

On Application of Petri Nets to Biological Pathways

March 2007

Chen Li

Graduate School of Science and Engineering
Yamaguchi University

Abstract

Title of Thesis: On Application of Petri Nets to Biological Pathways

Name of degree candidate: Chen Li

Degree and Year: Ph.D. in Science, 2007

Thesis directed by: Dr. Hiroshi Matsuno

Professor

Graduate School of Science and Engineering

Yamaguchi University, Japan

Systems biology is a new field that aims to integrate different levels of information to understand how biological processes function in a cell. The experimentally covered biological facts are usually summarized in a picture of network composed of figures of various shapes and several types of arrows reflecting the underlying biological images. Such pictures are called *biological pathways*, which can be classified into three categories: metabolic pathways, signaling pathways and gene regulatory networks. Many researches on biological pathway modelings using formal description methods have been made, and the systematic behaviors of the biological pathways have been observed by means of computer simulations. Generally in systems biology, mathematical modeling, simulation and analysis of biological systems play a critical role in helping biologists and biochemists explain and predict system's behavior.

Petri net is a formal description for modeling concurrent systems mainly applied to the artificial systems such as manufacturing systems and communication protocols. Petri nets have recently become widely accepted as a description method for biological pathways by researchers in computer science as well as those in biology.

This thesis discusses how to model, simulate and analyze signaling pathways in order to give systematic understanding of signaling pathways by using Petri net. The thesis is organized as follows: Chapter 1 gives an introduction of research background and presents the motivation of this thesis.

Chapter 2 presents the basic definitions of Petri nets and their extensions: timed Petri nets and hybrid functional Petri nets (HFPPN), which are used to construct models of biological pathways. The basic properties of them used in this thesis are also given.

Chapter 3 presents a modeling method based on Petri net by taking notice of molecular interactions and mechanisms of signaling pathways. Modeling rules and basic Petri net components representing various reaction types in signaling pathways are presented with detailed explanation. Finally, we demonstrate how our modeling method is practically used in modeling Interleukin-3 (IL-3) and Fas induced apoptotic signaling pathways as examples.

Chapter 4 gives structural analysis of modeled signaling pathways based on net theory. Firstly, we review the modeling method and structural analysis of metabolic pathways with Petri net. Then we discuss the characteristics of signaling pathways and introduce a new notion "activation transduction component" to express an enzymic activation process that has an elementary T-invariant in Petri net model as a counterpart. Algorithms are given to find activation transduction components. The results of algorithm are used to schematize the connection relations between activation transduction components in signaling pathways. Finally, we present an application of proposed method to modeled example of Thrombopoietin (TPO) signaling pathways.

Chapter 5 presents a simulation method with timed Petri nets and performs simulation experiments. We propose two basic principles and further three rules for determining transition speeds of timed Petri nets. Then we confirm the availability of proposed method by observing signal transductions from simulation experiments of Fas induced apoptotic signaling pathways as an example.

Chapter 6 introduces a pathway database website based on our new modeling method, which is available for the use of not only a biologist but also a researcher in computer science and/or engineering.

Chapter 7 concludes the results obtained in this thesis and discuss the research works remaining in future to be done.

学位論文内容要旨

学位論文題目：ペトリネット理論の生命パスウェイへの応用に関する研究
On Application of Petri Nets to Biological Pathways

指導教員：松野 浩嗣 教授

申請者名：李 晨 (リ シン)

平成 16 年度入学

山口大学大学院 理工学研究科 博士後期課程

自然共生科学専攻 複合系解析学講座

システム生物学は生物学的な反応が細胞の中でどのように機能するかを理解するため、さまざまなレベルに関する情報の統合を指向した新しい分野である。実験的に明らかにされた生物学的事実、さまざまな図形といくつかの種類、矢印で書かれたネットワークの図にまとめられており、基本的な生命科学の知識を反映している。そのようなネットワークの図は生命パスウェイと呼ばれ、代謝経路、シグナル伝達経路と遺伝子制御ネットワークの三つのカテゴリに分類することができる。生命パスウェイをモデル化する形式表現については多く研究されており、また計算機シミュレーションによる生命パスウェイにおけるシステムティックな挙動の観察も行われている。システム生物学は、生物システムの数学的モデル化、シミュレーション及び分析を通して、生物学者と生化学者がシステムの挙動を説明し、予測するために有効である。

ペトリネットは、コンカレントシステムをモデル化するための形式的な記述であり、主に製造システムや通信プロトコルなどのような人工的なシステムに応用されてきた。近年、ペトリネットは生命パスウェイを記述する一つの手法として情報科学及び生物学の研究者に広く受け入れられるようになってきた。

本論文ではペトリネットに基づくシグナル伝達経路のモデル化、シミュレーション及び解析の手法を示し、シグナル伝達経路のシステムティックな理解を与える。論文の構成は次の通りである。

1章では本論文の研究背景を紹介し、研究の目的を述べる。

2章ではシグナル伝達経路のペトリネットモデルを構築するための基盤となるペトリネット及びその拡張である時間ペトリネットとハイブリッド関数ペトリネットの定義を示す。同時にそれらの基本的な性質も与える。

3章はシグナル伝達経路における各細胞内分子の相互作用及びメカニズムに注目して、ペトリネットによるモデル化の手法を提案する。モデル化の規則及びシグナル伝達経路におけるさまざまな反応の種類に相当するペトリネットの構成要素を示し、詳しく説明する。最後に、インターロイキン-3 (Interleukin-3) のシグナル伝達経路と Fas によるアポトーシスを例に挙げ、ペトリネットに基づくモデル化の方法を示す。

4章ではペトリネット理論に基づくシグナル伝達経路のペトリネットモデルの構造的な解析手法を与える。まずペトリネットに基づいた代謝経路について、モデル化の手法と構造的な解析手法を概観する。次にシグナル伝達経路の特徴を述べる。ペトリネットにおける初等T-インバリエントに対応する酵素活性化のプロセスを表すため、「活性変換コンポーネント」という新しい概念を導入し、活性変換コンポーネントを求めるアルゴリズムを提案する。アルゴリズムの結果を用いて、シグナル伝達経路のモデルにおける活性変換コンポーネントの接続関係を図式化する。最後に、モデル化したトロンボポエチン (Thrombopoietin) のシグナル伝達経路を例に挙げ、提案した解析の応用例を示す。

5章は時間ペトリネットを用いて、シミュレーション実行に必要な反応時間を決定する手法を示し、実際にシミュレーション実験を行う。時間ペトリネットにおけるトランジションの遅延時間を決定するため、二つの基本原理と三つの発火規則を提案する。次に Fas リガンドによって誘導されるアポトーシスのモデルを例として、シミュレーション実験を行い、情報の伝達を観測し、提案された方法の有効性を確認する。

6章は提案したモデル化手法に基づいて構築した新しいデータベースのウェブサイトを紹介する。このサイトは生命パスウェイにおける細胞内分子の相互作用及び

メカニズムを表現したフラッシュアニメーションによるペトリネットモデルを提供する。このサイトは生物学者だけでなく情報科学，そして／または工学分野における研究者にとっても有用である。

7章は本論文で得られた結果をまとめ，今後の課題について述べる。

ON APPLICATION OF PETRI NETS TO BIOLOGICAL PATHWAYS

by

M.E. CHEN LI

Thesis submitted to the Graduate School of Science and Engineering
of Yamaguchi University on March 1, 2007,
in partial fulfillment of the requirements for the degree of
Doctor of Philosophy in Science

Advisory Committee:

Professor Hiroshi Matsuno, Chairman/Advisor

Professor Masahiro Fujishima

Professor Takashi Yamamoto

Professor Shigehiko Yumura

Professor Qi-Wei Ge

Lecturer Masaki Kawamura

© 2007 Yamaguchi University. All rights reserved.

Acknowledgments

First and foremost, I would like to express my sincere appreciation to my respected advisor, Professor Hiroshi Matsuno. His support, encouragement and advice have been immensely valuable both in personal and academic growth. I am particularly grateful for his daily warmhearted guidance. He directed my steps towards a new interdisciplinary field of systems biology that I am interested in very much.

I am also grateful to Professor Qi-Wei Ge, my main dissertation advisor and the supervisor of master's programs. Over the past six and half years, Professor Ge has been the most perceptive and patient mentor. Under the numerous discussions and idea exchanges with Professor Ge, this work has been improved and refined. All I can say is that without him, I would not be where I am today. I am so fortunate to have had his encouragement and helpful advice throughout the overseas study in Japan.

Special thanks go to my thesis committee members, Professor Masahiro Fujishima, Professor Takashi Yamamoto, Professor Shigehiko Yumura and Dr. Masaki Kawamura. Their careful reading and precious comments led to substantial improvement in the final product.

I would specially like to thank Professor Satoru Miyano (The University of Tokyo), Professor Youji Nagahisa and Associate Professor Mitsuru Nakata for their valuable advice, instruction and encouragement throughout this work.

I am grateful to Dr. Atsushi Doi and Dr. Masao Nagasaki at The University of Tokyo for their insightful comments and discussions. I am also extremely grateful to the assistance of my colleagues and co-workers: Mr. Shunichi Suzuki (TIS System Service Inc.), Mr. Kanji Hioka, Ms. Yoko Takeuchi, Ms. Nahomi Kan (Yamaguchi

Junior College), Mr. Goro Tsuji and Ms. Reiko Kato who are great colleagues and friends of mine over the past several years. I have truly enjoyed working with them.

I have also benefited from time spent with other colleagues at Professor Matsuno's and Ge's laboratories who have made my stay in Japan an enjoyable and rewarding experience. Special thanks to my nice classmate Ms. Misako Uragami with whom I have interesting scientific and private discussions and who has also given me helpful support in completing this thesis. Also I wish to especially thank my seniors Ms. Mieko Kawajiri and Ms. Chie Kimura, and my classmate of master's programs Ms. Risa Kamimura. They are so kind to look after me during these six years and I truly appreciate them from the bottom of my heart.

Last, I would also like to thank my parents, Shunyi and Zhixin for their endless encouragement and support. Without their love and great upbringing I would never have been able to accomplish this dissertation.

This work was partially supported by Grant-in-Aid for Scientific Research on Priority Areas "Systems Genomics" from the Ministry of Education, Culture, Sports, Science and Technology of Japan.

Notation

$x \in X$:	x is an element of set X .
$x \notin X$	x is not an element of set X .
$X \subset Y$:	Set X is contained in set Y .
$X \cup Y$:	Union of sets X and Y .
$X \cap Y$:	Intersection of sets X and Y .
$X - Y$:	Difference of sets X and Y .
$\sum x_i$:	The summation of all x_i .
ϕ :	Empty set.
N :	The set of natural numbers.
Z^+ :	The set of non-negative integers.
Z :	The set of integers.
$ X $:	The cardinality of set X .
$\max X$:	The maximum element of set X .
$X \leftarrow \{x_1, x_2, \dots, x_n\}$:	Add elements x_1, x_2, \dots, x_n to set X .
$L \leftarrow t_1 t_2 \dots t_n$:	Add items t_1, t_2, \dots, t_n to the end of list L in order.
$x \leftarrow x'$:	Assign a value of x' to variable x .

Contents

Abstract	i
Acknowledgment	ix
Notation	xi
Contents	xiii
1 Introduction	1
1.1 Research Background and Motivation	1
1.2 Organization of the Thesis	7
2 Definition of Petri nets	9
2.1 Definition and Basic Properties of Petri Nets	9
2.2 Timed Petri Nets	14
2.3 Hybrid Functional Petri Nets	14
3 Modeling of Signaling Pathways	21
3.1 Modeling Rules	21
3.2 Examples Modeling	33
3.2.1 Interleukin-3 Signaling Pathways	33
3.2.2 Fas-induced Apoptosis	39

4	Structural Analysis of Models	45
4.1	Analysis of Metabolic Pathways	45
4.1.1	Metabolic Pathways Overview	45
4.1.2	Elementary Flux Mode of Metabolic Pathways	47
4.1.3	Other Analyses of Metabolic Pathways with Petri Nets	52
4.2	Characterizing Signaling Pathways	54
4.2.1	Signal Propagation of Signaling Pathways	54
4.2.2	Activation Transduction Component and Elementary T-invariant	54
4.3	Algorithm to Find Activation Transduction Components	56
4.4	An Example – TPO Signaling Pathways	59
5	Simulation with Timed Petri Nets	69
5.1	Creating Timed Petri net for pathway simulation	69
5.2	Simulation Tools and Simulation Experiments	73
5.2.1	Biological Pathway Simulation Tools	73
5.2.2	Simulation Experiments of Fas-induced Apoptosis	76
5.3	Simulation Results and Discussions	80
6	Development of Pathway Database	83
6.1	Pathway Database Overview	83
6.2	<u>P</u> etri <u>N</u> et <u>P</u> athways (PNP) Description	90
6.2.1	Data Source and PNP Basement	90
6.2.2	Data Description	91
6.2.3	Data Searching	93
6.2.4	Data Update and Future Prospects	97

7 Conclusions	99
List of Figures	101
List of Tables	108
Bibliography	109
Appendix	121

Introduction

1.1 Research Background and Motivation

Systems biology, is a new field that aims to integrate different levels of information to understand how biological systems function in a cell. In systems biology, mathematical modeling, simulation and analysis of biological systems play a critical role in helping biologists and biochemists explain and predict behaviors of systems.

The experimentally covered biological facts are usually summarized in a picture of network composed of figures of various shapes (e.g. circles and rectangles) and several types of arrows (solid/dashed lines combined with filled/hollow/crossbar arrowheads) reflecting the underlying biological images (See Fig. 4.11). Such pictures are called *biological pathways*. Biological pathways can be classified into three categories: gene regulatory networks, metabolic pathways, and signaling pathways. Many researches on biological pathway modelings using formal description methods have been made [34], and the systematic behaviors of biological pathways have been observed by means of computer simulations.

With the study of cellular relationships and interactions of biological pathways, the modeling and analysis of biological networks have been investigated by using Petri nets. Petri net [61] is a formal description for modeling concurrent systems mainly applied to the artificial systems such as manufacturing systems [64] and communication protocols [82]. Petri nets have recently become widely accepted as a description method for biological pathways by researchers in computer science as

well as those in biochemistry [62].

Petri Net Based Formalism of Biological Pathways Biological pathways are reaction-networks of biological processes in a cell, which can be classified into three categories: metabolic pathways, gene regulatory networks, and signaling pathways. Due to the nature of concurrency of biological pathways, many researches using Petri nets on modeling biological pathways has been made. Metabolic pathways are the first biological pathways modeled by low-level Petri nets [27, 67].

After these works, several kinds of high-level Petri nets have been employed to model biological pathways: colored Petri net [19, 42, 80], stochastic Petri net [21, 59, 60], functional Petri nets [28], and hybrid Petri net [9, 10, 11, 14, 38, 46, 48, 49, 50, 51, 55, 79]. Differences in modeling biological pathways between colored Petri net, stochastic Petri net, and hybrid Petri net are well discussed in [22] based on characteristics of these Petri nets. For other mathematical formalisms of biological pathways such as Bayesian networks, Boolean Networks, differential equations, and rule-based formalisms, Jong summarized these mathematical formalisms in the review [34]. This review focused on gene regulatory systems, but these formalisms have been also applied to modeling of metabolic pathways and signaling pathways.

These attempts using Petri nets prove that there exist a variety of requirements in biological pathway modeling, and have been widely applied to study metabolic pathways and signaling pathways in both quantitative and qualitative approaches because of potential advantages of Petri net possessing intuitive graphical representation and capabilities for mathematical analysis. By using qualitative method, researchers could gain lots of important insights into the behaviors of the models at a relatively low cost in terms of effort and computational time, even without quantitative data. The qualitative analysis for even large scale and complex biological networks can be handled with the intuitive structural and behavioral properties defined by Petri nets.

Till now, many studies [19, 28, 48, 66, 67, 74, 80, 85] on modeling and analyzing

metabolic pathways using Petri net have been developed from the first paper by Reddy *et al.* in 1993 [67]. Metabolic pathways have such intrinsic characteristics that are series of chemical reactions catalyzed by enzymes, resulting in either the formation of a metabolic product to be used or stored by the cell, or the initiation of other metabolic pathways. In the works on modeling metabolic pathways, few discussions on formal description of metabolic pathways have been made so far. This is because there is no need to investigate the formalization method of metabolic pathways as the topic of pathway modeling owing to simple mechanism of metabolic pathways that can be expressed by a uniform network of catalytic reactions. In contrast, the mechanism of signaling pathways are generally more complex, consisting of distinct reactions such as complex formation, catalytic reaction, and translocation. Based on this observation, we need to propose a new modeling method for signaling pathways on account of potential advantages of Petri nets whose representation is easy to understand due to its graphical and precise nature. That is:

- (1) to propose a modeling method to describe signaling pathways consistently with the Petri net models of molecular interactions that enables biologists to intuitively understand the intrinsic structure and features of signaling pathways.

The aims of the modeling by Petri net for signaling pathways are: (i) to make the biologists intuitively understand the intrinsic structure and features of signaling pathways, and (ii) to make it possible to mechanically model larger and more complicated signaling pathway networks.

Qualitative Analyses of Biological Pathways with Petri Nets A signaling pathway is a set of chains of intracellular signaling events which starts by attaching ligands at receptors and ends by altering target proteins, which are responsible for modifying the behaviors of a cell. These signaling events are mediated by intracellular signaling proteins (enzymes as usual) that relay the signal into the cell by activating the next enzyme from inactive state to active state on receipt of signal in the chain. Many of the enzymes controlled by reactions such as phosphorylation are

enzymes themselves. In the enzymic cascades, an enzyme activated by phosphorylation phosphorylates the next enzyme in sequence. That is, the signal in signaling pathways propagates itself in the form of a series of chains consisting of sequential enzymic activation processes where a certain protein changes from “inactivate” state to “activate” state depending on the function of an upstream enzyme.

So far, a few researchers have tried to investigate relationships among complex molecular mechanisms and interactions, and further structural behaviors of signaling pathways by using Petri nets [8, 25, 41]. In the paper [25], Heiner *et al.* have explained how to model and validate the apoptosis pathways by using qualitative Petri nets. They have demonstrated a step-wise technique to model apoptosis signaling pathways. Further they have performed the model validation by using a standard Petri net analysis technique, and presented the biological meaning of the analysis results. Nevertheless, it is still expected to find a general methodology to analyze common signaling pathways by using Petri nets. Therefore, with the feature of signaling pathways, we need

- (2) to propose an analyzing method to inquire into the behaviors of sequential enzymic activation processes of signaling pathways and give a novel insight into the architecture of signaling pathways to grasp the structural and behavioral properties.

Quantitative Analyses of Biological Pathways with Petri Nets Petri nets have been employed for qualitative modeling and analysis of biological pathways since many theoretical investigations on Petri nets such as structural analysis of systems in the past have been made. In contrast, ordinary differential equations (ODEs) have been mainly used as the techniques for quantitative modeling and simulations. This approach provides mathematically well-founded and fine interpretations of biological pathways. Accordingly, some trials have been made to model and simulate signaling pathways using ODEs [23, 69]. Though ODE-based simulation can present quantitative behaviors of biological substances, it is hard to observe the whole system intuitively and grasp structural images of biological pathways from

the series of differential equations. One approach to cope with this problem is to use hybrid Petri net (HPN) [47, 48] which allows quantitative modeling and simulation of biological pathways with taking advantages of Petri net enabling graphical representation of biological pathways. It has likely been a common sense that Petri net is in good agreement with qualitative evaluation but not suitable for quantitative evaluation of biological pathways. However, there have been some attempts to use Petri net for quantitative evaluation.

Matsuno *et al.* [47] demonstrated that hybrid Petri net (HPN) has high potential to model and simulate biological pathways through the example of λ -phage genetic switch mechanism; for this pathway model, many ODE-based qualitative evaluations have been conducted. After this work, many biological pathways have been created with the technique of HPN or its extension as listed below.

- Gene Regulatory Networks
 - λ phage genetic switch [47]
 - circadian rhythms of fruit fly [51]
 - circadian rhythms of mouse [49]
 - cancer gene regulation (p53, MDM2, and p19ARF) [11]
- Signaling Pathways
 - apoptosis induced by protein Fas [51]
 - Notch-Delta signaling pathway in *Drosophila* [50]
 - gemcitabine chemotherapeutic drug pathway [60]
 - Huntington's disease [56]
 - role of interleukin-6 in the fate of haematopoietic stem cells [79]
 - Raf-1 kinase inhibitor protein on the extracellular signal regulated kinase [20]
- Metabolic Pathways
 - urea cycle and its regulation [6]
 - *lac* operon and glycolytic pathway [48]
- Protein Networks (cell cycle)

- cell division process of *Xeopus* [46]
- fission yeast cell cycle [14]

It can be considered that discrete nature of Petri net does not promote the use of Petri net for quantitative analysis of biological pathways. However, a few attempts aiming at quantitative analysis by discrete-based Petri net are found in the papers [19, 28, 63]. Hofestädt and Thelen [28] have introduced “functional Petri net” which allows to calculate dynamic biocatalytic process by using functions for specifying the arrow weight. With the functional Petri net, they illustrated the method to simulate biochemical networks. Interesting application of the functional Petri net is found in [37] which tries to infer the structure and the set of parameters of functional Petri net representing a metabolic pathway from observed data with the evolutionary algorithm. Popova-Zeugmann *et al.* [63] have introduced time Petri nets to bridge the gap between qualitative and quantitative models in steady state. They have presented structural techniques to decide the time-dependent realizability of a given transition sequence and to calculate its shortest and longest time length using linear programming for the analysis of the time Petri net model. In their research, the firing itself of a transition is supposed to take no time. In contrast, we deal with the following problem in this thesis:

- (3) to propose a method of determining the delay time of transitions of Petri net models automatically, i.e. the time taken in firing of each transition in order to observe flow speeds of different transductions leading intracellular responses to ultimate regulation, and perform simulations without establishing and tuning exact concentration.

1.2 Organization of the Thesis

This thesis is organized as follows: Chapter 1 gives an introduction of research background and presents the motivation of this thesis.

Chapter 2 presents the basic definitions of Petri nets and their extensions: timed Petri nets and hybrid functional Petri nets (HFPN), which are used to construct biological pathways. The basic properties of them used in this thesis are also given.

Chapter 3 reviews the modeling method for metabolic pathways with Petri net. Then we propose a modeling method based on Petri net by taking notice of molecular interactions and mechanisms of signaling pathways. Modeling rules and basic Petri net components representing various reaction types in signaling pathways are presents with detailed explanation. Finally, we demonstrate how our modeling method is practically used in modeling Thrombopoietin (TPO) and Fas induced apoptosis signaling pathways as an example. Other models of signaling pathways are also given.

Chapter 4 gives structural analysis of modeled signaling pathways based on net theory. We discuss the characteristics of signaling pathways and introduce a new notion “activation transduction component” to express an enzymic activation process that has an elementary T-invariant in Petri net model as a counterpart. Algorithms are given to find activation transduction components. The results of algorithm are used to schematize the connection relations between activation transduction components in signaling pathways. Finally, we present an application of proposed method to modeled examples of TPO and IL-3 signaling pathways.

Chapter 5 presents a simulation method with timed Petri nets and performs simulation experiments. We propose two basic principles and further three rules for determining transition speeds of timed Petri nets. Then we confirm the availability of proposed method by observing signal transductions from simulation experiments of Fas induced apoptosis signaling pathways as an example by using a Petri net based simulation tool “Cell Illustrator” [87].

Chapter 6 introduces a pathway database website based on our new modeling method, which is available for the use of not only a biologist but also a researcher in computer science and/or engineering.

Chapter 7 concludes the results obtained in this thesis and discuss the research works remaining in future to be done.

Definition of Petri nets

This chapter presents the basic definitions of Petri nets and their extensions: timed Petri nets and hybrid functional Petri nets. The basic properties of them, used in this thesis, are also given.

2.1 Definition and Basic Properties of Petri Nets

A Petri net N is defined by a 5-tuple $N=(T, P, E, \alpha, \beta)$ that corresponds to a bipartite graph, where T is a set of transitions t represented by bars or boxes ($|$ / $||$), P is a set of places p represented by circles (\circ) in a graph, E is a set of directed arcs e , $E=E^+ \cup E^-$, between places and transitions, where $e=(t, p) \in E^+$ and $e=(p, t) \in E^-$. α denotes the weight of arc $e(p, t)$ from place to transition, and β denotes the weight of arc $e(t, p)$ connected from transition to place. Figure 2.1 shows basic elements of Petri nets. Here, note that the presence of multiple arcs is shown by a single arc with a non-zero positive integer arc weight. For example, Fig. 2.2 represents a Petri net with same arc weights, where the set of places P is $\{p_1, p_2, p_3, p_4\}$, the set of transitions T is $\{t_1, t_2, t_3\}$, and the set of directed arcs E is $\{(p_1, t_1), (p_2, t_1), (t_1, p_3), (t_1, p_4), (t_2, p_2), (p_3, t_2), (p_4, t_2), (p_4, t_3), (t_3, p_1)\}$.

A transition without input places is called source transition that is always fireable, and a transition without output places is called a sink transition likewise. A place can hold a positive integer number of tokens as its content. An assignment of tokens in each place expressed in form of a vector is called marking M , which varies during

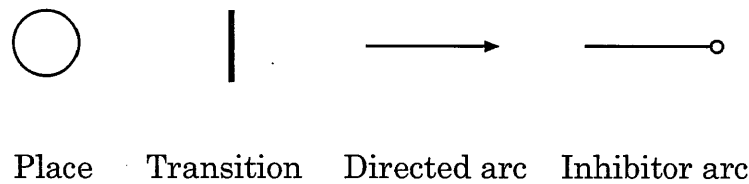


Fig. 2.1: Basic elements of Petri net.

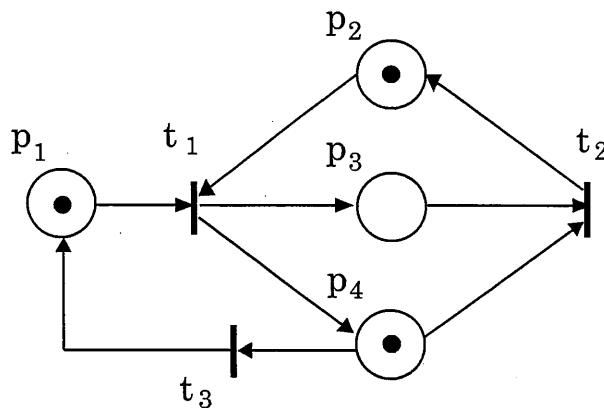


Fig. 2.2: An example of Petri net with unity arc weights.

execution of a Petri net. The number and position of tokens may change during the execution of a Petri net.

The execution of a Petri net is controlled by the number and distribution of tokens in the Petri net. A Petri net executes by firing transitions. A transition fires by removing tokens from its input places and creating new tokens which are distributed to its output places. A transition is fireable if each of its input places has at least as many tokens in it as arcs from the place to the transition. Figures 2.3 shows three cases of transition's firing rules as examples.

An inhibitor arc represents inhibitory function which is depicted as a line with a hollow circle at the end where the arrowhead normally appears. An inhibitor arc disables a transition to fire if the upstream place is occupied by a token, but does

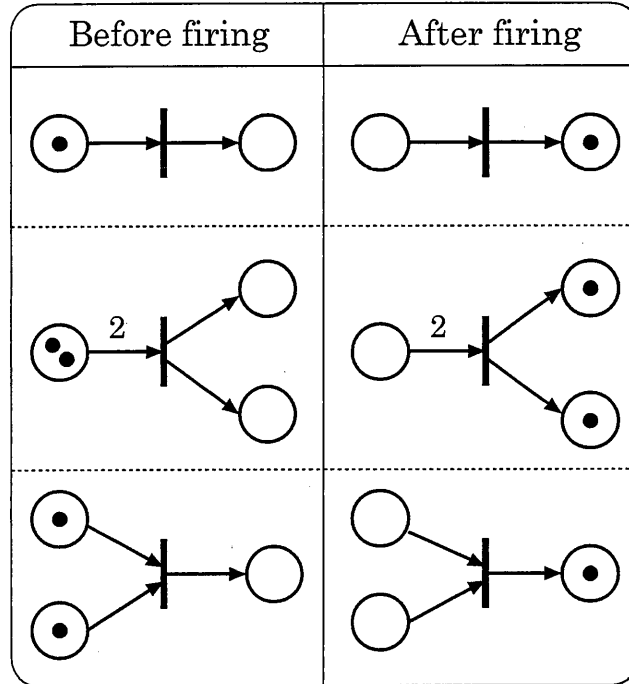


Fig. 2.3: Examples show firing rules of Petri net.

not consume the token. The followings are the mathematic definitions for Petri nets used in this Thesis as described below:

[Definition 1] A Petri net is denoted as $PN = (T, P, E, \alpha, \beta)$ that is a bipartite graph [61], where $E = E^+ \cup E^-$ and

T : a set of transitions $\{t_1, t_2, \dots, t_{|T|}\}$, where $|T|=m, m \geq 0$

P : a set of places $\{p_1, p_2, \dots, p_{|P|}\}$, where $|P|=n, n \geq 0$

E^+ : a set of arcs from transitions to places $e=(t, p)$

E^- : a set of arcs from places to transitions $e=(p, t)$

α : $\alpha(e)$ is the weight of arc $e=(p, t)$

β : $\beta(e)$ is the weight of arc $e=(t, p)$.

□

[Definition 2] Let PN be a Petri net.

- (1) ${}^{\circ}t$ (or t°) is a set of the input (or output) places of t and called the *pre-set* (or *post-set*) of transition t .
- (2) The structure of PN can be represented by a matrix, called *place-transition incidence matrix* (incidence matrix for short) C , whose n rows and m columns correspond to n places and m transitions. The matrix $C=C^+-C^-$ is defined as follows:

$$C^+(i, j) = \begin{cases} \beta(e) & \text{if } e=(t_j, p_i) \in E^+ \\ 0 & \text{otherwise;} \end{cases}$$

$$C^-(i, j) = \begin{cases} \alpha(e) & \text{if } e=(p_i, t_j) \in E^- \\ 0 & \text{otherwise.} \end{cases}$$

- (3) Token distribution to places is called *marking* and expressed by

$$M=(m_1, m_2, \dots, m_{|P|})^t, \text{ where, } m_i \text{ is the number of tokens at } p_i.$$

- (4) A transition sequence $\sigma=t_1t_2 \dots t_k$ is called *firing sequence* from M_I to M_F , if the firing simulation of σ on M_I can be carried out all the way to the last element of σ , which leads to the marking M_F . The marking transition is expressed by $M_I[\sigma]M_F$ and the firing numbers of all the transitions are expressed by a *firing count vector* $J=(j_1, j_2, \dots, j_{|T|})^t$. The relationship among C , J , M_I and M_F can be expressed by $M_F=M_I+CJ$. \square

The incidence matrix C of the Petri net shown in Figure 2.2 is as follows:

$$C = \begin{pmatrix} -1 & 0 & 1 \\ -1 & 1 & 0 \\ 1 & -1 & 0 \\ 1 & -1 & -1 \end{pmatrix}$$

Note that a Petri net PN represented by its incidence matrix must satisfy a condition that there is no self-loop in PN . The current marking of Fig. 2.2 is $M_0=(1, 1, 0, 1)$ that is the initial marking. Two transitions t_1 and t_3 are enabled and my fire. The result of firing t_1 in M_0 is a new marking $M_F=(0, 0, 1, 2)$, $M_0[t_1]M_F$. Transitions firings can continue as long as there exists at least one enabled transition. When there are no enabled transitions, the execution halts.

[Definition 3] Let PN and C be a Petri net and its incidence matrix, respectively [15, 58].

- (1) A non-negative integer vector J satisfying $CJ=0$ is called *T-invariant* and the set of transitions $T_J=\{t_i \in T | j_i \neq 0\}$ is called the *support* of J .
- (2) For a T-invariant J with the support T_J , if there exists no such T-invariant J' whose support $T_{J'}$ satisfies $T_{J'} \subset T_J$, then T_J is called *minimum support*. Further for a T-invariant J with minimum support T_J , if all the values $\{j_i | t_i \in T_J\}$ have no common divisor then J is called *elementary T-invariant*.
- (3) A subnet N_J is called “generated by a set of transition T_J ” if N_J is such a subnet that N_J is composed of all the transitions t included in T_J and all the places included in the pre-set and post-set of any $t \in T_J$.
- (4) An inhibitor arc e_i represents inhibitor function which is depicted as a line with a hollow circle at the end where the arrowhead normally appears. An inhibitor arc disables a transition to fire if the upstream place is occupied by a token, but does not consume the token. □

As defined above, a T-invariant is a non-negative integer vector that returns a Petri net’s marking to its initial marking. That is, a T-invariant is a firing sequence of transitions that expresses a periodic behavior of a Petri net and an elementary T-invariant expresses such a minimum periodic behavior that can not be divided furthermore.

[Firing rule of Petri nets N] A transition t is firable if each its input place p_I has at least α_e ($e=(p_I, t)$) tokens. A transition t fires to remove α_e ($e=(p_I, t)$)

tokens from each its input place p_I and deposit β_e ($e=(t, p_O)$) tokens to each its output place p_O . \square

2.2 Timed Petri Nets

Timed Petri nets are extension of Petri nets useful to performance evaluation and time-dependent analysis [53, 65, 75, 84]. For performance evaluation and time-dependent analysis, such as dynamic simulations of biological systems, the concept of time is necessary. However, it is not given in the definition of Petri nets. A timed Petri net $\overline{N}=(\overline{T}, \overline{P}, \overline{E}, \alpha, \beta)$ is a Petri net such that each transition is associated with time.

The firing rule of timed Petri net is extended as follows:

[Firing rule of timed Petri nets \overline{N}] (1) If the firing of a transition t_i is decided, tokens required for the firing are reserved. (2) When the delay time d_i of transition t_i passed, t_i fires to remove the reserved tokens from the input place of t_i and put tokens into the output places of t_i . \square

In a timed Petri net, the firing times per unit time f_i , called *firing frequency*, of a transition t_i is constrained by its delay time d_i , and the maximum of firing frequency is the reciprocal of d_i .

2.3 Hybrid Functional Petri Nets

Ordinary differential equations (ODEs) are widely accepted to express biological phenomena such as biochemical reactions. But in this work, it is rather difficult to observe the whole system intuitively such as a picture if the system constitutes a large network of cascades. Although the Petri net model allows very intuitive graphical representation, the mechanism of ODEs cannot be directly realized be-

cause the Petri net model deals with only integers as the contents of places. For sophisticated dynamic systems in which control mechanisms of genes and chemical reactions with enzymes are concurrently performed, it is more reasonable to use real numbers for representing the amounts of some objects, e.g. the concentrations of a protein, mRNA, complex of proteins, metabolites, etc.

The hybrid Petri net model (HPN) [3] has been introduced as an extension of the discrete Petri net model so that it can handle real numbers in a continuous way and it allows us to express explicitly the relationship between continuous values and discrete values while keeping the good characteristics of discrete Petri net soundly. Drath [12, 13] has also enhanced this notion to define the hybrid dynamic net model (HDN) for modeling more complex systems.

In HPN/HDN model, two kinds of places and transitions are used, discrete / continuous places and discrete / continuous transitions. A discrete place and a discrete transition are the same notions as used in the Petri net model. A continuous place holds a nonnegative real number as its content. A continuous transition fires continuously in the HPN/HDN model and its firing speed is given as a function of values in the places in the model. For graphical notations, discrete transition, discrete place, continuous transition and continuous place are drawn as shown in Fig. 2.4.

From the definition of HPN/HDN, the firing speed of a continuous place must be the same as the consuming speed through each arc from its source place and the contents of all source places are consumed with the same speed. This speed is also the same as the production speed through each arc from the transition. This is the unfavorable feature of HPN/HDN for biopathway simulation. For example, consider a reaction in which a dimer is cleaved to two monomers (Fig. 2.5 (a)). This reaction in the HDN model could be represented as shown in Fig. 2.5 (b) by using a test arc and a transition for amplification (note that the amounts consumed and produced in places by continuous transition firing are the same by definition while the amount of monomers is twice as large as that of dimers). But it is neither intuitive nor natural at all. It may be obvious that this feature of HPN/HDN is a

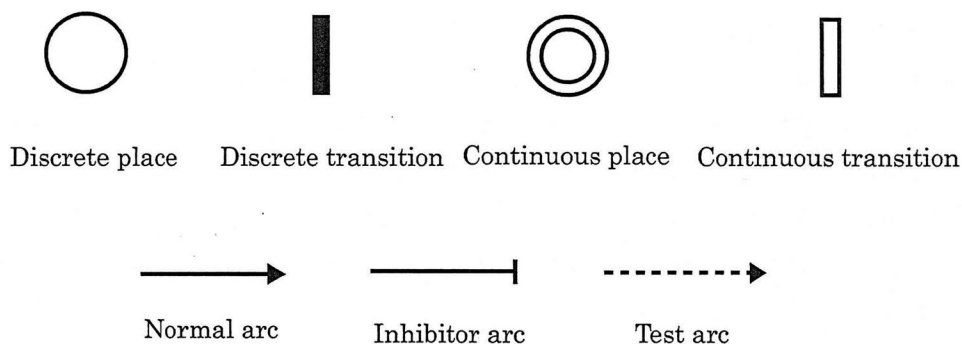


Fig. 2.4: Elements of hybrid (functional) Petri nets.

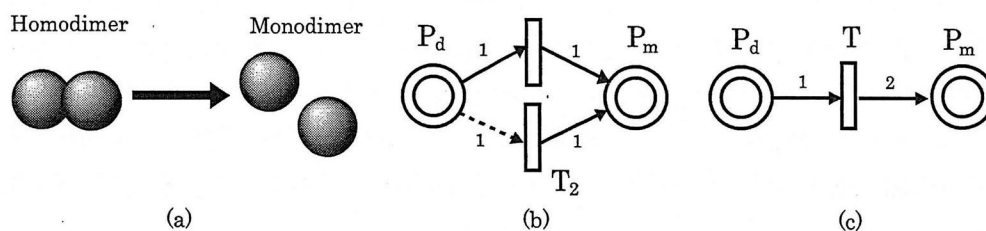


Fig. 2.5: Model for reaction decomposing dimers to monomers. (a) Reaction decomposing dimers to monomers. (b) Hybrid Petri net. In continuous places P_d and P_m , concentrations of the dimer and the monomer are stored, respectively. At continuous transitions T_1 and T_2 , same firing speeds are assigned as a reaction speed. Integers “1” represent weights of arcs. (c) hybrid functional Petri net model for the reaction. Note that, at the transition T, the reaction speed is assigned. P_d and P_m are the same as ones in (b). Different weights “1” and “2” are assigned to two arcs.

severe drawback in modeling biopathways.

On the other hand, some favorable features have been also introduced in Petri net theory. In addition to normal arc explained so far, inhibitory arc and test arc have been defined for convenience (Fig. 2.4). An inhibitory arc with weight r enables the transition to fire only if the content of the place at the source of the arc is less than or equal to r . For example, an inhibitory arc can be used to represent the function of “repress” in gene regulation. A test arc does not consume any content

of the place at the source of the arc by firing. For example, test arcs can be used to represent the transcription process since nothing is consumed by this process except for degradation.

[Definition 4] A hybrid functional Petri net (HFPN) is defined by extending the notion of transition of HPN/HDN [3, 12, 13] in the following way:

HFPN has five kinds of arcs; discrete input arc, continuous input arc, test input arc, discrete output arc, and continuous output arc. A discrete input arc (continuous input arc) is directed to a discrete transition (continuous transition) from a discrete/continuous place (continuous place) from which it consumes the content of the source place by firing. A test input arc is directed from a place of any kind to a transition of any kind. It does not consume the content of the source place. These three arcs are called input arcs. A discrete output arc is directed from a discrete transition to a place of any kind. A continuous output arc is directed from a continuous transition to a continuous place. These two arcs are called output arcs.

1. **Continuous transition:** A continuous transition T of HFPN consists of continuous/test input arcs a_1, \dots, a_p from places P_1, \dots, P_p to T and continuous output arcs b_1, \dots, b_q from T to continuous places Q_1, \dots, Q_q .

Let $m_1(t), \dots, m_p(t)$ and $n_1(t), \dots, n_q(t)$ be the contents of P_1, \dots, P_p and Q_1, \dots, Q_q at time t , respectively. The continuous transition T specifies the following:

- a. The firing condition is given by a predicate $c(m_1(t), \dots, m_p(t))$. As long as this condition is true, T fires continuously.
- b. For each input arc a_i , T specifies a function $f_i(m_1(t), \dots, m_p(t)) > 0$ which defines the speed of consumption from P_i when it is firing. If a_i is a test input arc, then we assume $f_i \equiv 0$ and no amount is removed from P_i . Namely, $d[a_i](t)/dt = f_i(m_1(t), \dots, m_p(t))$, where $[a_i](t)$ denotes the amount removed from P_i at time t through the continuous input arc a_i during the period of firing.
- c. For each output arc b_j , T specifies a function $g_j(m_1(t), \dots, m_p(t)) > 0$

which defines the speed of amount added to Q_j at time t through the continuous output arc b_j when it is firing.

Namely, $d[b_j](t)/dt = g_j(m_1(t), \dots, m_p(t))$, where $[b_j](t)$ denotes the amount of the contents added to Q_j at time t through the continuous output arc b_j during the period of firing.

2. **Discrete transition:** A discrete transition T of HFPN consists of discrete/test input arcs a_1, \dots, a_p from places P_1, \dots, P_p to T and discrete output arcs b_1, \dots, b_q from T to places Q_1, \dots, Q_q . Let $m_1(t), \dots, m_p(t)$ and $n_1(t), \dots, n_q(t)$ be the contents of P_1, \dots, P_p and Q_1, \dots, Q_q at time t , respectively. The discrete transition T specifies the following:

- a. The firing condition is given by a predicate $c(m_1(t), \dots, m_p(t))$. If this is true, T gets ready to fire.
- b. The delay function given by a nonnegative integer valued function $d(m_1(t), \dots, m_p(t))$. If the firing condition gets satisfied at time t , T fires in delay $d(m_1(t), \dots, m_p(t))$. However, if the firing condition is changed during this delay time, the transition T loses the chance of firing and the firing condition will be reset.
- c. For each input arc a_i , T specifies a nonnegative integer valued function $f_i(m_1(t), \dots, m_p(t)) > 0$ which defines the number of tokens (integer) removed from P_i through arc a_i by firing. If a_i is a test input arc, then we assume $f_i \equiv 0$ and no token is removed.
- d. For each output arc b_j , T specifies a nonnegative integer valued function $g_j(m_1(t), \dots, m_p(t)) > 0$ which defines the number of tokens (integer) are added to Q_j through arc b_j by firing. \square

In Fig. 2.6, examples of continuous transition and discrete transition are shown.

From the above definition, it may be obvious that in the HFPN model, the dimer-to-monomers reaction can be intuitively represented as Fig 2.5 (c). Not only this simple example but also more complex interactions can be easily and intuitively described with HFPN. The software CI [87] is developed and implemented based on

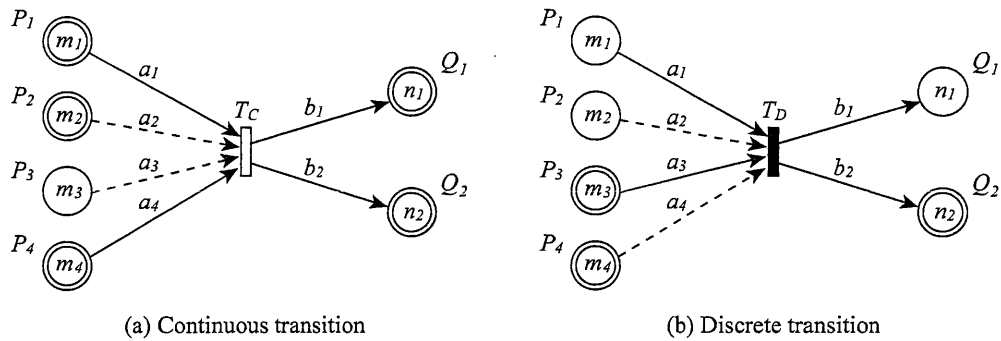


Fig. 2.6: Continuous and discrete transitions of hybrid functional Petri net. (a) An example of continuous transition. Four input arcs are attached to continuous transition T_C : two continuous input arcs from continuous places P_1 and P_4 , and two test input arcs from continuous place P_2 and discrete place P_3 . a_i is the weight of arc from place P_i for $i=1, 2, 3, 4$. Two continuous arcs are headed from the transition T_C to continuous places Q_1 and Q_2 , respectively. Variables b_1 and b_2 are assigned to these arcs as weights. (b) An example of discrete transition. Four input arcs are attached to discrete transition T_D : two discrete input arcs from discrete place P_1 and continuous place P_3 , and two test input arcs from discrete place P_2 and continuous place P_4 . a_i is the weight of arc from place P_i for $i=1, 2, 3, 4$. Two output arcs are headed from the transition T_D to discrete place Q_1 and continuous place Q_2 . Variables b_1 and b_2 are assigned to these arcs as weights.

this HFPN architecture.

Modeling of Signaling Pathways

In this chapter, we first propose a modeling method with Petri net by paying attention to molecular interactions and mechanisms, and then demonstrate how our modeling method is practically used in modeling signaling pathways mediated by Interleukin-3 (IL-3) as an example.

3.1 Modeling Rules

In this section, we give the modeling rules for signaling pathways with Petri net that can be naturally and explicitly modeled according to the following rules:

- (1) Places denote static elements including chemical compounds, conditions, states, substances and cellular organelles participating in the biological pathways. Tokens indicate the presence of these elements. The number of tokens is given to represent the amount of chemical substances. Current assignment of tokens to the places are expressed in form of a vector, namely a *marking* as defined in chapter 2.

For example, Fig. 3.1 (a) illustrates an association reaction. In Fig. 3.1 (b) and (c), each place represents one biological substance and compound. Tokens indicate the presence of substance A and B before the firing of transition t_1 . Current token distribute of the places is $M_I=(1, 1, 0)$.

- (2) Transitions denote active elements including chemical reactions, events, actions, conversions and catalyzed reactions. A transition fires by taking off tokens from its individual input places and creating new tokens that are dis-

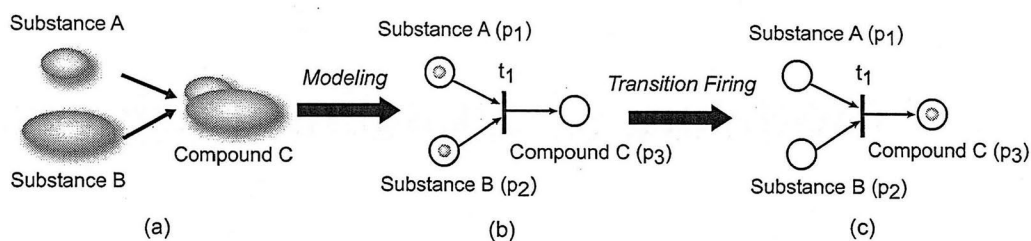


Fig. 3.1: An application of modeling rules to a simple reaction.

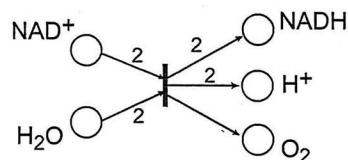
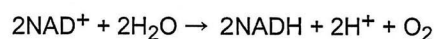


Fig. 3.2: Petri net model of a chemical reaction of light-induced phosphorylation, given by its stoichiometric equation.

tributed to its output places if its input places has at least as many tokens in it as arc weight from the place to the transition.

In Fig. 3.1 (b), t_1 represents the association reaction and t_1 is firable because the input places of t_1 have enough tokens than arc weight from the places to t_1 . The marking after the firing of t_1 is $M_F=(0, 0, 1)$ (see Fig. 3.1 (c)).

- (3) Directed arcs connecting the places and the transitions represent the relations between corresponding static elements and active elements. Arc weights α and β (defined in **Definition 1**) describe the quantities of substances required before and after reaction, respectively. Especially in case of modeling a chemical reaction, arc weights represent quantities given by stoichiometric equations of the reaction itself. Fig. 3.2 shows a Petri net model representing a chemical reaction of light-induced phosphorylation, given by its stoichiometric equation. Note that, weight of an arc is omitted if the weight is 1.

- (4) Since an enzyme itself plays a role of catalyzer in biological pathways and there occurs no consumption in biochemical reactions, an enzyme is exceptionally modeled in **Definition 5** below.
- (5) An inhibition function in biological pathways is modeled by an inhibitor arc.

Generally in Petri net theory, weights of arcs are supposed to be positive integer, however in this paper we assume weights of all arcs could be positive rational in representing degradation of compounds. All rational could be multiplied by a common denominator to obtain integers when analyzing signaling pathways to be shown in chapter 4. Note that using rational arc-weights involves taking risks of high computational costs and computational overflow.

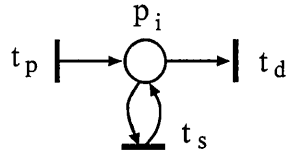


Fig. 3.3: An enzyme place in Petri net model.

[Definition 5] An enzyme in a biological pathway is modeled by a place, called *enzyme place*, as shown in Fig. 3.3.

- (1) Enzyme place p_i has a self-loop with same weight connected from and to t_s . Once an enzyme place is occupied by a token, the token will return to the place again to keep the firable state, if the transition t_s is fired.
- (2) Let t_p and t_d denote a token provider of p_i and a sink output transition of p_i , respectively, where the firing of t_p represents an enzyme activation reaction and the firing of t_d implies an extremely small natural degradation in a biological pathway. p_i holds up token(s) after firing transition t_p and the weights of the arcs satisfy $\alpha(p_i, t_d) \ll \alpha(p_i, t_s)$. \square

In cell biology, signaling pathways have been widely studied. They are information cascades of enzyme reactions from transmembrane receptors to the nucleus

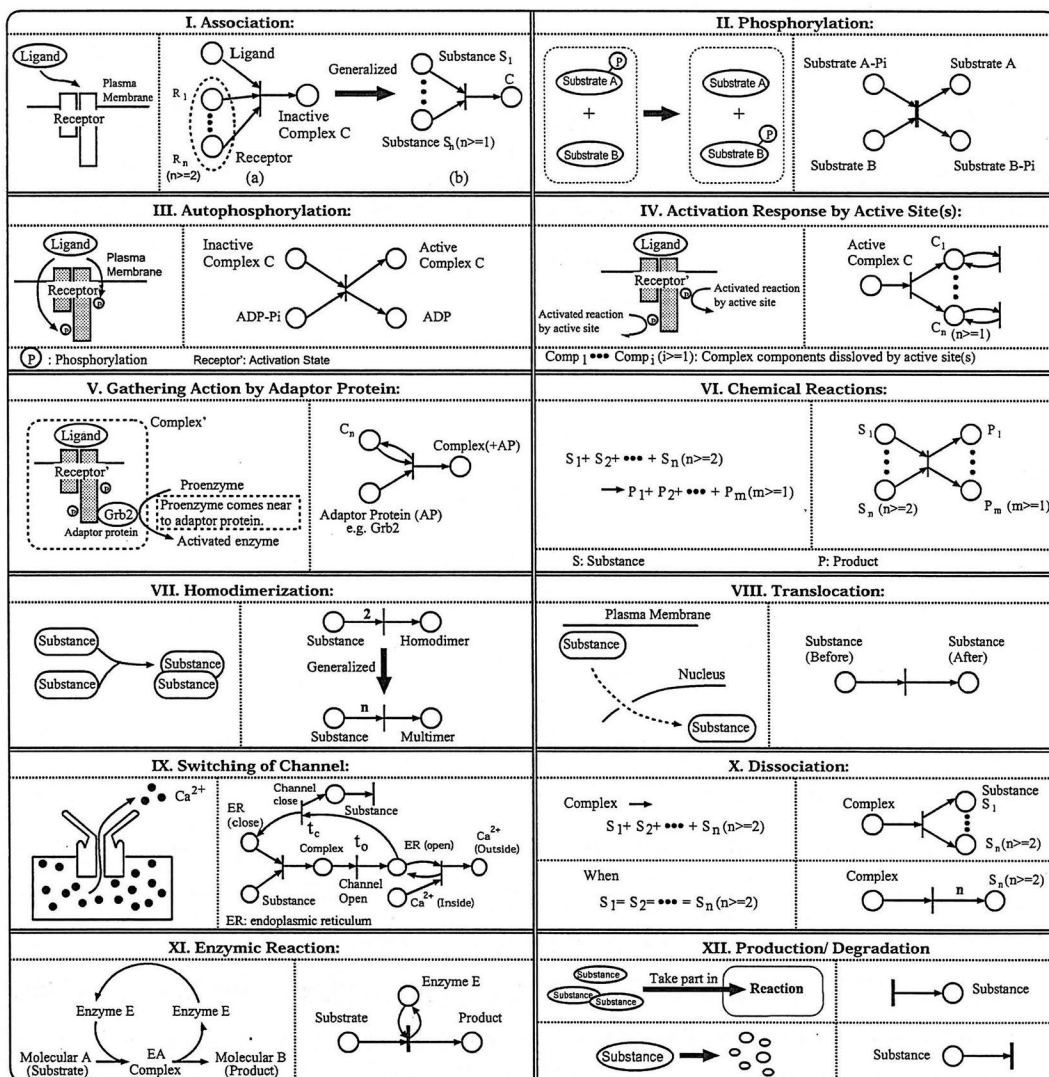


Fig. 3.4: Petri net models of various reaction types in signaling pathways.

DNA, which ultimately regulate intracellular responses such as programmed cellular proliferation, gene expression, differentiation, secretion and apoptosis. Numerous reaction types of molecular interaction mechanisms have been described by Petri net model [27], which suffices to give the description of the metabolic pathway presently [67]. For signaling pathways, as has been pointed [76], besides the catalytic reactions, the information among the molecular interactions such as complex formation, gathering action, translocation and channel switching, also need to be respectively modeled by Petri nets according to different types of interactions as long as the biological facts has been known.

To explicitly understand the structural complicated signaling pathways, the modeling of each essential molecular interaction by using Petri net is the first step in modeling the network of signaling pathways as a qualitative event system. With a focus on possible molecular interactions as long as we have known, In Fig. 3.4, we summarize various molecular interactions of signaling pathways (see left side of dashed line in Fig. 3.4) and their corresponding Petri net model (right side of dashed line). Both of them in a reaction type are described as a “block” labeled with roman numeral in this thesis. The description of each molecular interaction and corresponding model are given as follows. Each illustration corresponding to the explanation is also given subsequently.

[**I. Association:**]

It is a binding reaction to induce the formation of homo- or heterodimers and to generate a complex compound. Fig. 3.5 shows the ligand-receptor binding interaction and corresponding Petri net model that indicates the transition is unfirable in the absence of place of ligand although receptors exist. The number of input place of transitions is two or more while the output place number is one in association reaction. Obviously, we can expand the conception of association to the formation of model represented in Fig. 3.5 (b), generally representing the simultaneous association of substances $S_1, \dots, S_n (n \geq 1)$ forming a complex C in biological systems.

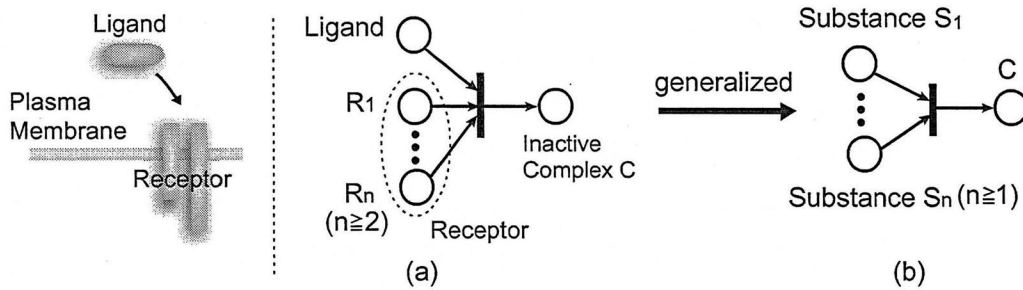


Fig. 3.5: Petri net model of I. association reaction.

[**II. Phosphorylation:**]

It is a reaction to add a phosphate (PO_4) group to a protein or a small molecule, and dephosphorylation that is the backward reaction of phosphorylation removing phosphate groups from a compound by hydrolysis (see Fig. 3.6).

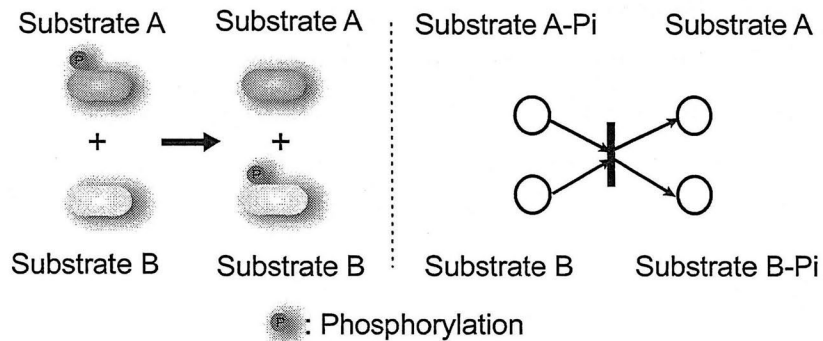


Fig. 3.6: Petri net model of II. phosphorylation.

[**III. Autophosphorylation:**]

Figure 3.7 or the block in Fig. 3.4 illustrates an autophosphorylation reaction that is a transphosphorylation reaction, frequently following the binding of a ligand to a receptor with intrinsic protein kinase activity on the left side. The Petri net model of this autophosphorylation reaction is given on the right side. Besides the

autophosphorylation reaction arising after the binding of a ligand to a receptor, autophosphorylation reactions are a common sight inside the signaling pathways. All these autophosphorylation reactions can be commonly modeled to the Petri net model as shown on the right side of dashed line in Fig. 3.7.

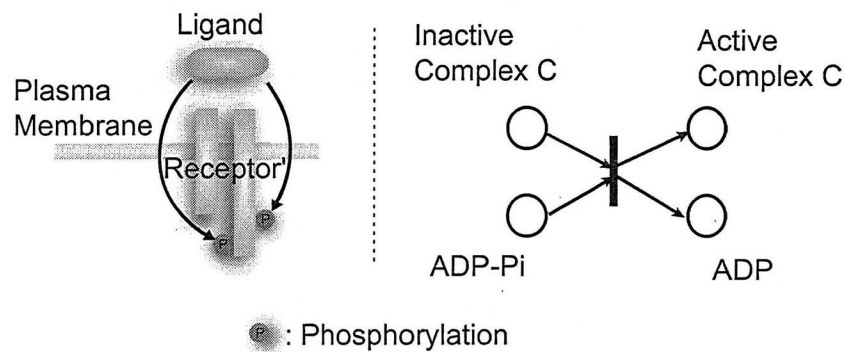


Fig. 3.7: Petri net model of III. autophosphorylation.

[**IV. Activation response by active site(s):**]

Generally continued activated ligand-receptor complex regulates varied majority of cellular pathways transmitting the signals within the cell. Few methods using Petri nets have been proposed to model such activated complex place possessing more than one transitions that can trigger down-stream signaling pathways [25]. Their methods are easily understood, but have some problems that, if the transition of such place fires to remove the token(s) in shared input place at one time epoch, it will disable rest transitions simultaneously although the token will return back the same input via a self-loop. Hence, we need a more appropriate model to express this system's behavior. Our basic consideration is that, if there have plurality of successive signaling pathways depending on distinct active site(s) (subunits) of activated complex, all the active site(s) shall be regarded as complex component(s) $C_1, \dots, C_n (n \geq 1)$ as shown in Fig. 3.8 or the block **IV** in Fig. 3.4.

[**V. Gathering action by adaptor protein:**]

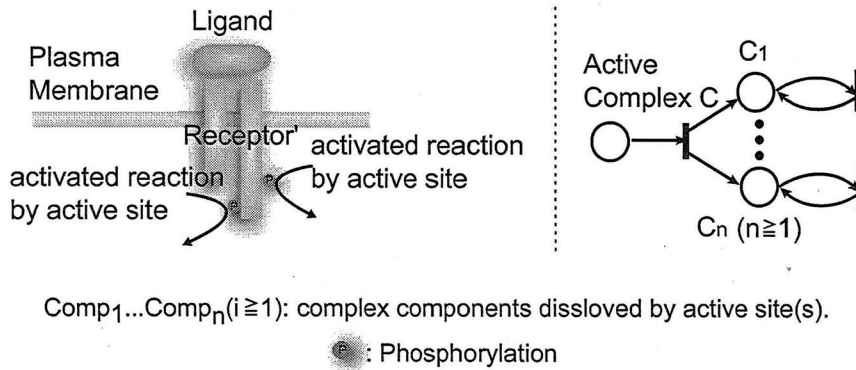


Fig. 3.8: Petri net model of IV. activation response by active site(s).

It is distinguished from association reaction. The main participator adaptor protein is an accessory protein to main proteins. These proteins lack the intrinsic enzymic activities themselves but instead mediate specific protein-protein interactions driving the formation of protein complexes. In Fig. 3.9, the adaptor protein Grb2 binds to the ligand-receptor complex. The proenzymes close to the complex comes near to Grb2 and becomes active form as shown on the left side in Fig. 3.9. Because the complex itself possesses the enzymic activities, the place of the complex are modeled with self-loop, where the place representing the adaptor protein has only one arc from the place to the transition (see the right side of Fig 3.9).

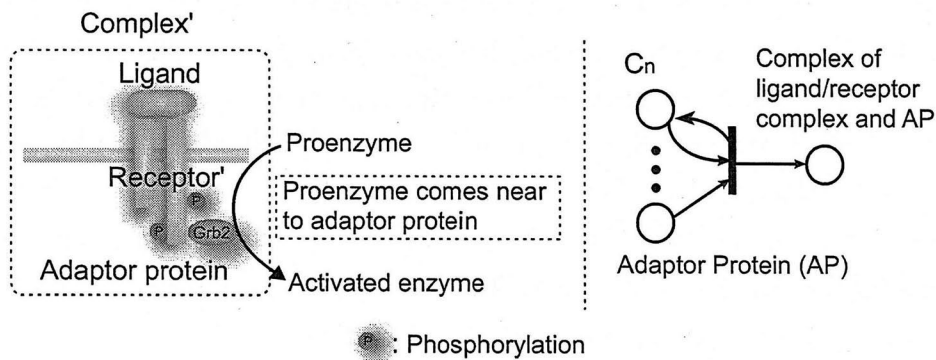
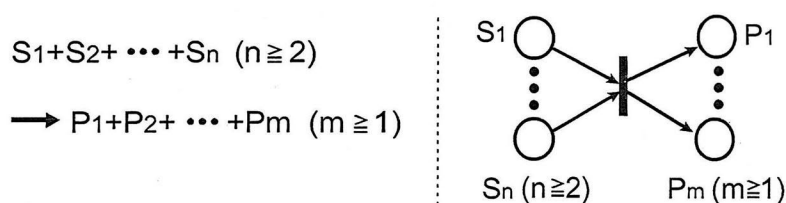


Fig. 3.9: Petri net model of V. Gathering action by adaptor protein.

[VI. Chemical reactions]

It is the most common reaction in signaling pathways, which the conversion of substances to products is ordinarily modeled as input places to output places, both belonging to the same transition.



S and P denote substrate and product, respectively.

Fig. 3.10: Petri net model of VI. chemical reactions.

[VII. Homodimerization:]

It is a polymerization reaction of two identical substances to shape a dimer similar to a kind of association reaction. A substance is modeled as an input place connected with a 2-weighted arc. It is easy to expand the conception to model the formation of multimer holding n -weight such as trimer and tetramer that is a complex of two or more equivalent polypeptides. The lower Petri net in Fig. 3.14 or the block **X** in Fig. 3.4 is constructed under the opposite consideration of modeling homodimerization reactions.

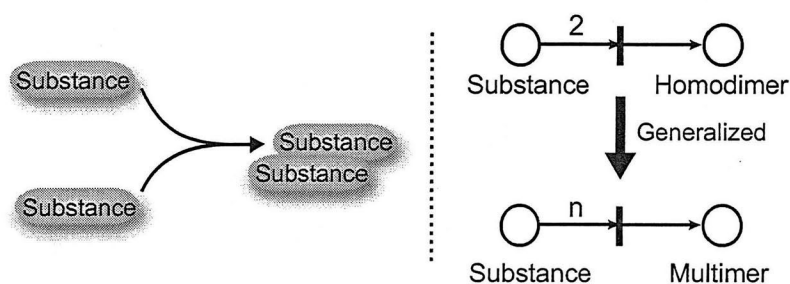


Fig. 3.11: Petri net model of VII. homodimerization.

[VIII. Translocation:]

It refers to the movement of molecules, substances or ions across cell membranes or via the bloodstream in biology. Figure 3.12 shows the nuclear translocation within a cell. A transition is modeled to indicate the movement action of substances before and after. In this reaction type, instead of using just one place to represent each substance, it is necessary to assign two places to distinguish between the substances based on their location inside the cell. It may be necessary to prescribe two or more places to represent the substances, when there are alternative physical features, transformations in the activity of the substances, or different biological functions.

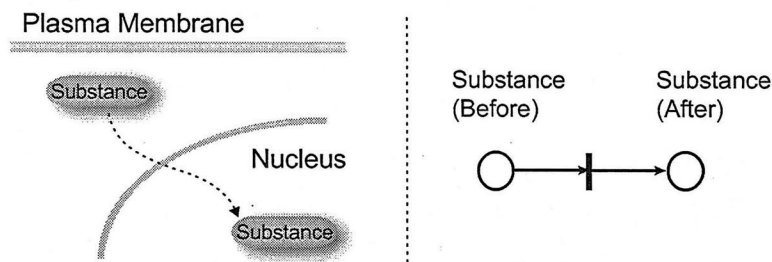


Fig. 3.12: Petri net model of VIII. translocation.

[IX. Switching of Channel:]

Intracellular signal pathways are largely carried out by second messenger molecules. Ca^{2+} acts as a second messenger molecule to carry out large intracellular signal inside the cell. Usually the concentration of free Ca^{2+} within the cell is very low; it is stored inside of organelles, mostly the endoplasmic reticulum. In order to become active, Ca^{2+} has to be released from the organelles into the cytosol.

Two transitions t_o and t_c are introduced to denote channel activity of “open” and “close”, respectively. t_o is enabled when input place holds up token(s) after the association of organelles and substances, whereas t_c is enabled as long as some stop mechanisms shutoff the channel.

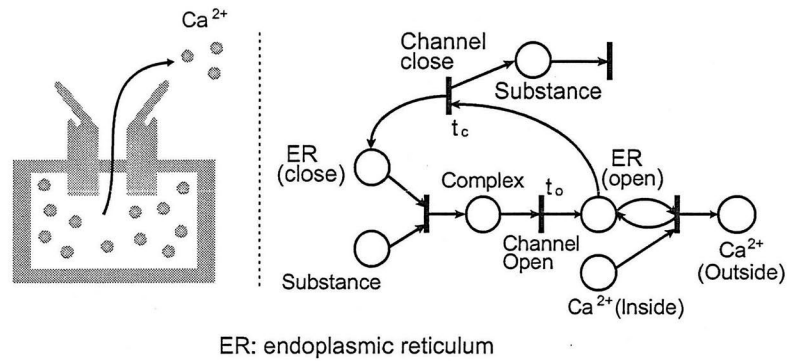


Fig. 3.13: Petri net model of IX. switching of channel.

[**X. Dissociation:**]

This is the opposite of [**I. Association**]. Dissociation process is a general process in which complexes and molecules separate or split into smaller molecules, ions. The number of input place of transitions is one while the output place number is two or more.

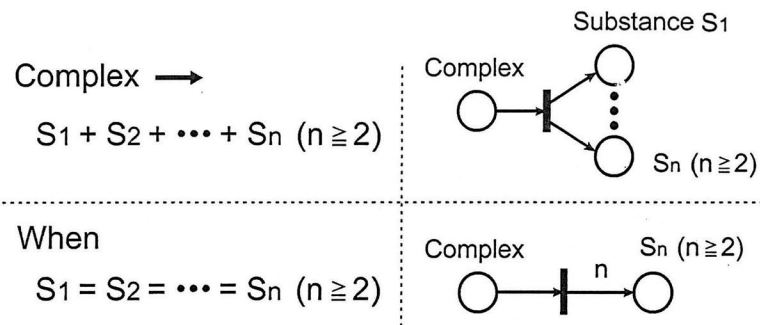


Fig. 3.14: Petri net model of X. dissociation.

[**XI. Enzymic Reaction:**]

Since an enzyme itself plays a role of catalyzer in biological pathways and there occurs no consumption in biochemical reactions, the reaction is modeled to a tran-

sition, whereas the substrate is modeled to enzyme place that has a self-loop with same arc-weight. That is, once an enzyme place is occupied by a token, the token will return to the place again to keep the firable state, if the transition is fired.

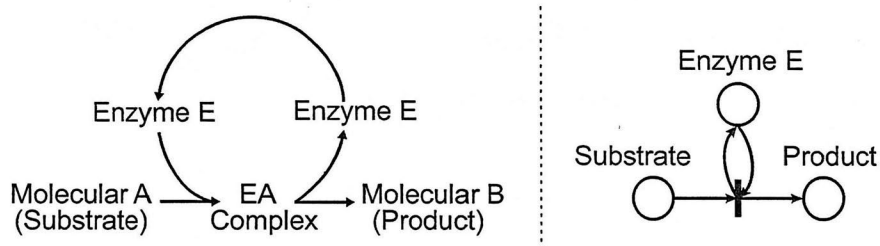


Fig. 3.15: Petri net model of XI. enzymic reaction.

[XII. Production/Degradation]

A source transition represents an activity to provide substances that will take part in the reactions. A sink transition denotes small and natural degradation of substance.

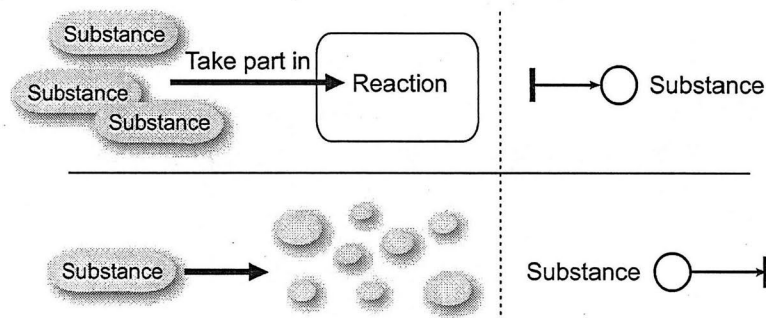


Fig. 3.16: Petri net model of XII. production/degradation.

3.2 Examples Modeling

3.2.1 Interleukin-3 Signaling Pathways

In this section, we give an example to demonstrate our modeling method. The example is the signaling pathway mediated by cytokine Interleukin-3 (IL-3).

■ Pathway Overview

IL-3 promotes the proliferation and differentiation of bone marrow-derived hematopoietic cells through binding to its receptor. Recently, several studies have already indicated that IL-3 inhibits apoptosis by stimulating the activation of cellular kinases. On the other hands, withdrawal of IL-3 leads to the activation of caspase proteases and a commitment to cell death.

An extracellular ligand activates IL-3 signaling pathway by binding to the receptors of IL-3 (IL-3R for short), resulting in dimerization of the two IL-3R alpha and beta, followed by tyrosine phosphorylation of IL-3R beta itself. Two signaling pathways are induced by binding to distinct functional domains in the IL-3R beta [33, 7, 36, 29, 1, 31, 52] as shown in Fig. 3.17.

[JAK/STAT Signaling Pathway]

Jak2 is activated by binding itself to the membrane proximal domain of IL-3R beta, which triggers the activation of Jak-STAT signaling pathway. The pathway includes following reactions:

1. Jak2 activates STAT5 by phosphorylating two residues of STAT5.
2. Two STAT5 shape a STAT5 homodimer.
3. STAT5 homodimer translocates to the nucleus, where they modulate expression of target genes.
4. STAT5 homodimer binds to c-FOS and shapes a complex of c-FOS/STAT5 homodimer.

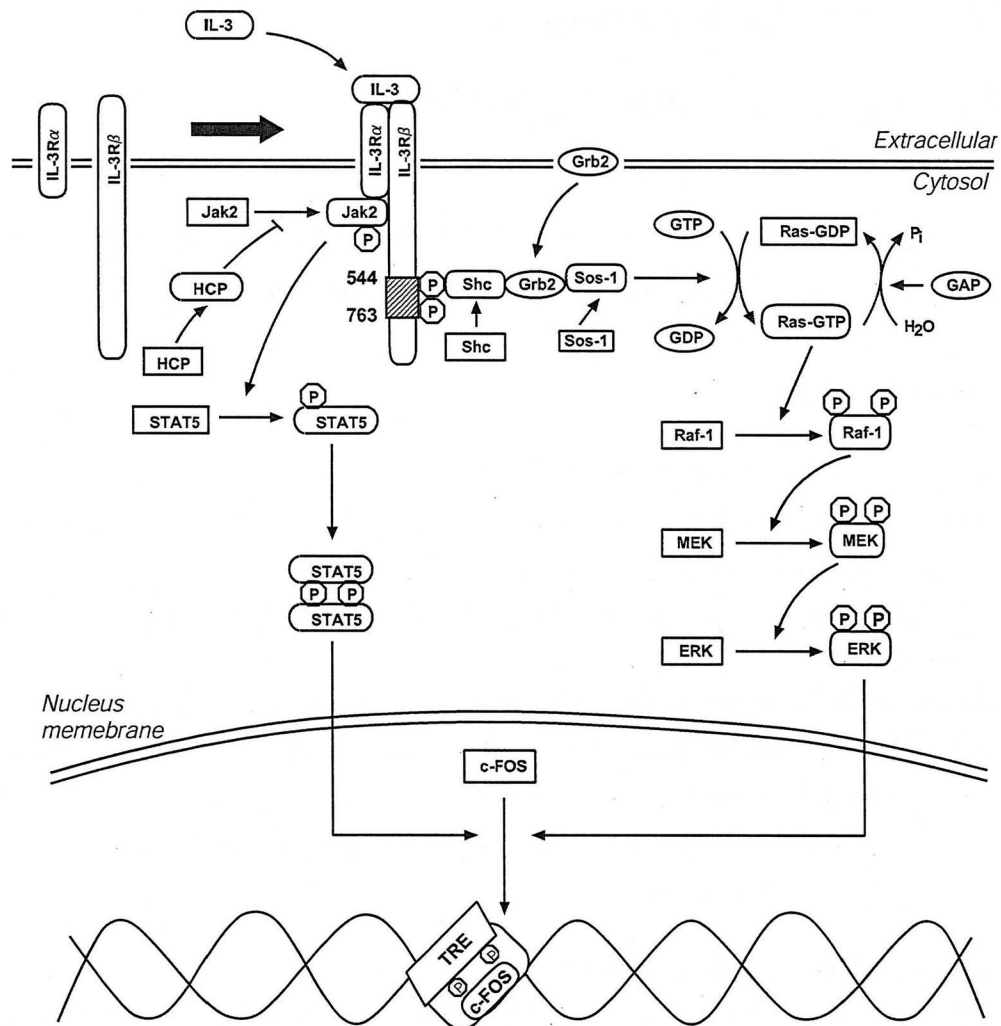


Fig. 3.17: The signaling pathway induced by IL-3.

5. ERK activates the complex of c-FOS/STAT5 homodimer.
6. c-FOS of the complex c-FOS/STAT5 homodimer binds to the TRE sequences on DNA, promotes the transcription of genes, and produces gene products.

[Ras-MAPK Signaling Pathway]

IL-3 also activates Ras-MAPK signaling pathway by recruitment of Shc in a mem-

brane distal domain of IL-3R beta. Subsequent activations involved in Ras-MAPK signaling pathways are as follows.

1. Grb2 binds to Shc of the complex Shc/ligand-receptor complex as an adaptor protein and triggers downstream activation.
2. Sos-1 is activated by Shc/Grb2.
3. Sos-1 changes Ras state from inactivated Ras-GDP to activated Ras-GTP. Activated Ras-GTP becomes inactive Ras-GDP by hydrolysis with GAP.
4. Ras-GTP activates Raf-1 by phosphorylating two residues of Ras-GTP.
5. Raf-1 activates MEK by phosphorylating two residues of MEK.
6. ERK is activated by the phosphorylation of MEK.
7. Activated ERK translocates to the nucleus and recruits *c-FOS* promoting the transcription of genes.

■ Petri Net Modeling

Figure 3.18 shows the whole Petri net model of IL-3 signaling pathway according to proposed modeling methods. In this subsection, we demonstrate how to model IL-3 signaling pathway using the modeling method proposed in Sect. 3.1.

The modeling operation starts from the source transitions (t_0 and t_1) denoting the activities that the substances take part in reactions. IL-3 ligands and corresponding receptor IL-3R alpha are assigned to the places (p_1 and p_2) connected from the source transitions (t_0 and t_1) respectively, in accordance with block **XII. Production/Degradation** of Fig. 3.4. IL-3 ligands bind to IL-3R alpha and induce a formation of IL-3/IL-3R alpha complex compound. A transition t_2 is used to represent this association reaction connecting from the input places (p_1 and p_2) as well as connecting to the output place p_3 of IL-3/IL-3R alpha complex applying the block **I. Association** in Fig. 3.4. After the formation of the complex (p_3), IL-3R beta has an immediate association with the complex and shapes a complex of IL-3/IL-3R alpha/IL-3R beta. Two places (p_3 and p_4) merge into a place p_5 denoting IL-3/IL-3R

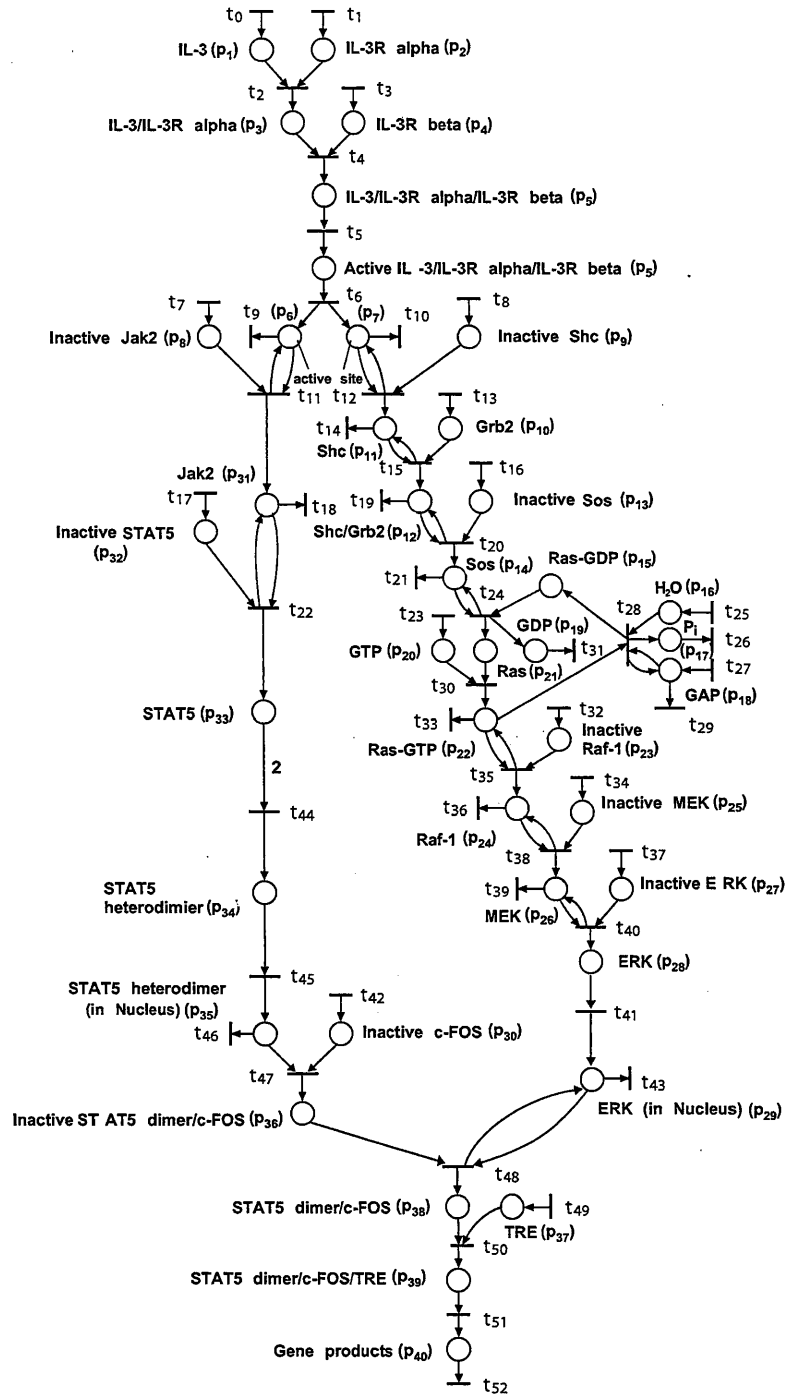


Fig. 3.18: Petri net model of Fig. 3.17.

alpha/IL-3R beta complex via the transition t_4 representing the association reaction. Autophosphorylation occurs following the binding of IL-3 ligand to IL-3R alpha and beta with intrinsic protein kinase activity denoted by the transition t_5 . Since the down-stream signaling pathways: JAK-STAT signaling pathway and Ras-MAPK signaling pathway are activated respectively by binding to distinct functional domains in the IL-3R beta, two functional domains are modeled by two places (p_6 and p_7) and the activation reaction is modeled as “Activation response by active sites” shown in block **IV. Activation response by active site(s)** of Fig. 3.4. In the following text, we only explain the modeling of JAK-STAT signaling pathway.

Since IL-3/IL-3R alpha/IL-3R beta complex possesses protein kinase activity, it next initiates the activation of Jak2 (p_8) and there occurs no consumption in the reactions. IL-3/IL-3R alpha/IL-3R beta complex (p_6) is modeled to an enzyme place (refer to [**Definition 5**]) with a self-loop. Similarly, Jak2 (p_{31}) catalyzes inactive STAT5 (p_{32}) to an active form (p_{33}) which is modeled as an enzymic reaction denoted by transition t_{22} . Next, two STAT5 (p_{33}) shape a STAT5 homodimer (p_{34}). A transition t_{44} is used to represent polymerization connecting from the input place p_{33} with a 2-weighted arc $e(p_{33}, t_{44})$ as well as connecting to the output place p_{34} of STAT5 homodimer applying the block **VII. Homodimerization** in Fig. 3.4. STAT5 homodimer further translocates to cell nucleus. A transition t_{45} is modeled to indicate the movement action of STAT5 homodimer inside and outside the nuclear membrane. Then STAT5 homodimer (p_{35}) binds to inactive c-FOS (p_{30}) and form a complex of STAT5 homodimer/c-FOS (p_{36}) which are modeled as an association reaction **I. Association** where transition t_{47} denotes the binding process.

At last, the transition t_{43} is used to model an enzymic reaction where ERK activated via the Ras-MAPK signaling pathway catalyzes c-FOS of STAT5 homodimer/c-FOS to an active form (p_{38}) which applies the reaction model of enzymic reaction as shown in block **XI**. Activated c-FOS of STAT5 homodimer/c-FOS (p_{38}) binds to the TRE sequences (p_{37}) on DNA which is modeled as an association reaction. Followed transcription and translation are modeled by transition t_{50} and corresponding

gene products are modeled by place p_{40} connecting to sink transition t_{51} indicating the natural degradation to the system environment (see block **XII. Production/Degradation** in Fig. 3.4).

In this way, modeling of IL-3 signaling pathway can be done according to simple modeling rules or by connecting the reaction types listed in Fig. 3.4. Table 3.1 summarizes the biological interpretation of each transition used in Petri net model of IL-3 signaling pathway.

Table 3.1: Biological interpretation of each transition in Fig. 3.20.

Transition	Reaction type	Biological interpretation
$t_0, t_1, t_3, t_7, t_8, t_{13}, t_{16}, t_{17}, t_{23}, t_{25}, t_{27}, t_{32}, t_{34}, t_{37}, t_{42}, t_{49}$	XII. Production/Degradation	The substances represented by output places transitions attend the reactions from system environment
t_5	III. Autophosphorylation	Autophosphorylation after binding of a ligand to a receptor with protein kinase activity
t_6	IV. Activation Response by Active Site(s)	The activation of JAK-STAT and/or Ras-MAPK signaling pathways depending on distinct functional domain of activated ligand-receptor complex
t_{44}, t_{45}	VII. Homodimerization	Polymerization reaction of some identical substances to shape a multimer
$t_2, t_4, t_{30}, t_{47}, t_{50}$	I. Association	Association reaction with the binding to induce the formation of a complex
$t_{11}, t_{12}, t_{15}, t_{20}, t_{22}, t_{24}, t_{28}, t_{35}, t_{38}, t_{40}, t_{48}$	XI. Enzymic reaction	Substrates are catalyzed to the productions; there occurs no consumption in biochemical reactions
$t_9, t_{10}, t_{14}, t_{18}, t_{19}, t_{21}, t_{26}, t_{29}, t_{31}, t_{33}, t_{36}, t_{39}, t_{43}, t_{46}, t_{52}$	XII. Production/Degradation	Natural degradation of substances
t_{41}	VIII. Translocation	The movement action of substances from cytoplasm to nucleus
t_{51}	Transcription and Translation	Transcription and Translation after the binding to a certain sequence on DNA

3.2.2 Fas-induced Apoptosis

In this subsection, we use the example of apoptosis to demonstrate our modeling method.

Apoptosis, a form of cell death characterized by cell shrinkage, membrane blebbing, nuclear breakdown, and DNA fragmentation, is a vital cell lifecycle decision point for development, maintenance of tissue homeostasis, and elimination of harmful cells in metazoan organisms [32, 57].

Caspases (cysteine-aspartic-acid-proteases) are a group of cysteine proteases existing as inactive zymogens that can be cleaved by other proteins within the cell resulting in the apoptotic process. Failure of apoptosis is one of the main contributions to tumor development and autoimmune diseases such as neurodegenerative diseases, AIDS and ischemic stroke [78]. Different cellular signals can initiate activation of apoptosis on different ways in dependence of the various kinds and biological states of cells. Fas-induced apoptosis has been studied in detail and its mechanism has been proposed. Fas ligand is a type II transmembrane protein belonging to TNF family, which signals apoptotic effects to nucleus through several major pathways as shown in Fig. 3.19.

Fas ligands, existing as trimers, bind to Fas receptor and promote receptor trimerization. Adaptor proteins FADD in turn associate with the receptors through an interaction between homologous death domain (DD) on the receptor and FADD. Furthermore, FADD contains death effector domain (DED) that allows binding of procaspase-8 to the receptor complex to form a death inducing signaling complex (DISC) [70, 81]. Upon the association with FADD through DED, procaspase-8 is autocatalytically activated to produce caspase-8. The activation of caspase-8 initiates the following two pathways (1) and (2) leading to the activation of downstream caspases.

(1) caspase-8 activates downstream caspases indirectly by cleaving Bcl-2 interacting protein (Bid) and COOH-terminal part of Bid (tBid) translocates onto mitochondria

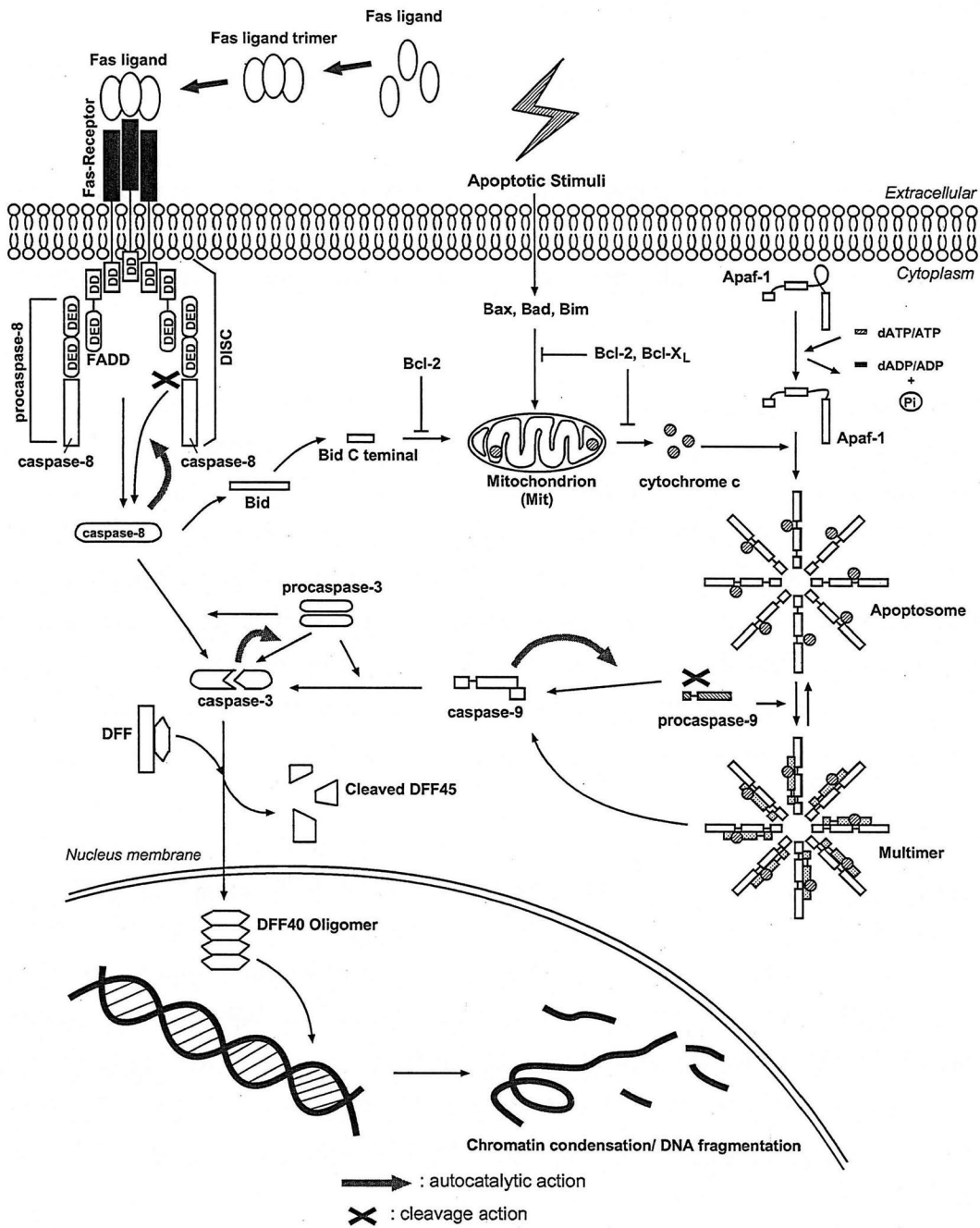


Fig. 3.19: Biological diagram of apoptosis pathways induced by Fas ligands.

(Mit for short) where it makes cytochrome c leak out and enter the cytosol. Released cytochrome c binds to apoptotic protease activating factor-1 (Apaf-1) together with dATP/ATP and procaspase-9 and achieve the caspase-9 activation based on three-step reactions as illustrated in Fig. 3.19 [30, 43, 86]:

- (i) dATP/ATP binds to Apaf-1 and is hydrolyzed to dADP or ADP, respectively;
- (ii) cytochrome c binds to Apaf-1 and promotes the multimerization of Apaf-1/cytochrome c complex, forming a so-called apoptosome made of at least eight subunits when dATP/ATP bound to Apaf-1 is hydrolyzed;
- (iii) Once apoptosome is formed, procaspase-9 is recruited to apoptosome, and it becomes activated through autocatalysis.

Activated caspase-9 releases from apoptosome to cleave downstream caspases such as caspase-3, and new procaspase-9 is activated through autocatalysis by either apoptosome or fresh activated caspase-9 [44].

(2) caspase-8 activates downstream caspases such as caspases-3 by directly cleaving them.

Activated caspase-3 cleaves DNA fragmentation factor (DFF) composed of 45kDa (DFF45) and 40kDa (DFF40) subunits. Cleaved DFF45 dissociates from DFF40, accompanied by DFF40 homo-oligomer formation that possess DNase activity [68, 83]. Finally, DFF40 oligomer induces DNA fragmentation and chromatin condensation that is regarded as an apoptotic hallmark.

Figure 3.20 shows the whole Petri net model of Fas induced apoptosis based on our modeling rules. The modeling operation starts from the source transition t_1 denoting an activity that the substances take part in reactions. Here we only explain the case of the pathway whose caspases are directly cleaved by caspase-8 (p_{10}) to trigger DNA damage: Fas ligands and corresponding receptor are assigned to places (p_1 and p_3) connected from the source transitions (t_1 and t_3) respectively, in accordance with block **XII** of Fig. 3.4. Since three Fas ligands shape a Fas ligand trimer, a transition t_2 is used to represent polymerization connecting from the input place p_1 with a 3-weighted arc $e(p_1, t_2)$ as well as connecting to the output place p_2 of Fas ligands trimer applying the block **VII** in Fig. 3.4. Next, the ligand-receptor

binding interaction occurs and corresponding Petri net model that two places (p_2 and p_3) merge into a place p_4 denoting ligand-receptor complex via the transition t_4 represents association reaction. Succeedent reactions for the production of intermediate products: ligand-receptor/FADD complex (p_6) and DISC (p_8) are modeled in the same way using both of block I, i.e. association reaction. procaspase-8 (p_7) contained in DISC (p_8) is autocatalytically cleaved to produce caspase-8 (p_{10}) which is modeled as a dissociation reaction **X** represented by t_9 . Since caspase-8 (p_{10}) next initiates the activation of downstream caspases and there occurs no consumption in the reactions, caspase-8 (p_{10}) is modeled to enzyme place with a self-loop to take part in four enzymic reactions including two autocatalytic activations of new caspase-8, activation of caspase-3 cascades and mitochondrial DNA damage pathways. The reaction that activated caspase-3 catalyzes DFF (p_{34}) to the productions of DFF40 and DFF45, is modeled as an enzymic reaction represented by t_{42} . DFF40 further form a DFF40 homo-oligomer (p_{39}) which applies the reaction model of homodimerization as shown in block **VII** represented by t_{44} . At last, the transition t_{49} is used to model the enzymic reaction where DFF40 oligomer acts as DNase to induce DNA fragmentation whose corresponding place p_{41} connects to sink transition t_{51} indicating the natural degradation to the system environment (see block **XI** and **XII**).

In this way, modeling of apoptosis can be done by connecting the reaction types listed in Fig. 3.4. The biological interpretation for each transition used in this model are summarized in Table 3.2. Note that this model is of no delay time for transitions.

Table 3.2: Biological interpretation of each transition in Fig. 3.20.

Transition	Reaction type	Biological interpretation
$t_1, t_3, t_5, t_7, t_{16}, t_{17}, t_{20}$ $t_{24}, t_{26}, t_{28}, t_{29}, t_{33}, t_{41}, t_{48}$ t_2, t_{32}, t_{44}	XII. Production/Degradation	The substances represented by output places transitions attend the reactions from system environment
$t_4, t_6, t_8, t_{23}, t_{34}$	VII. Homodimerization	Polymerization reaction of some identical substances to shape a multimer
t_9, t_{35}	I. Association	Association reaction with the binding to induce the formation of a complex
$t_{10}, t_{12}, t_{14}, t_{15}, t_{38}, t_{39},$ t_{40}, t_{42}, t_{49}	X. Dissociation	Complexes, substances separate or split into smaller molecules
$t_{11}, t_{13}, t_{18}, t_{30}, t_{31}, t_{36},$ $t_{37}, t_{43}, t_{45}, t_{46}, t_{47}, t_{50}, t_{51}$ t_{19}, t_{22}	XI. Enzymic reaction XII. Production/Degradation	Substrates are catalyzed to the productions; there occurs no consumption in biochemical reactions Natural degradation of substances
t_{21}, t_{25}, t_{27}	VIII. Translocation VI. Chemical reaction	The movement action of substances from cytoplasm to mitochondria membranes The conversion of substances to products by a chemical reaction

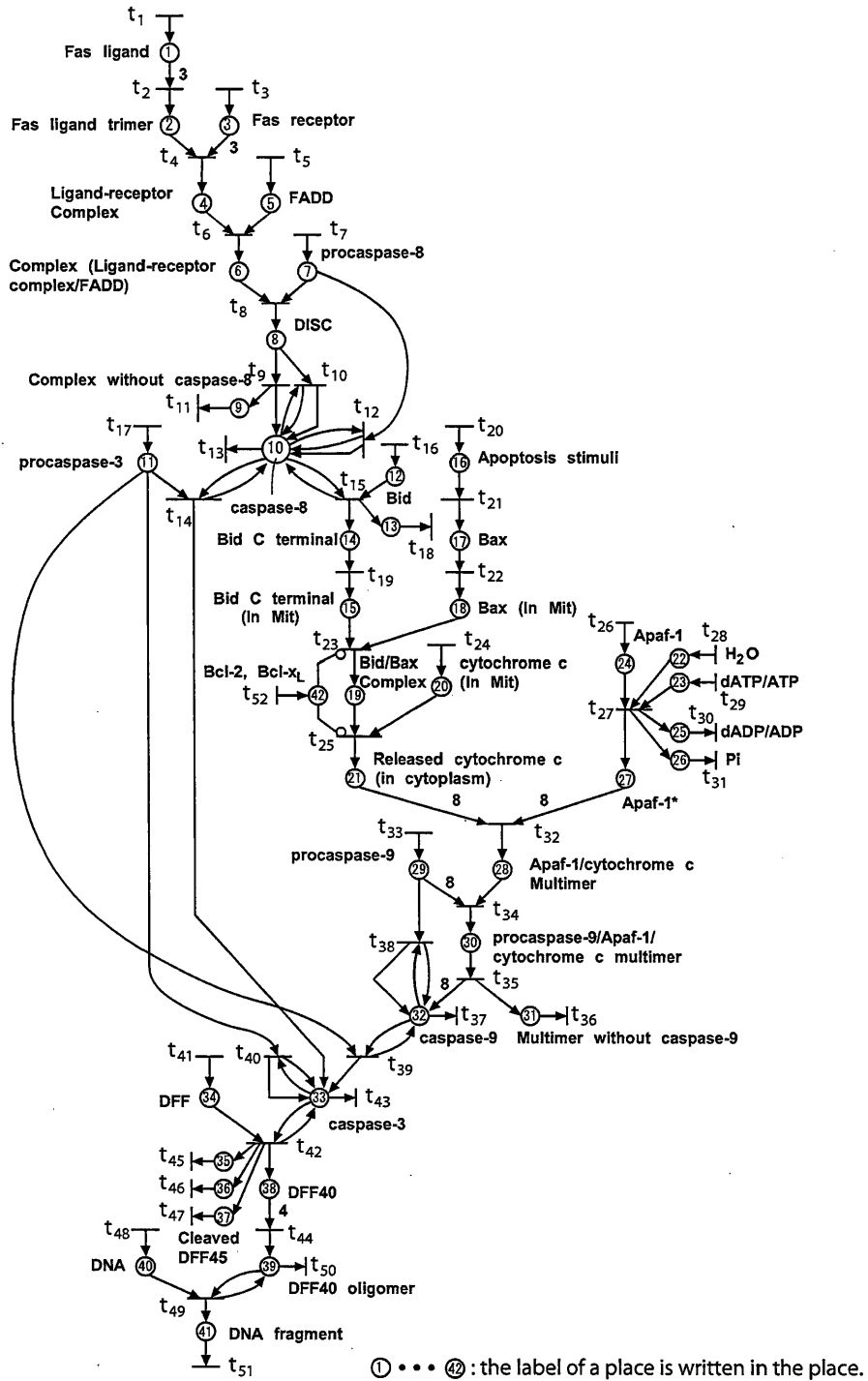


Fig. 3.20: Petri net model without time of figure 3.19.

Structural Analysis of Models

In this chapter, we give structural analyses of modeled signaling pathways based on Petri net theory.

This chapter, firstly presents a brief introduction of elementary flux modes into metabolic pathways that are known to correspond to elementary T-invariants of Petri net. Then, we introduce a new notation “activation transduction and component” to express an enzymic activation process that has an elementary T-invariant in Petri net model as a counterpart. Lastly, we design an algorithm to find such basic systematic components of signaling pathways by calculating a series of elementary T-invariants.

4.1 Analysis of Metabolic Pathways

This section focuses on the formalization and analysis of metabolic pathways using Petri nets. We shows that structural properties of the metabolic pathways can be described by T-invariant, P-invariant, siphon, and trap which exhibit the fundamental behavioral properties of Petri nets.

4.1.1 Metabolic Pathways Overview

Metabolism is the set of chemical reactions that occur in a cell, which enable it to keep living, growing and dividing. Metabolic processes are usually classified as:

- Catabolism: complex molecules are broken down into simpler substances, often resulting in a release of energy and power from nutrients.

- Anabolism: simple substances are synthesized into the complex materials of living tissue, usually through processes that demand energy and reducing power obtained from nutrient catabolism.

Cell metabolism involves extremely complex sequences of controlled chemical reactions called metabolic pathways. In biochemistry, a metabolic pathway consists of a series of chemical reactions occurring within individual cells, catalyzed by enzymes, resulting in either the formation of a metabolic product to be used or stored by the cell, or the initiation of other metabolic pathways. More than 2000 kinds of metabolic reactions have been commonly known, each metabolic reaction is catalyzed by a separate enzyme.

Ideas to use Petri nets for modeling and analyzing metabolic pathways have been popular from the quantitative and qualitative points of view. Two different types of vertices of Petri nets: places and transitions, have the metabolites and reactions as counterparts respectively in metabolic pathways [67]. Further in metabolic pathways, the stoichiometric coefficients described as arc-weights indicate the amounts of substances and products participated in a reaction. Thus, the stoichiometry matrix containing these coefficients corresponds to the incidence matrix of the Petri net if the Petri nets are pure [26]. A token indicates the presence or absence of a condition, a signal, or a resource. The number of tokens stands for the number of molecules of the existing metabolite. These modeling rules has been employed as standard formulating patterns in modeling metabolic pathways so far [24, 27, 40, 80, 85].

So far, besides the attempts to represent systems of metabolic pathways by setting up differential equations to investigate dynamics of concentration change in metabolites, the modeling using linear algebraic equations has also been launched under the assumption that the metabolites have reached a dynamic concentration equilibrium (steady state) due to the augmentation of the number of speed parameters.

In the following subsection, we use Petri nets for the qualitative analysis of metabolic pathways rather than for the analysis of dynamic behaviors. In particular, we discuss the structural attribute of metabolic pathways.

4.1.2 Elementary Flux Mode of Metabolic Pathways

Schuster et al. [72, 73] have proposed a concept of *elementary flux mode* (elementary mode or EM for short) developed from convex analysis to accurately reflect complete behaviors of a metabolic pathway with a set of linear paths. Elementary modes, which were defined as a minimal set of enzymes that could operate at steady state with all irreversible reactions proceeding in the appropriate direction, provide a mathematical tool to define and describe all metabolic routes. That is, for elementary modes, any disturbance to one enzyme belonging to this minimal set will result in a cessation of any flowing and a disruption of a dynamic concentration equilibrium of metabolites in the system [72, 73]. This allows detection of the full set of nondecomposable steady-state flows that the network can support, including cyclic flows. Any steady-state flux pattern can be expressed as a non-negative linear combination of these modes to form a unique set.

For example, Fig. 4.1 shows a metabolic network of chemical reactions. Metabolites are classified internal or external according to whether or not they fulfill the steady-state condition. In other words, the total rate of production of each internal metabolite equals the total rate of its consumption. In contrast, external metabolites (which are called sources and sinks) do not fulfill this condition because they participate in additional reactions that are not involved in the system under study.

In Fig. 4.1, V_1, \dots, V_7 denote enzymes; IM_1, \dots, IM_4 denote internal metabolic products; and EM_1, \dots, EM_3 denote external metabolites where EM_1 is source and EM_3 is sink. The flux V_1, V_4, V_7 between the cells and the systems are measured to be 10, 3, and 7 respectively. That is, the total rate of the consumption EM_1 is 10 and the rate of production of each internal metabolite (EM_2 and EM_3) is 3 and 7 as a result, because the systems fulfill the steady-state condition. Figures 4.2, 4.3, and 4.4 show all the elementary modes according to the algorithm proposed by *Schuster et al.* [72, 73]. Arc-weight in each figure shows the flux that the enzymes need to carry for the mode to function. In this example, the metabolic network can be decomposed

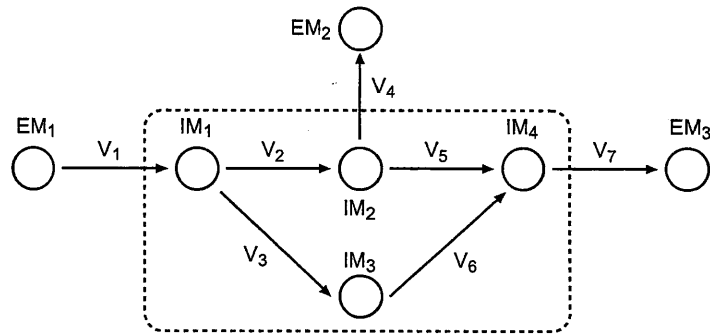


Fig. 4.1: A simple metabolic network of chemical reactions.

as $\alpha e_1 + \beta e_2 + \gamma e_3$ with e_1, e_2 and e_3 denoting three modes, and α, β and γ denoting positive coefficients because any flux pattern is a superposition of elementary modes with non-negative coefficients.

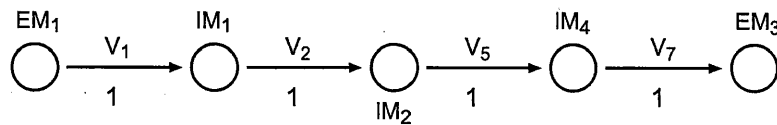


Fig. 4.2: Elementary mode 1 of Fig. 4.1.

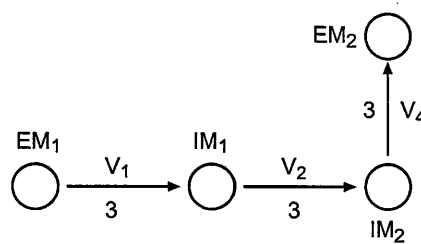


Fig. 4.3: Elementary mode 2 of Fig. 4.1.

It is interesting to note the relationship between elementary flux modes and elementary T-invariants of Petri net [85, 74]. Zevedei-Oancea *et al.* have found and

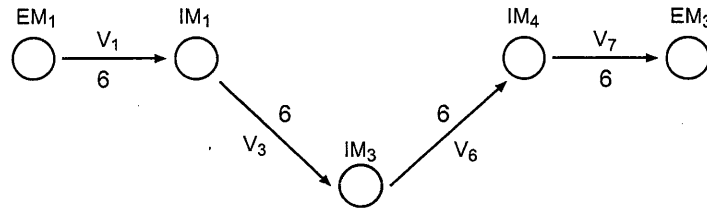


Fig. 4.4: Elementary mode 3 of Fig. 4.1.

discussed the other similarities between metabolic pathways and Petri net theory that elementary mode [72] corresponds to elementary T-invariants [85]. In the reference [80], elementary modes have been discussed to show the correspondence of elementary T-invariants to Petri nets. Further, Voss *et al.* have calculated elementary T-invariant from Petri nets that model glycolytic pathway and pentose phosphate pathway with showing the process to discover elementary modes using high-level Petri nets. Part of monosaccharide metabolism is used here for illustrating the relationship between elementary modes and elementary T-invariants.

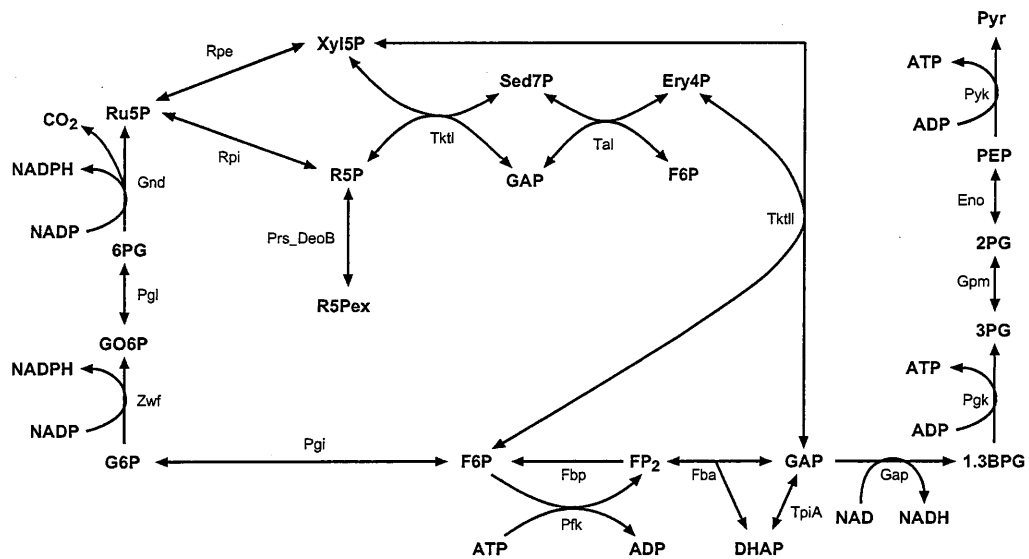


Fig. 4.5: Part of monosaccharide metabolism.

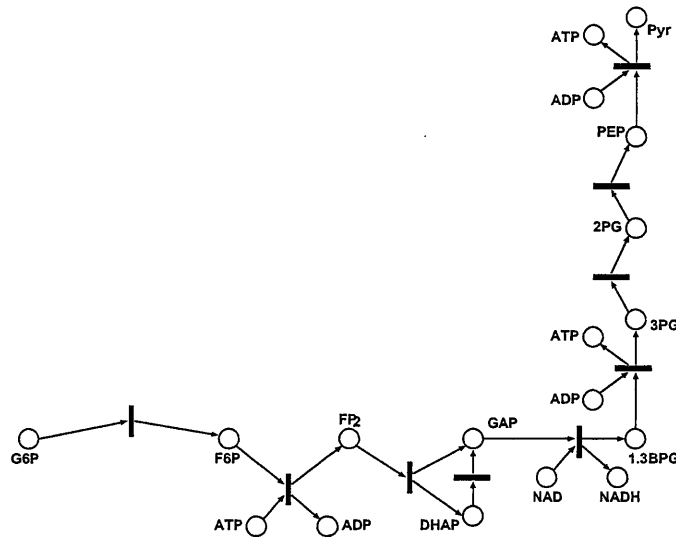


Fig. 4.7: Petri net model of one of the elementary modes.

In the reference [72], it has been discussed that there are 13 elementary modes in monosaccharide metabolism. Here we only give one of the elementary modes modeled as shown in Fig. 4.7 as an example.

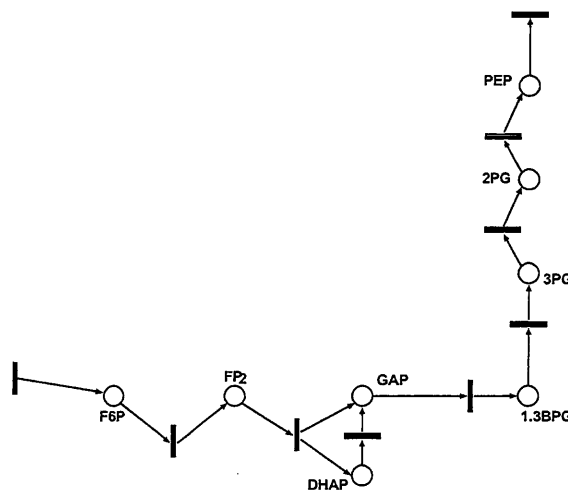


Fig. 4.8: The Petri net model removing the place representing external substances in Fig. 4.7.

We neglect the place denoting external substances in Fig. 4.7, because apart from the external substances (Pyr, NADH, Pi, ADP, ATP, G6P), internal substances have reached a dynamic concentration equilibrium (steady state). The Petri net model (see Fig. 4.8) without the places of external substances is exactly a corresponding net of an elementary T-invariant. This is because (1) each transition in the model fires as many times as the T-invariant indicated, the initial marking will be restored, i.e. the elementary mode always behaves periodically, and (2) it has no any other behavior except (1), i.e. the elementary mode cannot be decomposed furthermore. Therefore, elementary mode corresponds to elementary T-invariant of Petri net.

4.1.3 Other Analyses of Metabolic Pathways with Petri Nets

In 2003, Zevedei-Oancea *et al.* have found and discussed the other similarities between metabolic pathways and Petri net theory that conservation relations correspond to elementary and P-invariants [85]. In [80], elementary P-invariants have been calculated to represent the preservation law for the amounts of all metabolites in the system by Voss *et al.*, i.e. a positive linear combination of all concentrations (token numbers in Petri nets) is constant in time.

Moreover, the concepts of traps, siphon, deadlock and liveness have been considered to reveal some properties of metabolic pathways by Zevedei-Oancea *et al.*. They have revealed that

- (1) a trap is such a set of places corresponding to storage metabolites steadily increased during growth of an organism;
- (2) a siphon is such a set of places corresponding to storage metabolites gradually decreased during starvation;
- (3) the check for deadlock helps to determine whether a biochemical pathway can reach a false equilibrium where it is blocked;
- (4) the liveness of a system indicates that all transitions are able to fire infinitely.

They have also presented an example of *Trypanosoma brucei* metabolism to

detect siphons and traps for validation of their consideration.

Heiner, Koch and Voss have proposed a method for applying high-level Petri net to design and qualitatively analyze metabolic steady state models [80]. They have used colored Petri net with individual tokens which offers the possibility to distinguish the metabolites to detect and further give the interpretation of invariants.

As for intracellular interaction pathways, there also exist signaling pathways besides metabolic pathways. As we have stated above, the metabolic pathways can be described by elementary modes, in the following, we will inquire the characteristic behaviors of signaling pathways.

4.2 Characterizing Signaling Pathways

A signaling pathway is a set of chains of intracellular signaling events which starts by attaching ligands at receptors and ends by altering target proteins, which are responsible for modifying the behaviors of a cell. These signaling events are mediated by intracellular signaling proteins (enzymes as usual) that relay the signal into the cell by activating the next enzyme from inactive state to active state on receipt of signal in the chain.

4.2.1 Signal Propagation of Signaling Pathways

Many of the enzymes controlled by reactions such as phosphorylation are enzymes themselves. In the enzymic cascades, an enzyme activated by phosphorylation phosphorylates the next enzyme in sequence. That is, the signal in signaling pathways propagates itself in the form of a series of chains consisting of sequential enzymic activation processes where a certain protein changes from “inactivate” state to “activate” state depending on the function of an upstream enzyme. Therefore, it is important to inquire into the behaviors of sequential enzymic activation processes of signaling pathways.

4.2.2 Activation Transduction Component and Elementary T-invariant

We call a set of reactions and related substances that make an enzyme active as *activation transduction component*. Figure 4.9 (a) shows an activation transduction component of Ras activity regulation mechanism for enzyme Ras-GTP. Modeling this activation transduction component according to our modeling rules, it is clear that the activation transduction component corresponds to a subnet in which there is a T-invariant.

As we have mentioned, T-invariant is expressed by a vector and if each transition fires as many times as the vector indicates, the initial marking will be restored. In

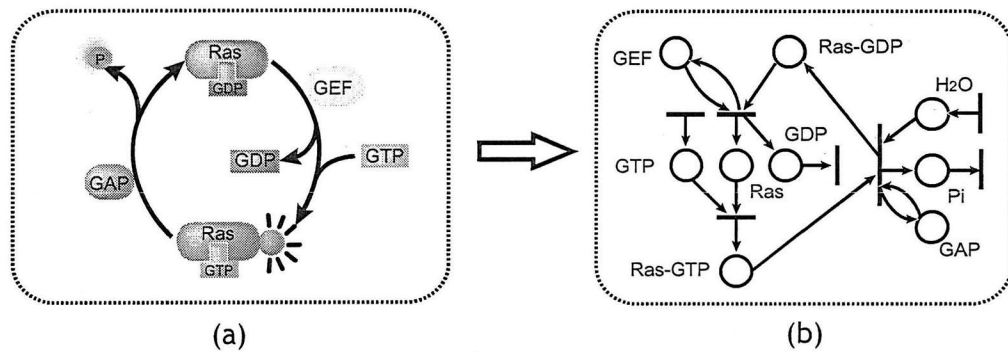


Fig. 4.9: The association between activation transduction component and elementary T-invariant with mapping a pathway to a Petri net model. (a) Activation transduction component of Ras activity regulation mechanism. (b) A Petri net model of (a) corresponding to a subnet of an elementary T-invariant.

Petri net modeled systems, a periodic behavior is represented by a T-invariant J and the corresponding net is such one N_J generated by T_J . This net N_J has such features that (i) before and after any firing sequence corresponding to a T-invariant, the tokens on each place in N_J are kept constant, and (ii) all the transitions in N_J take part in the firing sequence. An elementary T-invariant expresses fundamental periodic behaviors and is a T-invariant that can not be decomposed by non-negative rational linear combination of the other T-invariants.

In example of Fig.4.9, the Petri net model is exactly a corresponding net of an elementary T-invariant. This is because, (1) an activation transduction component always behaves periodically in order to transmit the signals from the precedent steps to the next as long as tokens on the enzyme place exists and during its process, no token will decrease or increase on any places, and (2) it has no any other behavior except (1), i.e., an activation transduction component can not be decomposed furthermore. Therefore, we can treat activation transduction components as corresponding nets of elementary T-invariants.

4.3 Algorithm to Find Activation Transduction Components

In this section, we show an algorithm to give relations among activation transduction components in signaling pathways in order to clarify how enzymic activation processes occur.

In a Petri net with inhibitor arcs, tokens in the place connected with an inhibitor arc never vary with the firing of the transition connected with the inhibitor arc, and thus we can simply delete the inhibitor arc. Therefore, in our algorithm Petri nets are supposed to have no inhibitor arcs.

We show an algorithm to identify a series of chains consisting of sequential activation transduction components by finding a series of elementary T-invariants from sink transition(s) except the sink transitions of enzyme places. Computation of elementary T-invariants has been studied for decades. Linear programming technique has been taken into account in computing some elementary T-invariants.[17] Based on this, an approach has been done trying to obtain all the elementary T-invariants.[4] An algorithm by repeating pivoting operations has been proposed by Avis *et al.*[5] Fourier-Motzkin method[45] and its improved method[77] are also well-known. In this paper, we adopt the method of Ge *et al.*[16] to compute all the elementary T-invariants of a Petri net by applying LP (Linear Programming) technique. In the reference,[16] Ge *et al.* have proposed an efficient method to generate all the elementary T-invariants by applying LP technique. They have proposed an algorithm **«Searching Basic-Feasible Solution with $x_s > 0$ »** to search all the elementary T-invariants in each of which the element x_s related to transition t_s is always non-zero. Note that the term of basic-feasible solution of LP is a basic solution that satisfies all the constraints. For the details of this algorithm, the readers are suggested to refer to Ref. Ge[16]. In the following, incidence matrix C of PN is supposed to be rewritten as $C \leftarrow C * \frac{1}{\alpha(p_i, t_d)}$ in order to compute elementary

T-invariants, where $\alpha(p_i, t_d) \ll 1$.

«Searching Activation Transduction Components»

- 1° Let PN be a given Petri net, and L_s be a list of sink transitions (except sink output transitions of enzyme places) in PN . Do $SN_J \leftarrow \phi$, $T_{sink} \leftarrow \{t | t \in L_s\}$, $T_{gen} \leftarrow \phi$ and initialize *FIFO* queue $Q \leftarrow \phi$.
- 2° If $Q \neq \phi$, pull a subnet N_{J_i} from Q and do the followings:
 - (i) let P_e and T_e be a set of enzyme places in N_{J_i} and a set of transitions providing tokens to the places of P_e , respectively;
 - (ii) let L_e be a list of transitions in $T_e - T_{gen}$, and do $L_s \leftarrow L_s \cdot L_e$, $T_{gen} \leftarrow T_{gen} \cup T_e$ and $PROV(N_{J_i}) = \{t | t \in T_e\}$.
- 3° If $L_s = \phi$ go to 4°, otherwise take out a transition t from the beginning of L_s and do $gen(t) \leftarrow \phi$. Obtain all the elementary T-invariants $\{J_i\}$ with $J_i(t) > 0$ by applying **«Searching Basic-Feasible Solution with $x_s > 0$ »**[16]. For each J_i , do the followings:
 - (i) obtain its corresponding subnet N_{J_i} (generated by the support T_{J_i} of J_i);
 - (ii) do $gen(t) \leftarrow gen(t) \cup \{N_{J_i}\}$;
 - (iii) if $N_{J_i} \notin SN_J$ is satisfied, then $SN_J \leftarrow SN_J \cup \{N_{J_i}\}$ and push N_{J_i} to Q .
- 4° If $Q = \phi$ then output T_{gen} , T_{sink} , $gen(t)$ for $t \in T_{gen} \cup T_{sink}$ and $PROV(N_{J_i})$ for $N_{J_i} \in SN_J$, and stop; otherwise go to 2°. □

In step 1° of the above algorithm, we mainly construct a transition list L_s to be used to search subnet chains (the sequential activation transduction components) from the bottom of the Petri net model, where SN_J denotes a set of subnets to be generated, and T_{gen} and T_{sink} denote the transitions that induce generation of these subnets. In 2°, for an obtained subnet N_{J_i} , we find the transitions T_e that provide tokens to the enzyme places in it, where L_e is used to update L_s and is so constructed as to avoid repeated appearance in L_s , and $PROV(N_{J_i})$ expresses the set of transitions that provide tokens to its enzyme places. In 3°, we compute all the elementary

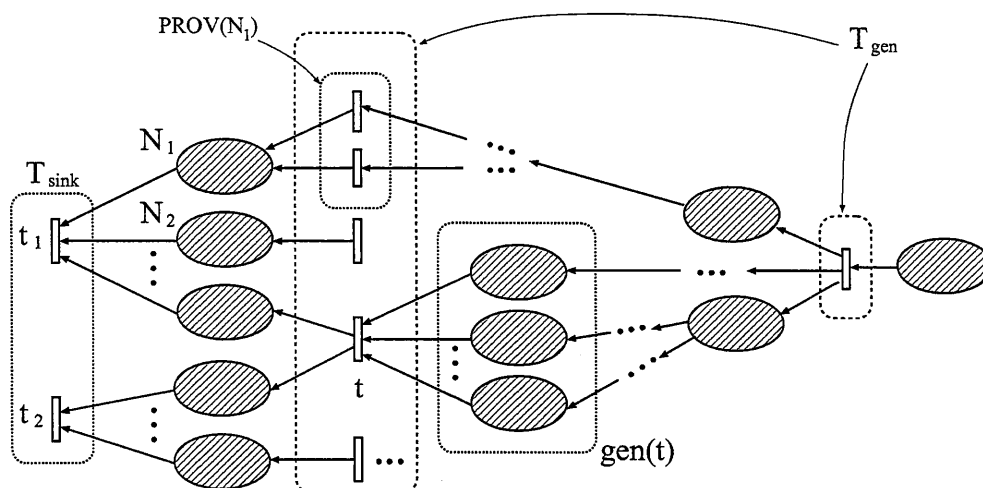


Fig. 4.10: An example of connection relations among subnets.

T-invariants that are determined by a transition t taken out from L_s and get all the corresponding subnets, where $gen(t)$ indicates the subnets derived from the transition t , SN_J is updated by all the obtained subnets. Q is so updated that the subnets pushed to it cannot appear more than once. It is not difficult to confirm that the time complexity to perform the algorithm is $O((|T_{gen}| + |T_{sink}|)(K_m|T||P|^2 + LP_s))$, where $K_m = \max\{|gen(t)| \mid t \in T_{gen} \cup T_{sink}\}$ and LP_s is the time complexity of linear programming.

By applying the following operations to the result of algorithm **«Searching Activation Transduction Components»**, $gen(t)$ and $PROV(N_{J_i})$, we can schematize the connection relations between the subnets that correspond to activation transduction components in signaling pathways.

- (1) Do $T_s \leftarrow T_{sink}$. For each $t \in T_s$, do $SN \leftarrow gen(t)$ and draw arrows from all subnets in SN to t . Do $T_s \leftarrow \phi$.
- (2) For each subnet $N \in SN$, do the followings:
 - (i) do $T'_s \leftarrow PROV(N)$, $T_s \leftarrow T_s \cup T'_s$;
 - (ii) for each $t \in T'_s$, draw arrows from t to N .

- (3) Do $SN \leftarrow \phi$. For each $t \in T_s$, do the followings:
 - (i) do $SN' \leftarrow gen(t)$ and $SN \leftarrow SN \cup SN'$;
 - (ii) for each $N \in SN'$, draw arrows from N to t .
- (4) Do $T_s \leftarrow \phi$. If $SN \neq \phi$ goto (2); otherwise stop.

Figure 4.3 illustrates an example of connection relations among subnets by doing the above operations. Note that hollow rectangle transitions denote the transitions in T_{sink} and T_{gen} to show the relationship between transitions and subnets.

4.4 An Example – TPO Signaling Pathways

In this section, we give examples to demonstrate our modeling and analyzing method.

The example is the signaling pathway mediated by thrombopoietin (TPO for short) that is a cytokine regulating hematogenesis and production of hematoblast. TPO signals its growth regulating effects to the cell through several major pathways including JAK/Stat, MAPK as shown in Fig.4.11.[18, 71, 2]

- (1) Tyrosine phosphorylation of Jak2 in membrane proximal domain of TPO receptor activates JAK/Stat pathways consisting of the activation of STATs, STATs' homo- and hetero- dimerization, translocating to nucleus, where they modulate expression of target genes.
- (2) Ras-MAPK pathways are activated by recruiting Shc in a membrane distal domain of TPO receptor. Grb2 is activated as an adaptor protein by binding to Shc and triggers subsequent activations of Sos, Ras, Raf-1, MEK, ERK, and RSK. Activated RSK translocates to nucleus and activates CREB that will bind to specific area of DNA to promote the transcription of genes.

We model the TPO signaling pathway to a Petri net model as shown in Fig.4.12 based on the modeling rules, whose incidence matrix C is rewritten to an integer matrix as follows:

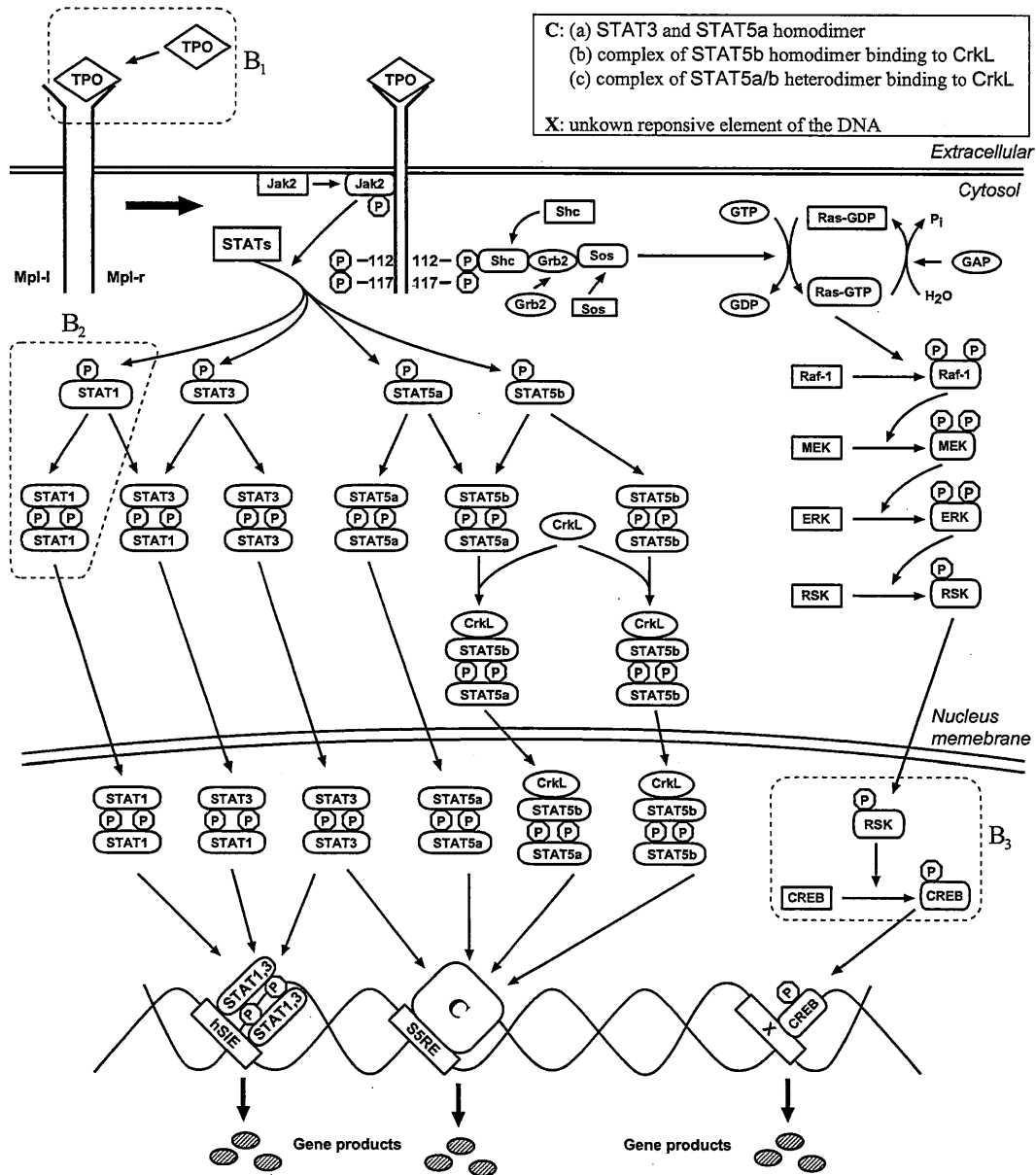


Fig. 4.11: TPO signaling pathway. The parts B₁, B₂ and B₃ surrounded by dashed lines are the three reaction examples, reactions of association, homodimerization and enzymic activation, which are the blocks I, VII and XI of Fig.3.4, respectively. Corresponding Petri net models of B₁, B₂ and B₃ are given in Fig.4.12 by the dashed-line-surrounded parts B'₁, B'₂ and B'₃, respectively.

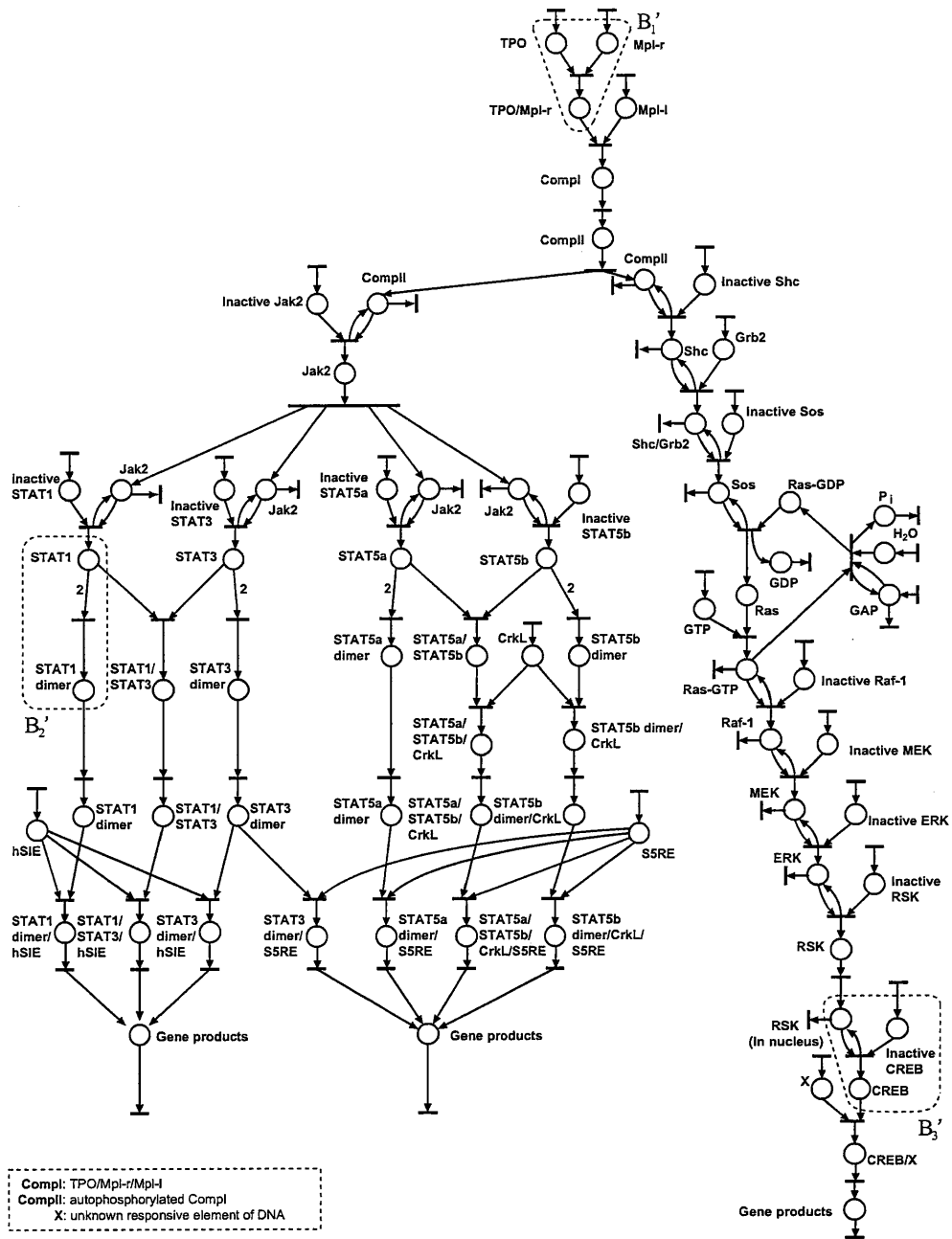


Fig. 4.12: Petri net model of the TPO signaling pathway shown in Fig. 4.11. Parts B₁′, B₂′ and B₃′ correspond to B₁, B₂ and B₃ of Fig.4.11, respectively. B₂′ reflects the complex formation of STAT1 making a homodimer from two monomers, and so the arc-weight is set to 2.

$$C = \begin{pmatrix} -2 & 0 & \cdots & 0 & \cdots & 0 & 0 \\ 0 & 2 & \cdots & 0 & \cdots & 0 & 0 \\ \vdots & \vdots & \vdots & \ddots & \vdots & \vdots & \vdots \\ 0 & 0 & \cdots & 0 & \cdots & -2 & 2 \\ 0 & 0 & \cdots & 0 & \cdots & 0 & -2 \end{pmatrix}$$

Note that, $\alpha(p_i, t_d)$ of the example is set to 0.5. In the following, we demonstrate how the algorithm is carried out.

First, we do step 1°, i.e., $L_s \leftarrow t_{20} \cdot t_{39} \cdot t_{95}$, $SN_J \leftarrow \phi$, $T_{sink} \leftarrow \{t_{20}, t_{39}, t_{95}\}$, $T_{gen} \leftarrow \phi$ and $Q \leftarrow \phi$. Then do 2°, $Q = \phi$ does not satisfy the condition $Q \neq \phi$ and goto 3°. Do 3°, since $L_s \neq \phi$ is not satisfied, take out a transition $t = t_{20}$ from the beginning of L_s . Then do $gen(t_{20}) \leftarrow \phi$ and $CJ_i = 0$ with $J_i(t_{20}) > 0$ by applying **«Searching Basic-Feasible Solution with $x_s > 0$ »**,

$$\begin{pmatrix} -2 & 0 & \cdots & 0 & \cdots & 0 & 0 \\ 0 & 2 & \cdots & 0 & \cdots & 0 & 0 \\ \vdots & \vdots & \vdots & \ddots & \vdots & \vdots & \vdots \\ 0 & 0 & \cdots & 0 & \cdots & -2 & 2 \\ 0 & 0 & \cdots & 0 & \cdots & 0 & -2 \end{pmatrix} \begin{pmatrix} x_1 \\ x_2 \\ x_3 \\ \vdots \\ x_{93} \\ x_{94} \\ x_{95} \end{pmatrix} = \begin{pmatrix} 0 \\ \vdots \\ 0 \end{pmatrix}$$

$$x_1, x_2, \dots, x_{94}, x_{95} \geq 0.$$

and obtain the elementary T-invariants $\{J_1, J_2, J_3\}$ as shown in Fig.4.13. The table in Fig.4.13 summarizes all elementary T-invariants of Petri net in Fig.4.12, in which we only show the non-zero transitions due to the space limitation. For each elementary T-invariant, do the followings (here, we only explain the case of J_1): (i) obtain corresponding subnet N_{J_1} ; (ii) do $gen(t_{20}) \leftarrow \{N_{J_1}\}$; (iii) since $N_{J_1} \notin SN_J$ is satisfied, do $SN_J \leftarrow \{N_{J_1}\}$ and push N_{J_1} to Q . In 4°, $Q \neq \phi$ does not satisfy $Q = \phi$ and go to 2°. In 2°, since $Q \neq \phi$ satisfies the condition, pull a subnet N_{J_1} from Q and do the followings: (i) $P_e \leftarrow \{p_{11}\}$, $T_e \leftarrow \{t_{11}\}$; (ii) do $L_s \leftarrow t_{39} \cdot t_{95} \cdot t_{11}$, $T_{gen} \leftarrow \{t_{11}\}$ and $PROV(N_{J_1}) =$

J_1	t_1	t_{12}	t_{14}	t_{15}	t_{16}	t_{17}	t_{18}	t_{19}	t_{20}											t_{95}					
	----	2	--	2	1	1	1	1	1	1															
J_2		t_{12}	t_{14}		t_{17}	t_{20}	t_{21}	t_{22}	t_{23}	t_{24}	t_{25}	t_{27}													
	----	1	--	1	----	1	----	1	1	1	1	1	1	1	1	1	1	1	1	1	1				
J_3					t_{17}	t_{20}			t_{25}	t_{27}	t_{28}	t_{29}	t_{30}	t_{31}											
	----				1	1	----		2	--	2	1	1	1	1	1	1	1	1	1	1				
J_4									t_{25}	t_{27}	t_{28}	t_{29}		t_{37}	t_{38}	t_{39}	t_{54}								
	----								2	--	2	1	1	----	1	1	1	----	1	----	1				
J_5		t_{32}	t_{34}	t_{35}	t_{36}	t_{39}	t_{40}	t_{41}		t_{54}															
	----	2	--	2	1	1	1	1	----	1	1	1	1	1	1	1	1	1	1	1	1				
J_6		t_{32}	t_{34}		t_{39}	t_{42}	t_{43}	t_{44}	t_{45}	t_{46}	t_{47}	t_{49}	t_{50}	t_{54}											
	----	1	--	1	----	1	1	1	1	1	1	1	1	1	1	1	1	1	1	1	1				
J_7					t_{39}				t_{47}	t_{49}	t_{50}	t_{51}	t_{52}	t_{53}	t_{54}	t_{55}	t_{56}								
	----				1	----			1	--	2	2	1	1	1	1	1	1	1	1	1				
J_8																				t_{89}	t_{91}	t_{92}	t_{93}	t_{94}	t_{95}
	----																			1	--	1	1	1	1
J_9		t_8	t_{10}	t_{11}	t_{13}	t_{26}	t_{33}	t_{48}																	
	----	1	--	1	1	--	2	----	2	----	2	----	2	----	2	----	2	----	2	----	2	----	2	----	2
J_{10}																				t_{84}	t_{87}	t_{88}	t_{90}		
	----																			1	--	1	1	1	2
J_{11}		t_1	t_2	t_3	t_4	t_5	t_6	t_7	t_9					t_{58}											
	1	1	1	1	1	1	1	1	--	2					2										
J_{12}															t_{81}	t_{85}	t_{86}								
	----														1	----	1	2	----						
J_{13}															t_{78}	t_{82}	t_{83}								
	----														1	----	1	2	----						
J_{14}															t_{75}	t_{79}	t_{80}								
	----														1	----	1	2	----						
J_{15}															t_{67}	t_{68}	t_{69}	t_{70}	t_{73}	t_{74}	t_{76}				
	----														1	1	1	1	----	1	1	--	1	----	1
J_{16}															t_{63}	t_{65}	t_{66}								
	----														1	----	1	2	----						
J_{17}															t_{71}	t_{72}									
	----														1	1	----								
J_{18}															t_{60}	t_{62}	t_{64}								
	----														1	--	1	--	2	----					
J_{19}															t_{57}	t_{59}	t_{61}								
	----														1	--	1	--	2	----					

..... : 0 . . . 0

Fig. 4.13: All elementary T-invariants of the Petri net in Fig.4.12.

$\{t_{11}\}$. Do 3°, since $L_s = \phi$ is not satisfied, take out $t = t_{39}$ from L_s and do $gen(t_{39}) \leftarrow \phi$. Obtain all the elementary T-invariants $\{J_4, J_5, J_6, J_7\}$, corresponding subnets $\{N_{J_4}, N_{J_5}, N_{J_6}, N_{J_7}\}$, $gen(t_{39}) \leftarrow \{N_{J_4}, N_{J_5}, N_{J_6}, N_{J_7}\}$ and $SN_J \leftarrow \{N_{J_1}, N_{J_2}, N_{J_3}\} \cup \{N_{J_4}, N_{J_5}, N_{J_6}, N_{J_7}\}$. Push $N_{J_4}, N_{J_5}, N_{J_6}, N_{J_7}$ to Q sequentially. In 4°, $Q \neq \phi$ does not satisfy $Q = \phi$ and go to 2°. In this way, do the steps sequentially until $Q = \phi$, then output $T_{gen}, T_{sink}, gen(t)$ for $t \in T_{gen} \cup T_{sink}$ and $PROV(N_{J_i})$ for $N_{J_i} \in SN_J$, and stop the algorithm. All the output of algorithm are shown in Table 4.1, and Fig.4.14 shows all the subnets of Petri net model in Fig.4.12.

By applying the operations proposed above to the results $T_{gen}, T_{sink}, gen(t)$, and $PROV(N_{J_i})$ of algorithm **«Searching Activation Transduction Components»**, we can draw corresponding arcs between subnets and transitions of T_{sink} and T_{gen} . And finally schematize the connection relations between all the subnets that correspond to activation transduction components in signaling pathways as shown Fig.4.15, in which there are 19 subnets $\{N_{J_1}, N_{J_2}, \dots, N_{J_{18}}, N_{J_{19}}\}$ obtained from elementary T-invariants shown in Fig.4.13.

Based on connection relations, each chain consisting of enzymic activation processes can be traced from the source subnets on the right side in Fig.4.15, e.g., searching from the top subnet $N_{J_{11}}$, the transition t_7 in $N_{J_{11}}$ fires to provide tokens to the subnet N_{J_9} and $N_{J_{19}}$, and the ligand-receptor complex (Comp11 for short) is activated. Once the enzyme of Comp11 is activate, the enzyme Shc in $N_{J_{19}}$ will be activated continuously by the firing of transition t_{59} to provide tokens to the subnet $N_{J_{18}}$. Activated enzyme Shc induces the activations of Shc/Grb2, Sos, Ras, Raf-1, MEK, ERK, RSK and CREB in turn by firing corresponding transitions to provide tokens to the subnets. In this way, the chains of enzymic activation processes from the extracellular stimulus to the DNA nucleus can be obtained.

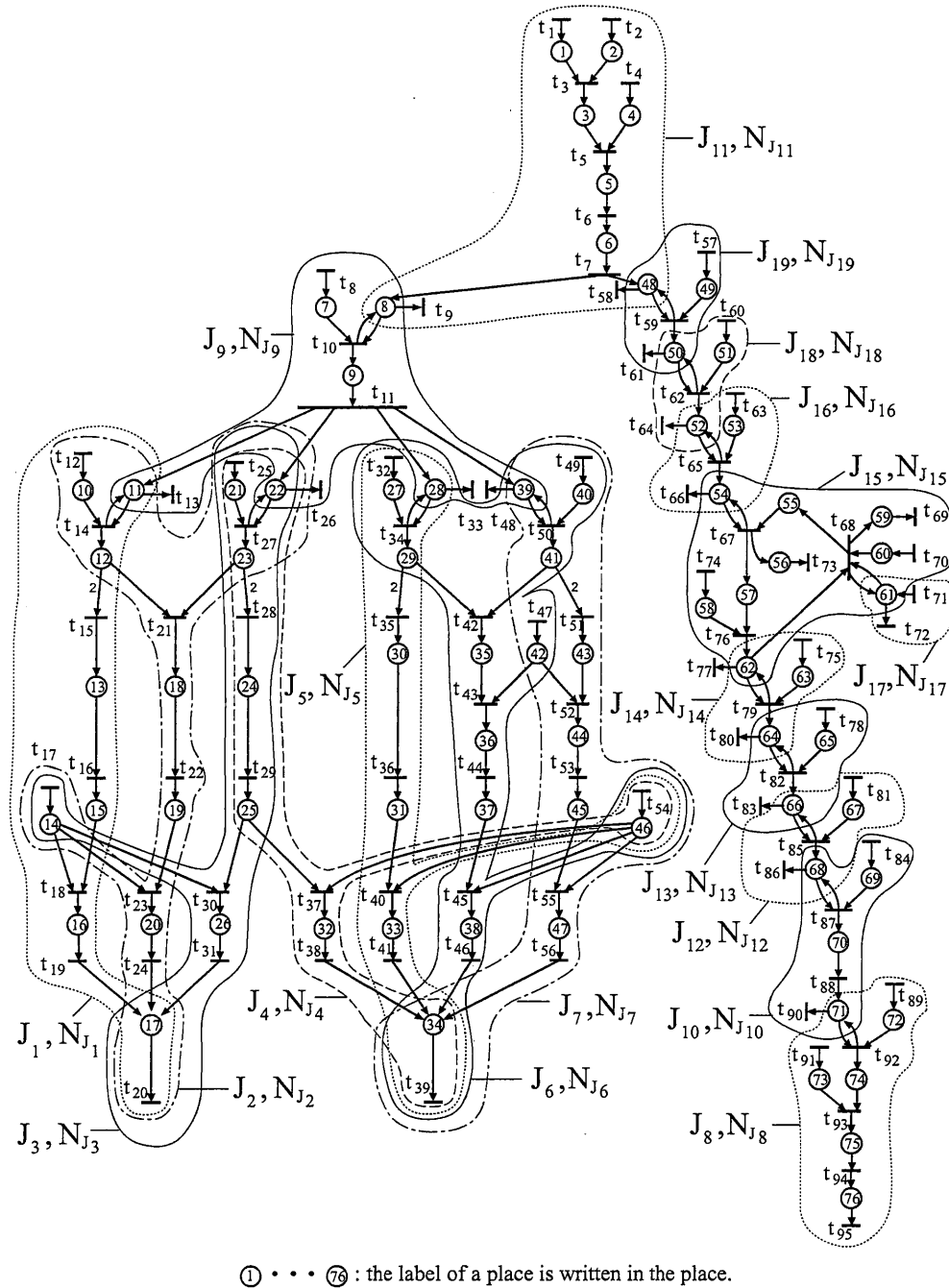


Fig. 4.14: All subnets obtained from elementary T-invariants as shown in Fig.4.13 of Petri net model.

Table 4.1: The results T_{sink} , T_{gen} , $gen(t)$, and $PROV(N_{J_i})$ by performing proposed algorithm.

T_{gen}	$\{t_7, t_{11}, t_{59}, t_{62}, t_{65}, t_{71}, t_{76}, t_{79}, t_{82}, t_{85}, t_{88}\}$		
T_{sink}	$\{t_{20}, t_{39}, t_{95}\}$		
$gen(t_7)$	$\{N_{J_{11}}\}$	$PROV(N_{J_1})$	$\{t_{11}\}$
$gen(t_{11})$	$\{N_{J_9}\}$	$PROV(N_{J_2})$	$\{t_{11}\}$
$gen(t_{20})$	$\{N_{J_1}, N_{J_2}, N_{J_3}\}$	$PROV(N_{J_3})$	$\{t_{11}\}$
$gen(t_{39})$	$\{N_{J_4}, N_{J_5}, N_{J_6}, N_{J_7}\}$	$PROV(N_{J_4})$	$\{t_{11}\}$
$gen(t_{59})$	$\{N_{J_{19}}\}$	$PROV(N_{J_5})$	$\{t_{11}\}$
$gen(t_{62})$	$\{N_{J_{18}}\}$	$PROV(N_{J_6})$	$\{t_{11}\}$
$gen(t_{65})$	$\{N_{J_{16}}\}$	$PROV(N_{J_7})$	$\{t_{11}\}$
$gen(t_{71})$	$\{N_{J_{17}}\}$	$PROV(N_{J_8})$	$\{t_{88}\}$
$gen(t_{76})$	$\{N_{J_{15}}\}$	$PROV(N_{J_9})$	$\{t_7\}$
$gen(t_{79})$	$\{N_{J_{14}}\}$	$PROV(N_{J_{10}})$	$\{t_{85}\}$
$gen(t_{82})$	$\{N_{J_{13}}\}$	$PROV(N_{J_{11}})$	$\{\phi\}$
$gen(t_{85})$	$\{N_{J_{12}}\}$	$PROV(N_{J_{12}})$	$\{t_{82}\}$
$gen(t_{88})$	$\{N_{J_{10}}\}$	$PROV(N_{J_{13}})$	$\{t_{79}\}$
$gen(t_{95})$	$\{N_{J_8}\}$	$PROV(N_{J_{14}})$	$\{t_{76}\}$
		$PROV(N_{J_{15}})$	$\{t_{65}, t_{71}\}$
		$PROV(N_{J_{16}})$	$\{t_{62}\}$
		$PROV(N_{J_{17}})$	$\{\phi\}$
		$PROV(N_{J_{18}})$	$\{t_{59}\}$
		$PROV(N_{J_{19}})$	$\{t_7\}$

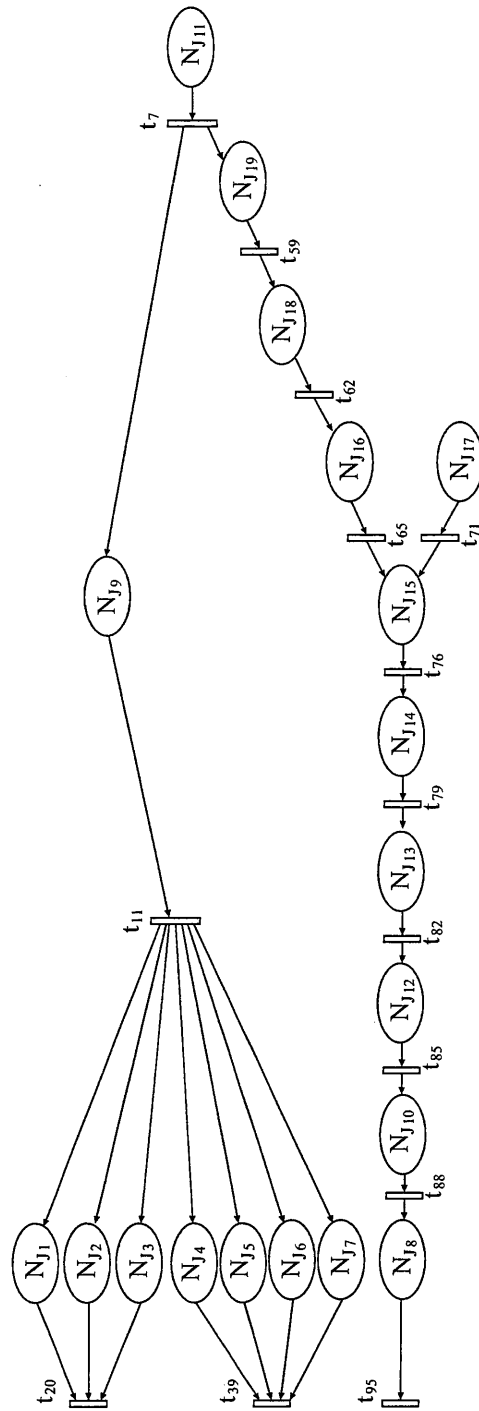


Fig. 4.15: Connection relations between all the subnets corresponding to activation transduction components in TPO signaling pathways.

Simulation with Timed Petri Nets

As described in Chapter 4, the Petri net model illustrated in Fig. 3.20 has been drawn. This model describes the structure of connection relation. The next task we should do is to confirm the validity of the model, that is whether proposed models accord with the biological facts of reactions or not. Therefore, we consider a new simulation method by which (i) the traces of signal transductions can easily be understood; and (ii) the transduction speeds of each pathways leading to cell death can be observed.

5.1 Creating Timed Petri net for pathway simulation

To control the transduction speeds of signals in a pathway, each transition in the Petri net model should have delay time reflecting the speed of corresponding biological reactions. Basic facts for deciding delay time can be obtained from biological experiments and scientific common principles. However, in the majority of cases, reliable data of detailed reactions have not been reported in biological literature. These observations lead us to develop a new method that determines transition speeds with which token flows in the modeled Petri net represent the signal transductions in the original signaling pathways.

[Basic principles]

- (1) The sum of consumption is equal to the production to keep the concentration equilibrium for each substance engaged in signaling pathways, i.e. for each

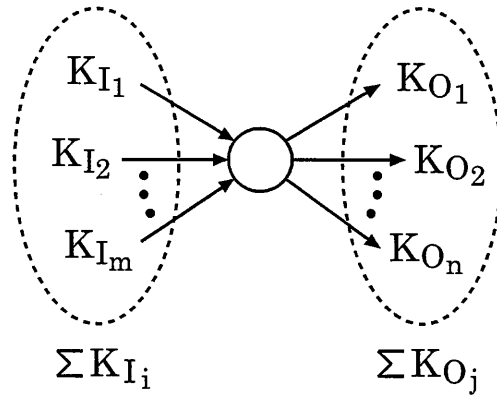


Fig. 5.1: Illustration for [Basic principles] (1).

place the token amounts flowed in and flowed out per unit time are equivalent:

$$\sum_{i=1}^m K_{I_i} = \sum_{j=1}^n K_{O_j} \quad (5.1)$$

$\sum_{i=1}^m K_{I_i}$ and $\sum_{j=1}^n K_{O_j}$ are the total token amounts flowed in and flowed out per unit time, respectively (see Fig. 5.1).

- (2) As defined in section 2.1, delay time d_i is the reciprocal of the maximum of firing frequency f_i , and it is obvious that the token amounts flowed in and flowed out for each place per unit time are expected to be kept equivalent under the fastest firing frequency f_i . Therefore, in this paper we decide d_i by calculating f_i .

Note that, in this paper we suppose that apoptosis pathway is such a biological system that if required substances are assembled, the reactions promptly become possible. Thus, what we have to discuss is how to assign the delay time to each transition in timed Petri net \bar{N} . In the following, we give such delay time determination rules for each transition.

[Strategy for determining transition speeds]

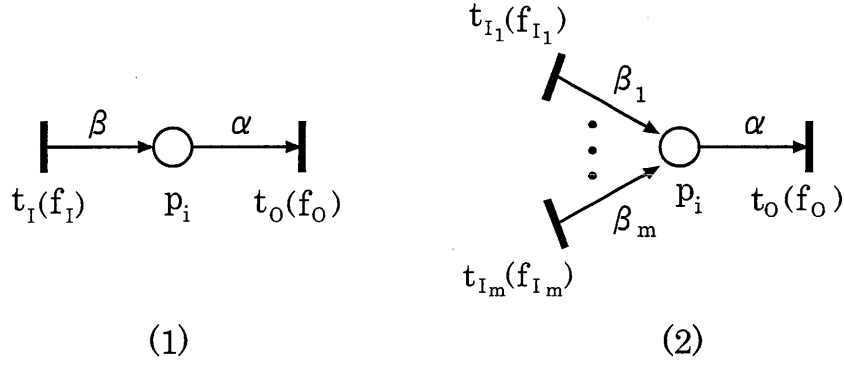


Fig. 5.2: Two connection cases in **Rule (1)**.

Rule (1): if there is such a place p_i that the number of input transitions is one or more while the number of output is one, the maximum of firing frequencies $\{f_i\}$ satisfy the following equation:

$$\sum_{i=1}^m \beta_i \cdot f_{I_i} = \alpha \cdot f_O \quad (5.2)$$

where α and β_i are the weights of arcs $e(p_i, t_O)$ and $e(t_{I_i}, p_i)$, respectively. t_{I_i} and t_O are the input and output transitions of place p_i . Furthermore, f_{I_i} , f_O are the maximum of firing frequencies of t_{I_i} , t_O , respectively (see Fig. 5.2).

Rule (2): if there is a place p_i whose output transitions are in conflict, the maximum of firing frequencies $\{f_i\}$ satisfy following linear equation and inequality:

$$\left\{ \begin{array}{l} \sum_{i=1}^m \beta_i \cdot f_{I_i} = \sum_{j=1}^m \alpha_j \cdot f_{O_j} \\ 2 \cdot \frac{f_{O_n}}{\alpha_n} \geq \frac{f_{O_1}}{\alpha_1} \geq \frac{f_{O_2}}{\alpha_2} \geq \dots \geq \frac{f_{O_n}}{\alpha_n} \end{array} \right. \quad (5.3)$$

where α_j and β_i are the weights of $e(p_i, t_{O_j})$ and $e(t_{I_i}, p_i)$ respectively, and α_j satisfies

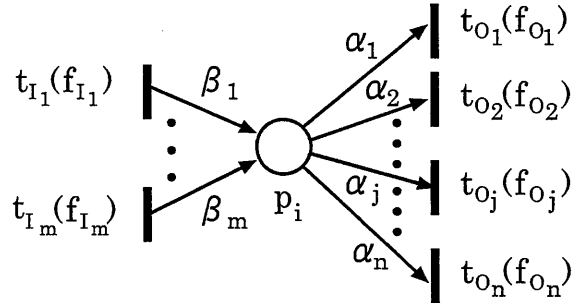


Fig. 5.3: Conflict situation applied to **Rule (2)**. Transitions $t_{O_1}, t_{O_2}, \dots, t_{O_j}, \dots, t_{O_n}$ are in *conflict* since firing either will remove the token from p_i , disabling the other transitions [61].

$\alpha_1 \geq \alpha_2 \geq \dots \geq \alpha_n$. t_{I_i}, t_{O_j} are the input and output transitions of place p_i , and f_{I_i}, f_{O_j} are the maximum of firing frequencies of t_{I_i} and t_{O_j} , respectively as shown in Fig. 5.3.

Rule (3): use a small value as the maximum of firing frequencies to sink transition connected from the enzyme place.

In the above **Rule (1)**, the equation is applied to such a place that has a single output transition. Obviously, this single transition can fire smoothly only according to the delay time. However, in apoptosis Petri net model, there exist the situations that transitions (e.g. t_{14}, t_{39} and t_{40}) are in conflict since firing either will remove the token from the input place disabling the other transitions. As we have stated above, biological experiments for measuring such reactions have not been executed yet in the majority of cases. Therefore, in this paper we assume such enabled transitions in conflict have the same chance to fire. Under this assumption, the first equation of **Rule (2)** is designed to obey **Basic principle (1)**, and the second inequality is considered for two reasons that: (i) the right-hand member $\frac{f_{O_1}}{\alpha_1} \geq \frac{f_{O_2}}{\alpha_2} \geq \dots \geq \frac{f_{O_n}}{\alpha_n}$ is designed to guarantee the firing of t_{O_1} with the maximum arc-weight α_1 that t_{O_1} do not fire later than the firing of t_{O_n} with minimum arc-weight α_n ; (ii) the left-hand member $2 \cdot \frac{f_{O_n}}{\alpha_n} \geq \frac{f_{O_1}}{\alpha_1}$ is in order to make the transition t_{O_1} not fire too fast than the

t_{O_n} that has the minimum arc-weight (make the first firing of t_{O_n} earlier than the second firing of t_{O_1} to be exactly). **Rule (3)** is designed to express the moderately slow and small natural degradation of enzymes.

Furthermore, when using timed Petri net to simulate the apoptosis, the self-loops of enzyme places are replaced by test arcs with threshold due to the attribute that a test arc does not consume any content of the place at the source of the arc by firing. The firing rules are defined as follows:

- (1) When the value of threshold equals 1, nothing need to be done since the transition at the sink of test arc can fire constantly as long as the place at the source of test arc is occupied by tokens;
- (2) When the value of threshold is more than 1, the test arc is handled as general arc and the transition at its sink has to comply with the above rules in order to guarantee the firing of the transition connected from the test arc.

In the following, we demonstrate how our model is practically executed (simulated). The model is simulated by biological pathway simulator – Cell Illustrator (CI) [87].

5.2 Simulation Tools and Simulation Experiments

5.2.1 Biological Pathway Simulation Tools

Cell Illustrator [87] is a simulation tool for modeling and simulation of biological pathways which employs the hybrid functional Petri net with extension (HFPNe) as a basic architecture [9, 54]. Nagasaki *et al.* [55] proposed a new powerful Petri net architecture HFPNe which involves all the functions of existing high-level Petri nets. In other words, each of low-level Petri net, stochastic Petri net, colored Petri net, and hybrid Petri net can be treated as a subset of the HFPNe. Precise definition of the HFPNe as well as relationships with other Petri nets are described in [55]. Figure 5.4 shows a screen shot of Cell Illustrator which displays Huntington's

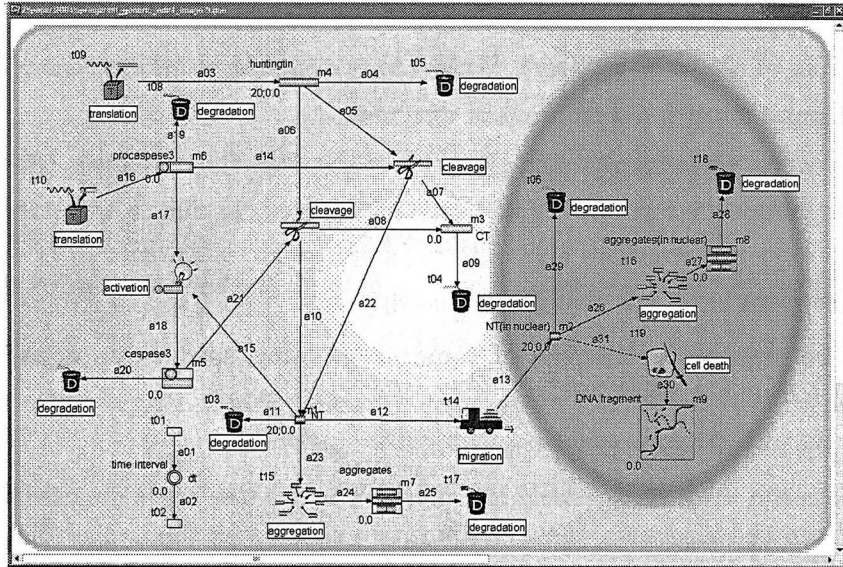


Fig. 5.4: Huntington's disease HFPNe model in the screen shot of Cell Illustrator [56].

disease model with HFPNe. In this figure, Petri net elements of places and transitions have been changed to pictures of biological images which reflect the roles of these elements. These changes make pathway models with HFPNe more familiar to biologists. Figures 5.5, 5.6 show the graphical user interface (GUI) and elements of Petri net used in Cell Illustrator [9].

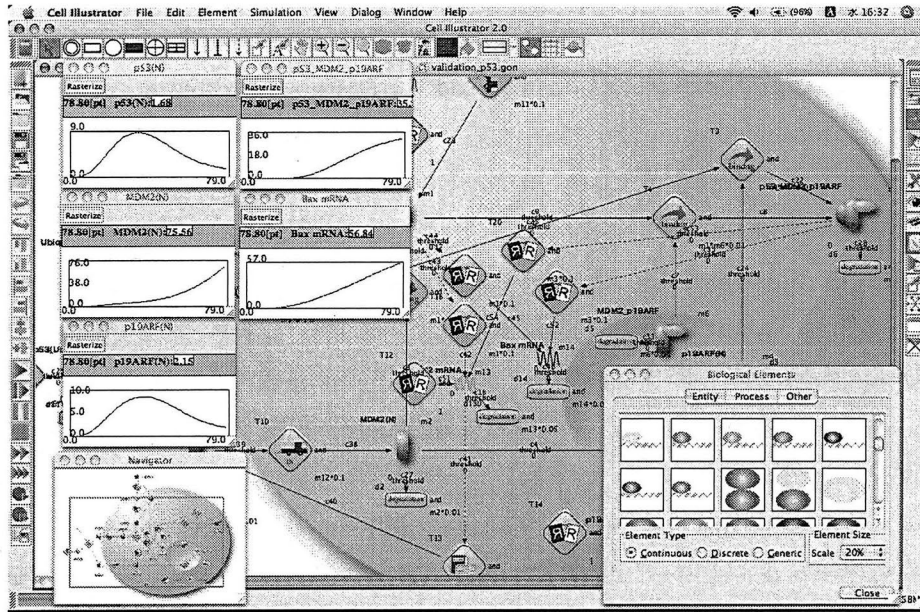


Fig. 5.5: A screenshot of Cell Illustrator editing a biological pathway. The user can build the biological pathway as a pathway model with the graphical user interface. Simultaneously, the simulation of the model is executable.

	Cell Illustrator (software)		
	Original symbols of HFPN		Examples of biological images
Type	Discrete	Continuous	Discrete and Continuous
Place			
Transition			
Arc			
	Normal	Test	Inhibitory

Fig. 5.6: Elements of Petri net used in Cell Illustrator. The user can use biological images instead of simple symbols of the Petri net.

5.2.2 Simulation Experiments of Fas-induced Apoptosis

In this subsection, the explanations of several transitions belonging to the Petri net model of Fas-induced apoptosis (see Fig. 3.20) are detailedly given to demonstrate how our method is practically used in constructing a timed Petri net model according to delay time determination rules.

Figure 5.7 illustrates the timed Petri net model of apoptosis. In Fig. 5.7, the place p_2 of Fas ligand trimer is such a place that the number of input and output transitions is respectively one, so that the maximum of firing frequencies f_4 satisfy the equation of **Rule (1)**, i.e. $\beta \cdot f_2 = \alpha \cdot f_4$, where, since $\beta = \alpha = 1$, and $f_2 = 1$, then $f_4 = 1$ is obtained.

Next, in calculating the delay time of t_9 and t_{10} , we apply **Rule (2)** because t_9 and t_{10} have a common place p_8 , and are in conflict. Based on the equation of $\beta \cdot f_8 = \alpha_1 \cdot f_9 + \alpha_2 \cdot f_{10}$, since $\beta = \alpha_1 = \alpha_2 = 1$, $f_8 = 1$, and f_9 and f_{10} are assumed to have the same firing chance, $f_9 = f_{10} = 1/2$ are obtained, then $d_9 = d_{10} = 2$ are obtained accordingly. That is, the transition t_9 and t_{10} have the equal chance to fire after d_9 or d_{10} . Note that β is the arc-weight of $e(t_8, p_8)$. α_1 and α_2 are the arc-weight of $e(p_8, t_9)$ and $e(p_8, t_{10})$, respectively. The delay time d_{37} of the transition t_{37} is assigned to 10 as an example that is based on **Rule (3)** due to the feature of small and natural degradation of caspase-9.

Furthermore, applying timed Petri net model allows to replace the initial marking instead of the source transitions, because of the facts that survival cells receive a certain number of extracellular stimuli and the amount of substances involved in corresponding reaction is not infinite (but enough many). And the number of initial tokens can be obtained. For example, the number of initial tokens for the place p_1 of Fas ligand equals $\alpha \cdot f_2 = 3 \cdot 1 = 3$ obtained by applying **Rule (1)** due to its single output transition t_2 . Note that, the delay time of the most apical transition is supposed to 1.

With the processes to decide the delay time of transitions to timed Petri net model, the delay time for transitions can be determined and the number of initial

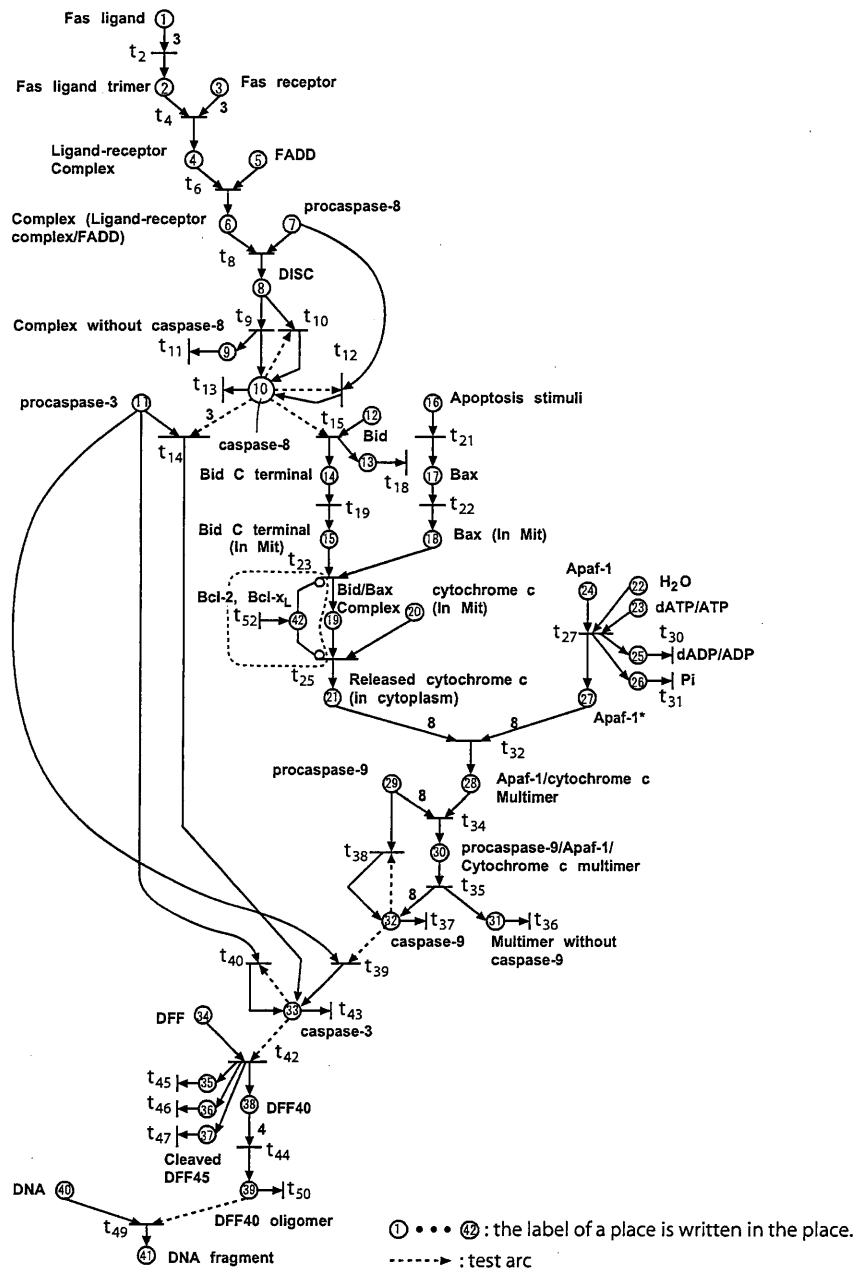


Fig. 5.7: Timed Petri net model of apoptosis based on Fig. 3.20. The block surrounded by dashed lines does not take part in the simulation of timed Petri net models because of the assumption that apoptosis pathways propagate the 'signal' without receiving the signals from any signal pathway having a relation to t_{52} when simulating the timed Petri net.

Table 5.1: The number of initial tokens for the output places of source transitions.

Place p_i	Biological substance	Initial tokens
p_1	Fas ligand	6
p_3	Fas receptor	6
p_5	FADD	6
p_7	procaspase-8	7
p_{11}	procaspase-3	28
p_{12}	Bid	8
p_{16}	Apoptosis stimuli	8
p_{20}	cytochrome c	8
p_{22}	H ₂ O	8
p_{23}	dATP/ATP	8
p_{24}	Apaf-1	8
p_{29}	procaspase-9	9
p_{34}	DFF	4
p_{40}	DNA	10

tokens of places can be given as listed in tables 5.1 and 5.2. The constructed timed Petri net model (Fig. 5.7) of apoptosis is simulated by using Cell Illustrator with the decided delay time and the number of initial tokens.

In the Petri net model as shown in Fig. 3.20, the production of Bcl-2/BCL-x_L is generally influenced by the activities of other signaling pathways, thus the place p_{42} of Bcl-2/BCL-x_L and input transition t_{52} are specially adopted to represent these activities. However, the apoptosis pathway of this thesis is supposed to propagate the 'signal' without receiving the signals from any signal pathway having a relation to t_{52} when simulating the timed Petri net. That is, the transition t_{52} does not fire. Therefore, the simulation of timed Petri net models can be performed without inhibitor arcs.

Table 5.2: Transition speeds in timed Petri net model for apoptosis illustrated in Fig. 5.7.

Transition t_i	Reaction type	Delay time d_i [sec]	Transition t_i	Reaction type	Delay time d_i [sec]
t_2	VII. Homodimerization	1	t_{30}	XI. Degradation	1
t_4	I. Association	1	t_{31}	XI. Degradation	1
t_6	I. Association	1	t_{32}	VII. Homodimerization	8
t_8	I. Association	1	t_{34}	I. Association	8
t_9	X. Dissociation	2	t_{35}	X. Dissociation	8
t_{10}	XI. Enzymic reaction	2	t_{36}	XI. Degradation	8
t_{11}	XII. Degradation	2	t_{37}	XI. Degradation	10
t_{12}	XI. Enzymic reaction	1	t_{38}	XI. Enzymic reaction	8
t_{13}	XII. Degradation	10	t_{39}	XI. Enzymic reaction	1.5
t_{14}	XI. Enzymic reaction	1.5	t_{40}	XI. Enzymic reaction	1.5
t_{15}	XI. Enzymic reaction	1	t_{42}	XI. Enzymic reaction	1
t_{18}	XI. Degradation	1	t_{43}	XI. Degradation	10
t_{19}	VII. Translocation	1	t_{45}	XI. Degradation	1
t_{21}	VI. Chemical reaction	1	t_{46}	XI. Degradation	1
t_{22}	VII. Translocation	1	t_{47}	XI. Degradation	1
t_{23}	I. Association	1	t_{49}	XI. Enzymic reaction	1
t_{25}	VI. Chemical reaction	1	t_{50}	XI. Degradation	10
t_{27}	VI. Chemical reaction	1			

5.3 Simulation Results and Discussions

Here we show experimental results obtained by simulating the timed Petri net model of Fas-induced apoptosis. Our experiments are carried out by using the simulator – Cell Illustrator. The followings can be found from the waveforms of the simulation results as shown in Fig. 5.8:

- (1) The response of DNA fragments to Fas ligands is expressed as the token behaviors in Fig.5.8 (a): Fas ligand concentration reaches zero at the time 2.0 [sec], and DNA fragments that is often considered as an indicator of cell death, start to increase after the time 19.0 [sec]. Apoptotic pathways are working to propagate signals from Fas ligands to the DNA;
- (2) the diagram (b) shows the number of tokens and further the activation order of three kinds of caspases involved in apoptosis pathways:
 - (i) caspase-8 is activated ahead of caspase-3 and caspase-9;
 - (ii) caspase-3 is activated afterwards which is activated directly by caspase-8 and the amount of caspase-3 has a notable augment that can be observed as the result of the autocatalytic activation;
 - (iii) caspase-9 begins to be activated after a short time from the activation of caspase-3. This is due to the activation of caspase-9 which relies on the mitochondrial DNA damage pathways that include the reactions such as the release of cytochrome c from mitochondria, the formation of apoptosome and so on.

By comparing the behaviors of simulation results executed by Matsuno *et al.* [51], we can observe that:

- (1) both of the diagram (a) and (b) in Fig. 5.8 have the approximate same waveforms as the simulation results in Ref. [51], i.e. the amount of DNA destruction is increased along with the decrease of Fas ligands due to the complex formation of Fas ligand trimer with the lapse of time.
- (2) the activation order of three kinds of caspases is caspase-8, caspase-3, caspase-

9, which is exactly the same as the one derived from the simulation in Ref. [51].

Since the simulation results reported by Matsuno *et al.* [51] have been successfully obtained by using “hybrid Petri nets”, our proposed simulation method may probably provide quite promising results based on timed Petri net model. However, hybrid Petri nets use continuous places and transitions. The reaction rates of transitions are assigned as real numbers and the parameters for initial concentration of substances and transition speeds are carefully tuned by hand. In general, lots of trial and error processes have been performed until appropriate parameters for simulation are determined. The simulation is precise and is executed in very small time interval. The parameter tuning processes consume too much time. Therefore, with the simulation results, the appropriateness of the timed Petri net model of apoptosis is verified that the simulation method may probably provide a number of valuable insights.

In addition, since Cell Illustrator possesses the excellent graphical user interface, the timed Petri net of apoptosis can be simulated in the animation method. In this way, the different apoptotic pathways can be pursued by tracing the flow of tokens as follows:

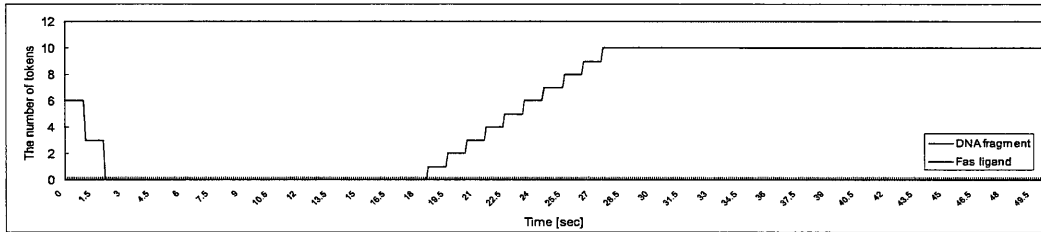
(1) Fas ligand induced pathway:

Fas ligand/Fas receptor/FADD/DISC/procaspase-8/caspase-8/procaspase-3/
caspase-3 pathway

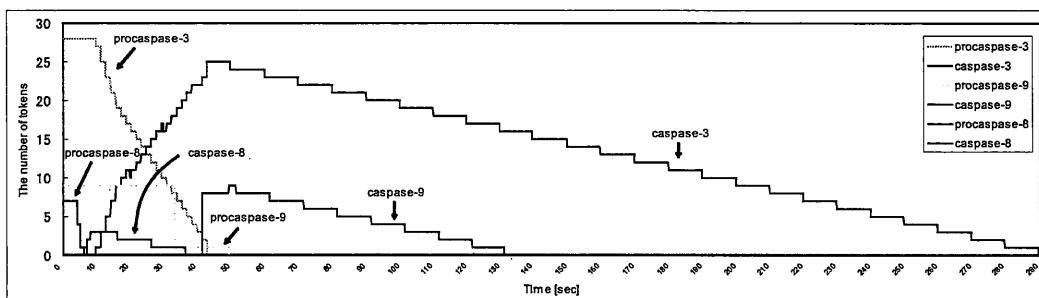
(2) Mitochondrial DNA damage pathway:

Fas ligand/Fas receptor/FADD/DISC/procaspase-8/ caspase-8/Bid/Bax/
cytochrome c/Apaf-1/apoptosome/ caspase-9/caspase-3 pathway.

In contrast, the continuous Petri net models have no such feature to make the biologists intuitively understand the intrinsic structure and behavioral properties of signaling pathways by simulating the models.



(a) Simulation results of Fas ligand and DNA fragmentation.



(b) Simulation results of procaspases and caspases.

Fig. 5.8: Simulation results of timed Petri net model of apoptosis in Fig. 5.7. (a) Token numbers representing DNA fragments increase in response to the initial amount of tokens of Fas ligands. (b) Concentration behaviors of (pro-)caspases working in the apoptotic pathway. The order of expression of the caspases in this graph is exactly the same as the order of them in Ref. [51], which is obtained by manual tuning of transitions in the apoptotic pathway.

Development of Pathway Database

With the rapid technological innovations and changes in biology and biochemistry, more and more produced biological data have been accumulated and systematically stored in specific databases.

6.1 Pathway Database Overview

Biological experts delineate pathways by reading the literature and stored them on pathway databases. In this section, we introduce several web-based databases of biological pathways and detailedly introduce our new website “Petri Net Pathways” available for the analyze of biological pathways with Petri nets.

Currently, there are more than 1000 public and commercial biological databases that usually contain genomics and proteomics data including nucleotide sequences of genes or amino acid sequences of proteins, function, structure, localisation on chromosome, clinical effects of mutations and similarities of biological sequences.

Biological databases play an important role in helping researchers to understand and explain biological phenomena ranging from the structure of molecules, interactions and their mechanisms, to the whole organisms and to understanding the evolution of species. The biological knowledge of databases is usually stored amongst many different specialized databases that include public repositories of gene data such as GenBank [88] or the protein DataBank (the PDB) [89], and the private databases like those used by research groups involved in certain projects or those held by biotech companies.

By far a special issue of the journal “*Nucleic Acids Research*” (NAR) [90] has been

regarded as the most important resource for biological databases. The database list and the database descriptions are freely available, and the all the publicly available online databases related to computational biology and bioinformatics are categorized as follows [90]:

- Nucleotide sequence databases
- RNA sequence databases
- Protein sequence databases
- Structure databases
- Genomics databases (non-vertebrate)
- Metabolic and signaling pathways
- Human and other vertebrate genomes
- Human genes and diseases
- Microarray data and other gene expression databases
- Proteomics resources
- Other molecular biology databases
- Organelle databases
- Plant databases
- Immunological databases

Here, we only introduce several well-constructed databases concerning with signaling pathways which provide clear and fast access.

■ [**KEGG: Kyoto Encyclopedia of Genes and Genomes]**

KEGG is a knowledge database for systematic analyses of bioinformatics or computational research, which integrates biological information about networks of molecular interactions concerning with genome, protein, metabolism and signal transduction. The KEGG database was initiated and has been developed by the Kanehisa Laboratories in the Bioinformatics Center of Kyoto University and the Human Genome Center of the University of Tokyo. The KEGG databases are daily updated and is freely available [35].

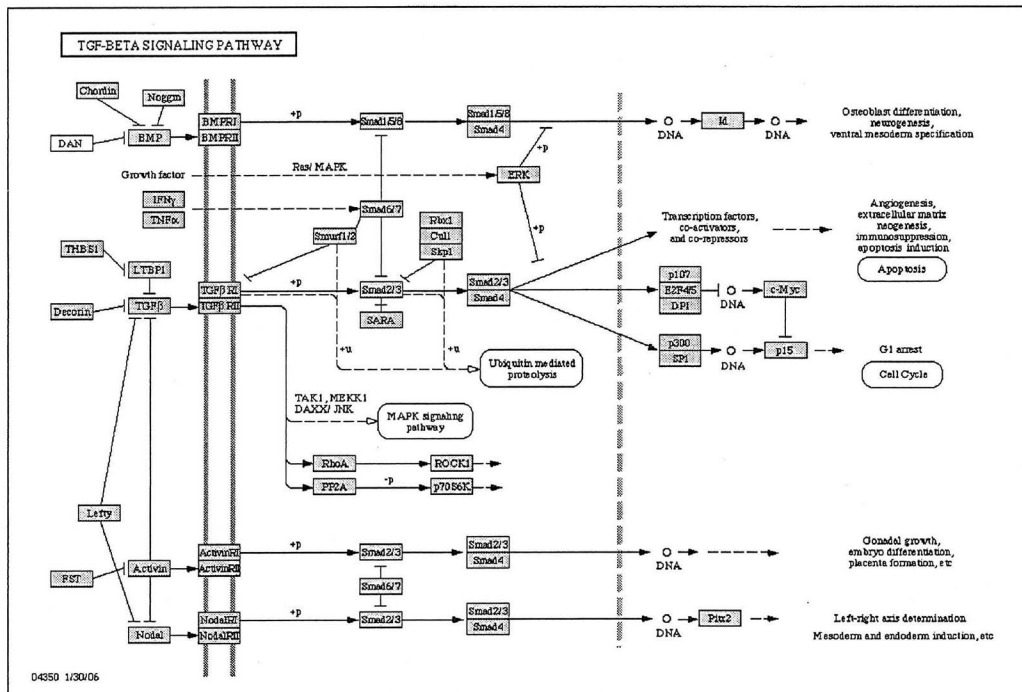


Fig. 6.1: The TGF-beta signaling pathways of Homo sapiens (human) in the screenshot of KEGG PATHWAY database.

The biological database consists of following four main databases [91]:

KEGG PATHWAY - Including pathway maps representing graphical represents of cellular processes, such as metabolism, membrane transport, signal transduction and cell cycle, which are manually drawn on the molecular interaction and reaction networks for metabolism, other cellular processes, and human diseases. Figure 6.1 shows the screenshot of Transforming Growth Factor-beta (TGF-beta) signaling pathways which is collected in KEGG PATHWAY database, in which a rectangle represents gene product, mostly protein including DNA, a circle represents other molecule of chemical compound and an ellipse represents another map. The other notations about the KEGG PATHWAY database such as arrows, protein-protein interactions, gene expression relations and enzyme-enzyme relations, are given on the internet via http://www.genome.jp/kegg/document/help_pathway.html.

KEGG BRITE - Functional hierarchies and binary relations of KEGG objects, including genes and proteins, compounds and reactions, drugs and diseases, and cells and organisms.

KEGG GENES - Gene catalogs of all complete genomes and some partial genomes with ortholog annotation, enabling KEGG PATHWAY mapping and BRITE mapping.

KEGG LIGAND - A composite database of chemical substances and reactions representing knowledge on the chemical repertoire of biological systems and environments.

■ [SPAD: Signaling Pathway Database]

SPAD is a database integrating the information of genetic function and signal transduction systems, which is free of charge and has been operated and developed by Molecular Gene Technics, Graduate School of Genetic Resources Technology, Kyushu University.

SPAD is classified into four categories according to the following signal molecules at a cell's surface (i.e. an extracellular signal):

- Growth Factor
- Cytokine
- Hormone
- Stress

that triggers the intracellular signaling pathway. The purpose of SPAD database is to use graphical representation to describe molecular interactions and functions between protein-protein, protein-DNA as well as protein-DNA sequences.

Figure 6.2 illustrates the signaling pathway mediated by TGF-beta that is included in the category of Growth Factor. An ellipse represents active form of component while a rectangle represents inactive form of component. Ten kinds of colors of icons are employed to indicate different molecules or substances depending on their functions. Two forms of arrows are utilized to represent experimentally known signaling pathways and unknown signaling pathways. The legends of signaling pathway figures in SPAD can be accessed online via

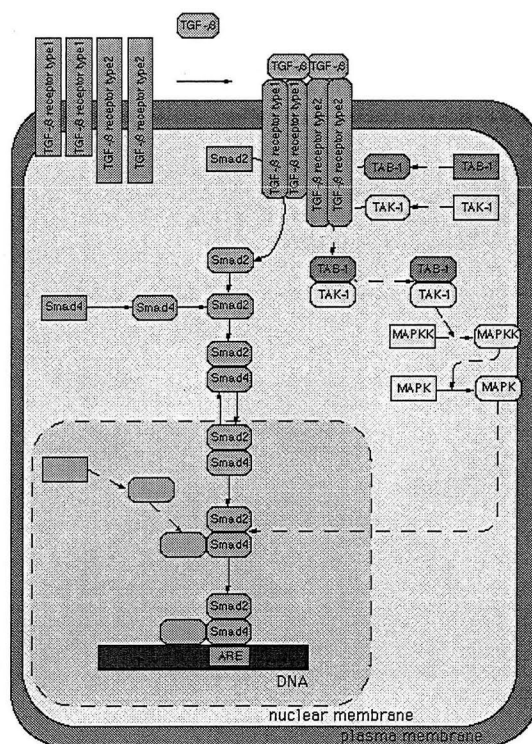


Fig. 6.2: The signaling pathways TGF-beta in the screenshot of SPAD database, available online: <http://www.grt.kyushu-u.ac.jp/spad/pathway/tgf-beta.html>.

<http://www.grt.kyushu-u.ac.jp/spad/legend.html>. Furthermore, All the signaling pathway maps in SPAD are clickable, in which the substance is linked to another pages having the relevant data of the substance such as synonym, structure/function, journal information and so on.

■ [TRANSPATH]

This website provides information about (mostly mammalian) signal transduction molecules and reactions [92, 39]. The data about molecules participating in signaling pathways and the reactions they are involved in, resulting in a complex network of

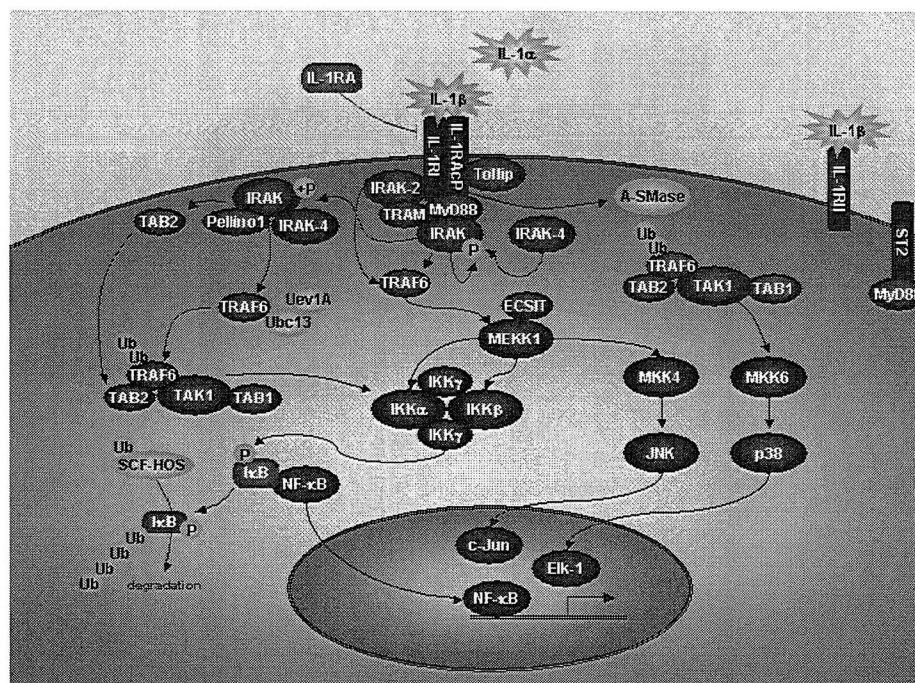


Fig. 6.3: The signaling pathways mediated by Interleukin-1 in the screenshot of TRANSPath.

interconnected signaling components.

TRANSPath focuses on signaling cascades that change the activities of transcription factors and thus alter the gene expression profile of a given cell. TRANSPath is a commercial biological database.

■ [BioCarta: Charting Pathways of Life]

BioCarta is an interactive web-based, user contributed collection of pathways information especially for human and mouse genomes. BioCarta is a commercial enterprise that supplies “uniquely sourced and characterized reagents and assays for biopharmaceutical and academic research”. The users are usually engaged in the new field of proteomics comprising the study of protein expression and function. But BioCarta

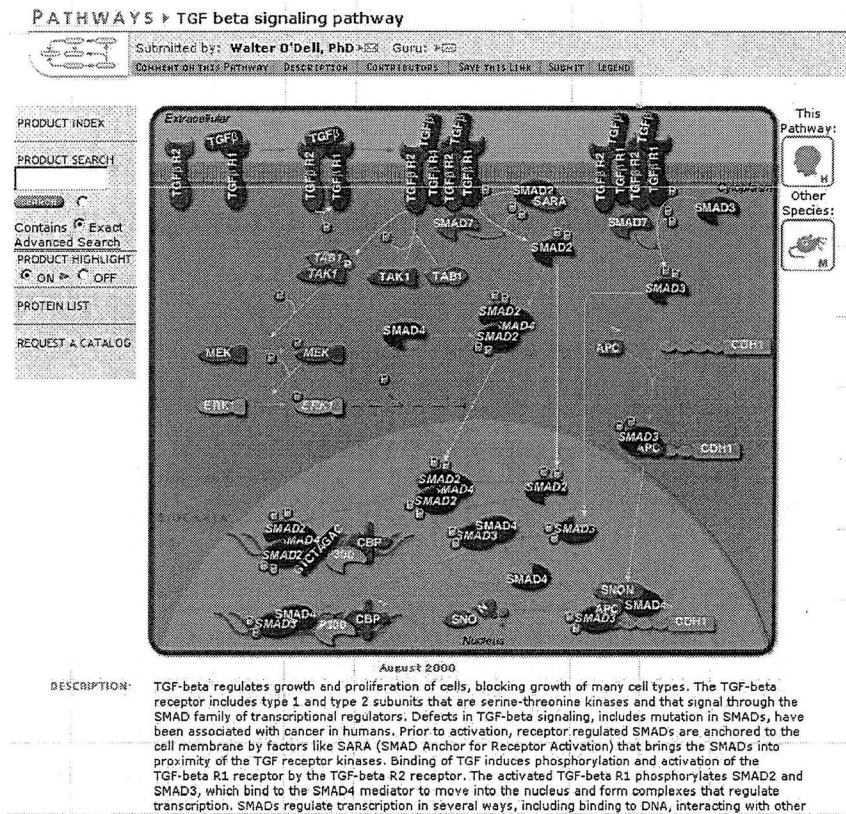


Fig. 6.4: The TGF-beta signaling pathways in the screenshot of BioCarta.

is less about their business than it is a interesting provider of known pathways. All the pathways in BioCarta are given in alphabetical order. Symbols “H” and “M” next to each pathway stand for Human and Mouse. Provided pathways are clickable and will be led to a detailed page [93].

Figure 6.4 shows a screen shot of TGF-beta signaling pathway of BioCarta pathways. Users can get more detail (e.g. description, contributors, revision history and references) about clicked pathway and comprised gene. Specific gene can be clicked to open a new window which is highlighted by a rotary triangle. The users can also

swap from Human to Mouse informations and vice versa using the icons at upper right corner.

6.2 Petri Net Pathways (PNP) Description

All above pathway databases are useful for overview the interactions. However, the dynamic behaviors of biological systems can not be observed from these pathways without special knowledge for mathematics. So, we launch an interactive web-based pathway database "Petri Net Pathways" (PNP for short) [94] that stores signaling pathway models by Petri nets as well as these biological explanations with flash animation that shows behaviors of signal flows. The website is available for the use of not only a biologist but also a research in computer science and/or engineering who has a will to participate in the research of systems biology with the knowledge and experience of the Petri net theory. Moreover, it may be useful in developing computational simulation involved in understanding signaling pathways. PNP allows free searching for protein as well as signaling pathway information, and is part of the research projects of Biopathway Analysis Center, Faculty of Science, Yamaguchi University.

6.2.1 Data Source and PNP Basement

The data source of PNP database mainly comes from the literature. Biological experts delineate the pathways by reading the literature, extracting important informations, and utilize them for further compilation. Simultaneously, we plan to up a easy and dynamic web-based submission form for information exchange serving as an interactive web-based resource for researchers, educators and students.

PNP was launched in April 2006 and is constructed and equipped to run on Linux X-windows. PNP includes data sources and referred literature that has a linkage to external public search service for references such as Entrez PubMed [95]. Figure 6.5

Petri Net Pathways

Contents

- Introduction
- Pathways
- Signaling Pathways
- List of Proteins
- References
- Publications
- Links
- Contact us

Site Index

Pathways

- IL-1
- G-protein
- TPO
- IL-6
- IGF-1

List of Proteins

- adenyl cyclase
- ADP
- AKT
- AMPK
- AP-1
- APRE
- ATP
- CaM
- cAMP
- CBP
- c-Fos
- c-Jun
- CK II
- CN
- CRE
- CREB
- CrKL
- DAG
- EBB
- eIF
- Elk-1
- ER
- ERK
- G alpha/o
- G

References

- Alberts, B., et al., Molecular Biology of the Cell -fourth edition- 871-2, Garland Science, 2002. (IGF-1)

Topics

NEW! The pathway (TGF-beta) has been newly arrived! (November,27, 2006)

Past Topics

Diagram: A diagram showing the interaction of Elk-1 and SRE with a DNA site. Elk-1 and SRE bind to the DNA site, leading to the transcription and translation of gene products, which are then degraded.

Logos: Cell Signaling Database, PATHWAY DATABASE in Cell Molecular Biology, CSML, Matsuno Lab.

Text: This website is constructed under the support of the Grand-in-Aid for Scientific Research on Priority Areas "System Genomics" from the Ministry of Education, Culture, Sport, Science and Technology in Japan.

Footer: Copyright (C) 2007, Biopathway Analysis Center, Faculty of Science, Yamaguchi University.

Fig. 6.5: PNP interface.

shows PNP interface. The next three figures are screen copies of introduced symbols employed in PNP.

6.2.2 Data Description

[Symbols of Biological Pathways]

In PNP, several symbols are defined to illustrate biological pathways with images and arrows in this website. We symbolize an active and an inactive state of a protein as well as a nonactive substance constituting biological pathways as shown

in Fig. 6.6.

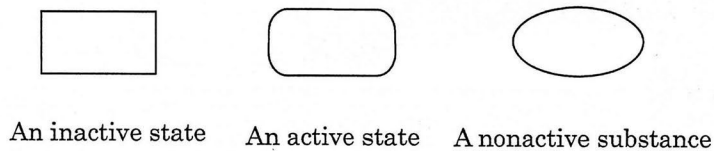


Fig. 6.6: Symbols of states.

We also classify substances into nine categories by the function of the substance:

- signal molecule
- cell receptor
- protein kinase
- transcription factor
- protease
- sequence on DNA bound by transcription factor
- substance related to G-protein families
- protein phosphatase and others

Arrows in Fig. 6.7 represent behaviors of promoting or inhibiting reactions. The reactions of phosphoric acid, ubiquitin and calcium ion are represented in Fig. 6.8 respectively.

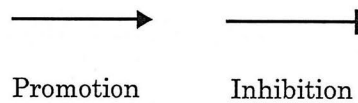


Fig. 6.7: Reaction behaviors of promotion or inhibition.

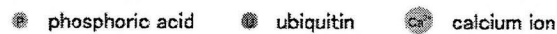


Fig. 6.8: Other symbols in PNP.

Above statement of biological pathway symbols is summarized and can be accessed through the route of “Introduction→Biological pathway symbols” at the left side of top page or jump to the address:

http://genome.ib.sci.yamaguchi-u.ac.jp/~pnp/bp_symbols.html directly.

6.2.3 Data Searching

For researchers to benefit from the data stored in a database, it is important that users can access to the information easily and rapidly. To achieve this purpose, two searching methods have been considered:

[Searching From Pathways Field]

From the top page, users can select provided signaling pathways from the Pathways Field on the upper right corner (see Fig. 6.9).

After clicking, from Fig. 6.10 users can get more detailed information on selected signaling pathways. Figure 6.10 shows the interface consisting of three parts concerning with the object pathways.

- **Biological pathway** - delineated by biological experts according to experimental facts from literature. Every biochemical reactions are clickable. A mouse's placement on interested molecular interaction will arise a dialogue balloon in which minute explanations about the interaction are given and corresponding Petri net model will appear after the click on the interactions. Simultaneously, concerned literature and online information are be given at the lower right part – Reference corner.
- **Petri net model** - modeled depending on clicked reactions which is constructed based on proposed modeling method introduced in Chapter 3. All the Petri net models are dynamic and can be simulated. Click on the button at the Petri net Field, the simulation will be executed to observe the flow of signal transduction within the cell.

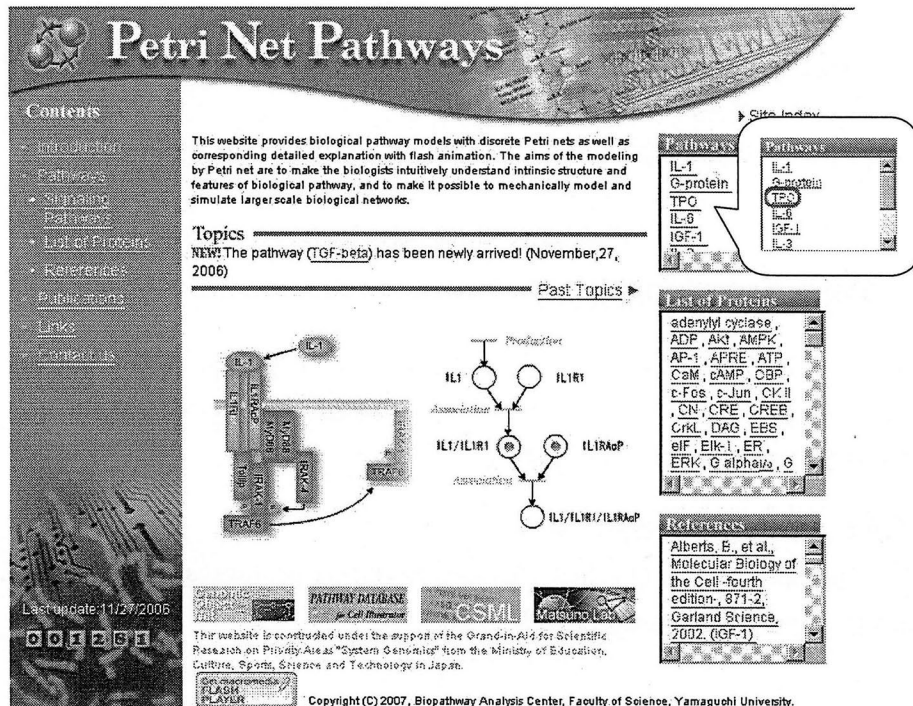


Fig. 6.9: Screenshot of searching from Pathways Field.

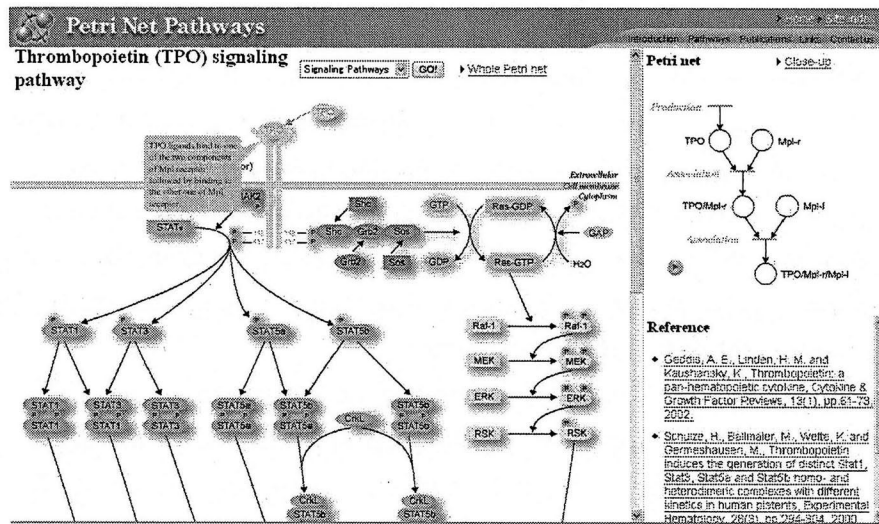


Fig. 6.10: Interface of the pathway selected from the Pathways Field.

- **Reference** - enumerated by every biological reaction. The Reference Field includes the data sources of paper and internet-references that have the linkages to public online database of references.

[**Searching From Menu of Top Page**]

Users are recommended to click “Pathways” on the menu at the left side of top page, see Fig. 6.11.

Figure 6.12 shows the screen copy of pathways. Stored signaling pathways in PNP are given and the users can click on object pathways to load the interface of target pathways identical to the result searched by first method.

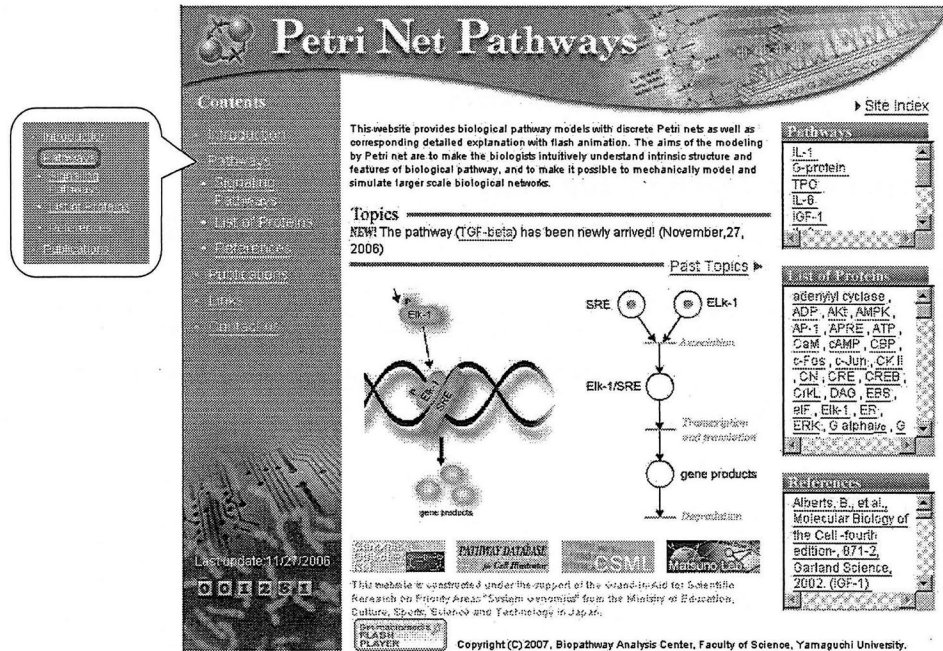


Fig. 6.11: Screenshot of searching from menu.

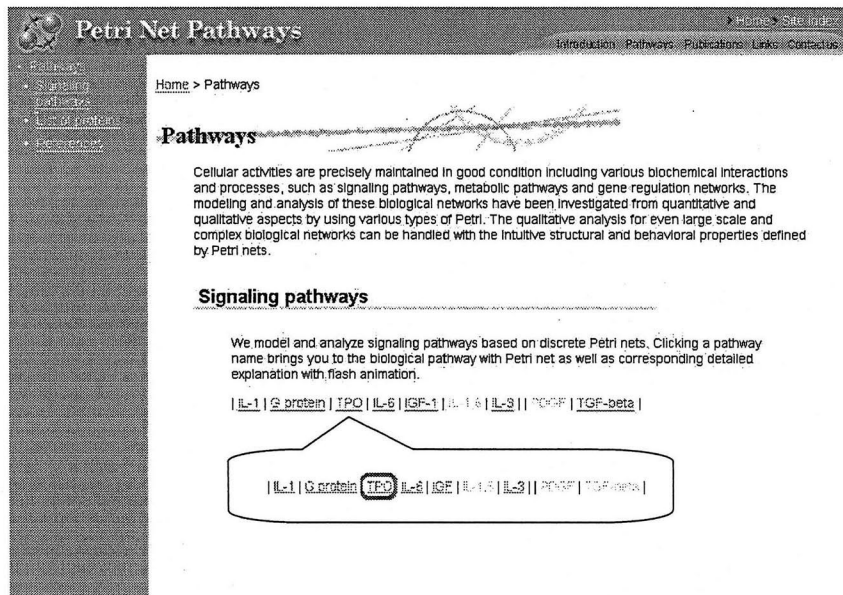


Fig. 6.12: Screenshot of summarized pathways after clicking.

6.2.4 Data Update and Future Prospects

PNP is regularly updated to add signaling pathways as long as new experimental fact as been known. The latest data release of PNP was on November 27, 2006. Currently, PNP contains 7 signaling pathways, about 137 proteins, 109 cited references. The pathways include IL-1, G-protein, TPO, IL-6, IGF-1, IL-3, TGF-beta.

The authors would like to encourage users to give valuable suggestion to improve the accuracy of PNP by using web-based submission or contacting webmaster directly by email. As the future work, the following items have to be performed:

- (i) Adding more biological pathways including metabolic pathways as well as gene regulatory networks.
- (ii) Employing the simulation techniques proposed in Chapter 5, in order to mechanically simulate timed Petri net models and obtain precious insights from the results of analyses and simulations.
- (iii) Making it possible to facilitate the exchange of Petri net model data in different formats, such as hybrid functional Petri net models.

Conclusions

Along with the progress of biological techniques to measure substances in a cell, a whole sketch of biological pathways in a cell will become uncovered. For the systematic understanding of biological pathways, computer simulation is indispensable, since it is too hard to grasp dynamic behaviors in a cell even for a small network consisting of small number of substances.

Petri net is a promising method for biological pathway modeling and simulation because it has the following characteristics;

- “firm mathematical foundation” enabling formal and clear representation of biological pathways as well as their structural analyses, and
- “visual representation of networks” which provides intuitive understanding of biological pathways without any mathematical descriptions which are basically difficult for ordinary biologists.

This thesis has discussed how to model, simulate and analyze signaling pathways in order to give systematic understanding of signaling pathways on the basis of Petri net theory.

In Chapter 3, we have proposed a modeling method based on Petri net by taking notice of molecular interactions and mechanisms of signaling pathways. We first have given modeling rules for signaling pathways with Petri net that can be naturally and explicitly modeled. Then we have focused on the molecular interactions and mechanisms, and presented 12 reactions types (e.g. autophosphorylation, chemical reaction, gathering action and so on) and corresponding Petri net models as long as the biological facts have been known with detailed explanation. Finally, we have demonstrated how our modeling method is practically used in modeling Interleukin-3

(IL-3) and Fas induced apoptotic signaling pathways as examples.

In Chapter 4, we have proposed methodology to give structural analysis of modeled signaling pathways based on Petri net theory. In order to describe the contribution of Petri net theory in analyzing structural properties of metabolic pathways using T-invariant, we have presents a brief introduction of elementary flux modes into metabolic pathways that are known to correspond to elementary T-invariants of Petri net. Then we have discussed the characteristics of signaling pathways and introduced a new notion “activation transduction component” (ATC) to express an enzymic activation process that has an elementary T-invariant in Petri net model as a counterpart. The purpose is to inquire into the behaviors of sequential enzymic activation processes of signaling pathways. And the features of signaling pathways have been given that the signal propagates itself through a series of sequential enzymic activation processes where a certain enzyme changes from “inactivate” state to “activate” state depending on the functions of upstream enzymes. We also have revealed that such an ATC corresponds to the subnet generated by the elementary T-invariant representing a fundamental periodic behavior. This is because, the subnet has such features that, (i) before and after any firing sequence corresponding to an elementary T-invariant, the tokens on each place in the subnet are kept constant; and (ii) all the transitions in subnet take part in the firing sequence. We have also proposed an algorithm to give relations among ATCs in signaling pathways in order to clarify how enzymic activation processes occur. The results of algorithm have been used to schematize the connection relations between activation transduction components in signaling pathways. It can give us a new insight into the architecture of signaling pathways to grasp structural and behavioral properties of them. Finally, we have presented an application of proposed method to modeled examples of TPO signaling pathways.

In Chapter 5, we have presented a simulation method with timed Petri nets that is an extension of Petri net, and performed simulation experiments. We have proposed a method to determine transition speeds of a Petri net, based on the simple principles - the number of tokens flowed into a place is equivalent to the one flowed

out from the place -. This method allows a modeled Petri net of a signaling pathway to be enhanced as signal transductions in the pathway that can be observed. Then we have confirmed the availability of proposed method by observing signal transductions from simulation experiments of Fas induced apoptosis signaling pathways as an example using a Petri net based simulator “Cell Illustrator”. The procedures of proposed simulation method also have automatically determined flow speeds of different transductions leading intracellular responses to ultimate regulation, which are determined along with the transition speeds of Petri net.

In Chapter 6, we first have introduced several well-constructed databases concerning with signaling pathways which are useful for overview molecular interactions. Then we have given a minute description of our new modeling method based database website “Petri Net Pathways” (PNP) available for the use of not only a biologist but also a researcher in computer science and/or engineering. PNP can give dynamic behaviors of biological systems even without special knowledge for mathematics and it is an interactive web-based pathway database that stores signaling pathway models by Petri nets as well as these biological explanations with flash animation describing behaviors of signal flows.

In Chapter 7, we have concluded the results obtained in this thesis and discuss the research works remaining in future to be done.

Future works in the research field related to this thesis are remained to be done as follows:

- (i) to improve our algorithm to analyze Petri net models including inhibitor arcs;
- (ii) to develop our current method further to analyze more complicated models and investigate the related properties;
- (iii) to simulate other Petri net modeled biological pathways; and
- (iv) to find efficient method of converting timed Petri net model to a continuous one that enables higher predictive precision.

List of Figures

2.1	Basic elements of Petri net.	10
2.2	An example of Petri net with unity arc weights.	10
2.3	Examples show firing rules of Petri net.	11
2.4	Elements of hybrid (functional) Petri nets.	16
2.5	Model for reaction decomposing dimers to monomers. (a) Reaction decomposing dimers to monomers. (b) Hybrid Petri net. In continuous places P_d and P_m , concentrations of the dimer and the monomer are stored, respectively. At continuous transitions T_1 and T_2 , same firing speeds are assigned as a reaction speed. Integers “1” represent weights of arcs. (c) hybrid functional Petri net model for the reaction. Note that, at the transition T, the reaction speed is assigned. P_d and P_m are the same as ones in (b). Different weights “1” and “2” are assigned to two arcs.	16

2.6	Continuous and discrete transitions of hybrid functional Petri net. (a) An example of continuous transition. Four input arcs are attached to continuous transition T_C : two continuous input arcs from continuous places P_1 and P_4 , and two test input arcs from continuous place P_2 and discrete place P_3 . a_i is the weight of arc from place P_i for $i=1, 2, 3, 4$. Two continuous arcs are headed from the transition T_C to continuous places Q_1 and Q_2 , respectively. Variables b_1 and b_2 are assigned to these arcs as weights. (b) An example of discrete transition. Four input arcs are attached to discrete transition T_D : two discrete input arcs from discrete place P_1 and continuous place P_3 , and two test input arcs from discrete place P_2 and continuous place P_4 . a_i is the weight of arc from place P_i for $i=1, 2, 3, 4$. Two output arcs are headed from the transition T_D to discrete place Q_1 and continuous place Q_2 . Variables b_1 and b_2 are assigned to these arcs as weights.	19
3.1	An application of modeling rules to a simple reaction.	22
3.2	Petri net model of a chemical reaction of light-induced phosphorylation, given by its stoichiometric equation.	22
3.3	An enzyme place in Petri net model.	23
3.4	Petri net models of various reaction types in signaling pathways. . . .	24
3.5	Petri net model of <u>I. association reaction</u>	26
3.6	Petri net model of <u>II. phosphorylation</u>	26
3.7	Petri net model of <u>III. autophosphorylation</u>	27
3.8	Petri net model of <u>IV. activation response by active site(s)</u>	28
3.9	Petri net model of <u>V. Gathering action by adaptor protein</u>	28
3.10	Petri net model of <u>VI. chemical reactions</u>	29
3.11	Petri net model of <u>VII. homodimerization</u>	29
3.12	Petri net model of <u>VIII. translocation</u>	30
3.13	Petri net model of <u>IX. switching of channel</u>	31
3.14	Petri net model of <u>X. dissociation</u>	31

3.15	Petri net model of <u>XI. enzymic reaction.</u>	32
3.16	Petri net model of <u>XII. production/degradation.</u>	32
3.17	The signaling pathway induced by IL-3.	34
3.18	Petri net model of Fig. 3.17.	36
3.19	Biological diagram of apoptosis pathways induced by Fas ligands.	40
3.20	Petri net model without time of figure 3.19.	44
4.1	A simple metabolic network of chemical reactions.	48
4.2	Elementary mode 1 of Fig. 4.1.	48
4.3	Elementary mode 2 of Fig. 4.1.	48
4.4	Elementary mode 3 of Fig. 4.1.	49
4.5	Part of monosaccharide metabolism.	49
4.6	Petri net model of Fig. 4.5.	50
4.7	Petri net model of one of the elementary modes.	51
4.8	The Petri net model removing the place representing external substances in Fig. 4.7.	51
4.9	The association between activation transduction component and elementary T-invariant with mapping a pathway to a Petri net model. (a) Activation transduction component of Ras activity regulation mechanism. (b) A Petri net model of (a) corresponding to a subnet of an elementary T-invariant.	55
4.10	An example of connection relations among subnets.	58
4.11	TPO signaling pathway. The parts B_1 , B_2 and B_3 surrounded by dashed lines are the three reaction examples, reactions of association, homodimerization and enzymic activation, which are the blocks I , V II and XI of Fig.3.4, respectively. Corresponding Petri net models of B_1 , B_2 and B_3 are given in Fig.4.12 by the dashed-line-surrounded parts B'_1 , B'_2 and B'_3 , respectively.	60

4.12	Petri net model of the TPO signaling pathway shown in Fig. 4.11. Parts B'_1 , B'_2 and B'_3 correspond to B_1 , B_2 and B_3 of Fig.4.11, respectively. B'_2 reflects the complex formation of STAT1 making a homodimer from two monomers, and so the arc-weight is set to 2.	61
4.13	All elementary T-invariants of the Petri net in Fig.4.12.	63
4.14	All subnets obtained from elementary T-invariants as shown in Fig.4.13of Petri net model.	65
4.15	Connection relations between all the subnets corresponding to activation transduction components in TPO signaling pathways.	67
5.1	Illustration for [Basic principles] (1).	70
5.2	Two connection cases in Rule (1).	71
5.3	Conflict situation applied to Rule (2). Transitions $t_{O_1}, t_{O_2}, \dots, t_{O_j}, \dots, t_{O_n}$ are in <i>conflict</i> since firing either will remove the token from p_i , disabling the other transitions [61].	72
5.4	Huntington's disease HFPNe model in the screen shot of Cell Illustrator [56].	74
5.5	A screenshot of Cell Illustrator editing a biological parkway. The user can build the biological pathway as a pathway model with the graphical user interface. Simultaneously, the simulation of the model is executable.	75
5.6	Elements of Petri net used in Cell Illustrator. The user can use biological images instead of simple symbols of the Petri net.	75
5.7	Timed Petri net model of apoptosis based on Fig. 3.20. The block surrounded by dashed lines does not take part in the simulation of timed Petri net models because of the assumption that apoptosis pathways propagate the 'signal' without receiving the signals from any signal pathway having a relation to t_{52} when simulating the timed Petri net.	77

5.8	Simulation results of timed Petri net model of apoptosis in Fig. 5.7. (a) Token numbers representing DNA fragments increase in response to the initial amount of tokens of Fas ligands. (b) Concentration behaviors of (pro-)caspases working in the apoptotic pathway. The order of expression of the caspases in this graph is exactly the same as the order of them in Ref. [51], which is obtained by manual tuning of transitions in the apoptotic pathway.	82
6.1	The TGF-beta signaling pathways of Homo sapiens (human) in the screenshot of KEGG PATHWAY database.	85
6.2	The signaling pathways TGF-beta in the screenshot of SPAD database, available online: http://www.grt.kyushu-u.ac.jp/spad/pathway/tgf-beta.html	87
6.3	The signaling pathways mediated by Interleukin-1 in the screenshot of TRANSPATH.	88
6.4	The TGF-beta signaling pathways in the screenshot of BioCarta.	89
6.5	PNP interface.	91
6.6	Symbols of states.	92
6.7	Reaction behaviors of promotion or inhibition.	92
6.8	Other symbols in PNP.	92
6.9	Screenshot of searching from Pathways Field.	94
6.10	Interface of the pathway selected from the Pathways Field.	94
6.11	Screenshot of searching from menu.	96
6.12	Screenshot of summarized pathways after clicking.	96

List of Tables

3.1	Biological interpretation of each transition in Fig. 3.20.	38
3.2	Biological interpretation of each transition in Fig. 3.20.	43
4.1	The results T_{sink} , T_{gen} , $gen(t)$, and $PROV(N_{J_i})$ by performing proposed algorithm.	66
5.1	The number of initial tokens for the output places of source transitions.	78
5.2	Transition speeds in timed Petri net model for apoptosis illustrated in Fig. 5.7.	79

References

- [1] S. Akira, Functional roles of STAT family proteins: lessons from knockout mice, *Stem Cells*, **17**, 1999.
- [2] W.S. Alexander, Thrombopoietin and the c-Mpl receptor: insights from gene targeting, *IJBCB*, **31**:1027–1035, 1999.
- [3] H. Alla and R. David, Continuous and hybrid Petri nets, *J. Circ. Syst. Comp.*, **8**(1):159–188, 1998.
- [4] T. Araki, T. Tanida, T. Watanabe, and K. Onaga, A linear programming-based algorithm for successively enumerating elementary invariants of Petri nets, *Technical Report of IEICE*, **CAS89–89**:125–132, 1989.
- [5] D. Avis and K. Fukuda, A pivoting algorithm for convex hulls and vertex enumeration of arrangements and polyhedra, *Discrete Comput. Geom.*, **8**:295–313, 1992.
- [6] M. Chen and R. Hofestädt, Quantitative Petri net model of gene regulated metabolic networks in the cell, *In Silico Biology*, **3**(3):347–365, 2003.
- [7] W. Chen, M.O. Daines, and G.K. Khurana Hershey, Turning off signal transducer and activator of transcription (STAT): the negative regulation of STAT signaling, *J. Allergy Clin. Immunol.*, **114**(3), 2004.
- [8] C. Choi, T. Crass, A. Kel, O. Kel-Margoulis, M. Krull, S. Pistor, A. Potapov, N. Voss, and E. Wingender, Novel consistent modeling of signaling pathways

- and its implementation in the TRANSPATH database, *Genome Informatics*, **15**:244–254, 2004.
- [9] A. Doi, *Modeling and simulation of biological pathways with hybrid functional Petri net*, PhD thesis, Yamaguchi University, March 2006.
- [10] A. Doi, M. Nagasaki, S. Fujita, H. Matsuno, and S. Miyano, Genomic Object Net II: Modeling biopathways by hybrid functional Petri net with extension, *Applied Bioinformatics*, **2**:185–188, 2004.
- [11] A. Doi, M. Nagasaki, H. Matsuno, and S. Miyano, Simulation based validation of the p53 transcriptional activity with hybrid functional Petri net, *In Silico Biology*, **6**(001), 2006. Available online: <http://www.bioinfo.de/isb/2006/06/0001/>.
- [12] R. Drath, Hybrid object nets: An object oriented concept for modeling complex hybrid systems, In *Proc. Hybrid Dynamical Systems, 3rd International Conference on Automation of Mixed Processes, ADPM'98*, pp. 437–442, 1998.
- [13] R. Drath, U. Engmann, and S. Schwuchow, Hybrid aspects of modeling manufacturing systems using modified Petri nets, In *Proc. 5th Workshop on Intelligent Manufacturing Systems*, Granado, Brasil. Available online: <http://www.systemtechnik.tu-ilmeneau.de/~drath/Download/Brasil98.ps.zip>.
- [14] S. Fujita, M. Matsui, H. Matsuno, and S. Miyano, Modeling and simulation of fission yeast cell cycle on hybrid functional Petri net, *IEICE Trans. Fundamentals*, **E87-A**(11):2919–2928, 2004.
- [15] Q.W. Ge, *An analytical study of Petri net structures in communications and computations*, PhD thesis, Hiroshima University, December 1990.
- [16] Q.W. Ge, T. Fukunaga, and M. Nakata, On generating elementary T-invariants of Petri nets by linear programming, In *Proc. ISCAS2005*, pp. 168–171, 2005.

Available online: <http://genome.ib.sci.yamaguchi-u.ac.jp/~pnp/papers/gqw-iscas2005.pdf>.

- [17] Q.W. Ge, T. Tanida, and K. Onaga, Construction of a T-base and design of a periodic firing sequence of a Petri net, In *Proc. 8th Mathematical Programming Symposium*, Japan, pp. 51–57, 1987.
- [18] A.E. Geddis, H.M. Linden, and K. Kaushansky, Thrombopoietin: a pan-hematopoietic cytokine, *Cytokine & Growth Factor Reviews*, **13**:61–73, 2002.
- [19] H.J. Genrich, R. Küffner, and K. Voss, Executable Petri net models for the analysis of metabolic pathways, *International Journal on Software Tools for Technology Transfer*, **3**(4):394–404, 2001.
- [20] D. Gilbert and M. Heiner, From Petri nets to differential equations – an integrative approach for biochemical network analysis, In *Proc. ICATPN 2006*, vol. 4024 of *Lecture Notes in Computer Science*, Springer, pp. 181–200, 2006.
- [21] P.J.E. Goss and J. Peccoud, Quantitative modeling of stochastic systems in molecular biology by using Stochastic Petri nets, In *Proc. Natl. Acad. Sci. USA 95*, pp. 6750–6755, 1998.
- [22] S. Hardy and P.N. Robillard, Modeling and simulations of molecular biology systems using Petri nets: Modeling goals of various approaches, *J. Bioinf. and Comput. Biol.*, **2**(4):619–637, 2004.
- [23] M. Hatakeyama, S. Kimura, T. Naka, T. Kawasaki, N. Yumoto, M. Ichikawa, J. Kim, K. Saito, M. Saeki, M. Shirouzu, S. Yokoyama, and A. Konagaya, A computational model on the modulation of mitogen-activated protein kinase (MAPK) and Akt pathways in heregulin-induced ErbB signalling, *Biochem J.*, **373**(2):451–463.
- [24] M. Heiner and I. Koch, Petri net based model validation in systems biology, In *Proc. 25th International Conference on Application and Theory of Petri*

- nets*, Proc. ICATPN2004 (LNCS3099), Lecture Notes in Computer Science, Springer, pp. 216–237, 2004.
- [25] M. Heiner, I. Koch, and J. Will, Model validation of biological pathways using Petri nets, demonstrated for apoptosis, *Biosystems*, **75**(1–3):15–28, 2004.
- [26] R. Heinrich and S. Schuster, *The regulation of cellular systems*, Chapman and hall, New York, 1996.
- [27] R. Hofestädt, A Petri net application to model metabolic processes, *Syst. Anal. Mod. Simul.*, **16**:113–122, 1994.
- [28] R. Hofestädt and S. Thelen, Quantitative modeling of biochemical networks, *In Silico Biol.*, **1**(1):39–53, 1998.
- [29] C.M. Horvath, STAT proteins and transcriptional responses to extracellular signals, *TIBS*, **25**, 2000.
- [30] Y. Hu, M.A. Benedict, L. Ding, and G. Nunez, Role of cytochrome c and dATP/ATP hydrolysis in Apaf-1-mediated caspase-9 activation and apoptosis, *EMBO J.*, **18**(13):3586–3595, 1999.
- [31] K. Imada and W.J. Leonard, The Jak-STAT pathway, *Mol. Immunol.*, **37**(1–2):1–11, 2000.
- [32] M.D. Jacobson, M. Weil, and M.C. Raff, Programmed cell death in animal development, *Cell*, **88**(3):347–354, 1997.
- [33] D.E. Johnson, Regulation of survival pathways by IL-3 and induction of apoptosis following IL-3 withdrawal, *Frontiers in Bioscience*, **3**(d313–324), 1998.
- [34] H.D. Jong, Modeling and simulation of genetic regulatory systems: A literature review, *J. Comput. Biol.*, **9**(1):67–103, 2002.

-
- [35] M. Kanehisa and S. Goto, KEGG: kyoto encyclopedia of genes and genomes, *Nucleic Acids Res.*, **28**(1), Jan 1, 2000.
- [36] T. Kisseleva, S. Bhattacharya, J. Braunstein, and C.W. Schindler, Signaling through the JAK/STAT pathway, recent advances and future challenges, *Gene*, **285**(1–2):1–24, 2002.
- [37] J. Kitagawa and H. Iba, *Identifying metabolic pathways and gene regulation networks with evolutionary algorithms*, Evolutionary Computation in Bioinformatics, 2003.
- [38] S. Kotani, T. Ishihara, and A. Hotta, Functional analysis of cell-cycle regulatory molecules using system biological technique, *Experimental Medicine*, **23**(9 (extra number)):220–228, 2005. (in Japanese).
- [39] M. Krull, N. Voss, C. Choi, S. Pistor, A. Potapov, and E. Wingender, TRANSPATH: an integrated database on signal transduction and a tool for array analysis, *Nucleic Acids Res.*, **31**(1):97–100, 2003.
- [40] R. Küffner, R. Zimmer, and T. Lengauer, Pathway analysis in metabolic databases via differential metabolic display (DMD), *Bioinformatics*, **16**(9):825–836, 2000.
- [41] D.Y. Lee, R. Zimmer, S.Y. Lee, D. Hanisch, and S. Park, Knowledge representation model for systems-level analysis of signal transduction networks, *Genome Informatics*, **15**(2):234–243, 2004.
- [42] D.Y. Lee, R. Zimmer, S.Y. Lee, and S. Park, Colored Petri net modeling and simulation of signal transduction pathways, *Metabolic Engineering*, **8**(2):112–122, 2006.
- [43] P. Li, D. Nijhawan, I. Budihardjo, S.M. Srinivasula, M. Ahmad, E.S. Alnemri, and X. Wang, Cytochrome c and dATP-dependent formation of Apaf-

- 1/caspase-9 complex initiates an apoptotic protease cascade, *Cell*, **91**(4):479–489, 1997.
- [44] X. Luo, I. Budihardjo, H. Zou, C. Slaughter, and X. Wang, Bid, a Bcl2 interacting protein, mediates cytochrome c release from mitochondria in response to activation of cell surface death receptors, *Cell*, **94**(4):481–490, 1998.
- [45] J. Martinez and M. Silva, A simple and fast algorithm to obtain all invariants of a generalized Petri nets, In *Proc. Second European Workshop on Application and Theory of Petri nets, Informatik-Fachberichte*, vol. 52, Springer-Verlag, pp. 301–310, 1982.
- [46] M. Matsui, S. Fujita, S. Suzuki, H. Matsuno, and S. Miyano, Simulated cell division processes of the *Xenopus* cell cycle pathway by Genomic Object Net, *Annual collection of articles of the Journal of Integrative Bioinformatics*, **1**:95–104, 2004. Available online: http://journal.imbio.de/index.php?paper_id=3.
- [47] H. Matsuno, A. Doi, M. Nagasaki, and S. Miyano, Hybrid Petri net representation of gene regulatory network, In *Pacific Symp. on Biocomputing*, vol. 5, pp. 341–352, 2000.
- [48] H. Matsuno, S. Fujita, A. Doi, M. Nagasaki, and S. Miyano, Towards biopathway modeling and simulation, In *Proc. 24th ICATPN*, vol. 2679 of *Lecture Notes in Computer Science*, Springer, pp. 3–22, 2003.
- [49] H. Matsuno, S.T. Inouye, Y. Okitsu, Y. Fujii, and S. Miyano, A new regulatory interaction suggested by simulations for circadian genetic control mechanism in mammals, *J. Bioinf. and Comput. Biol.*, **4**(1):139–153, 2006.
- [50] H. Matsuno, R. Murakami, R. Yamane, N. Yamasaki, S. Fujita, H. Yoshimori, and S. Miyano, Boundary formation by Notch signaling in *Drosophila* multicellular systems: Experimental observations and a gene network modeling by Genomic Object Net, In *Pacific Symp. on Biocomputing*, vol. 8, pp. 152–163, 2003.

-
- [51] H. Matsuno, Y. Tanaka, H. Aoshima, A. Doi, M. Matsui, and S. Miyano, Biopathways representation and simulation on hybrid functional Petri net, *In Silico Biol.*, **3**(3):389–404, 2003.
- [52] J.A. McCubrey, L.S. Steelman, P.W. Moye, P.E. Hoyle, C. Weinstein-Oppenheimer, F. Chang, M. Pearce, M.K. White, R. Franklin, and W.L. Blalock, Effects of deregulated Raf and MEK1 expression on the cytokine-dependency of hematopoietic cells, *Adv. Enzyme Regul.*, **40**:305–337, 2000.
- [53] P.M. Merline and D.J. Farber, Recoverability of Communication protocols: implications of a theoretical study, *IEEE Trans. on Comm.*, **24**(9):1036–1043, 1976.
- [54] M. Nagasaki, *A Platform for Biopathway Modeling Simulation and Recreating Biopathway Databases Towards Simulation*, PhD thesis, The University of Tokyo, 2004.
- [55] M. Nagasaki, A. Doi, H. Matsuno, and S. Miyano, A versatile Petri net based architecture for modeling and simulation of complex biological processes, *Genome Informatics*, **15**(1):180–197, 2004.
- [56] M. Nagasaki, A. Doi, H. Matsuno, and S. Miyano, Computational modeling of biological processes with Petri net-based architecture, *Bioinformatics Technologies*, :179–242, 2005.
- [57] S. Nagata, Apoptosis by death factor, *Cell*, **88**(3):355–365, 1997.
- [58] K. Onaga and Q.W. Ge, Structural Analysis of T-invariance of Petri Nets, *Trans. of the IEICE*, **J70–A**(2):185–194, 1987.
- [59] J. Peccoud, Stochastic Petri nets for genetic networks, *Medicine Sciences*, **14**(8–9):991–993, 1998.

-
- [60] M.P. Peleg, D. Rubin, and R.B. Altman, Using Petri net tools to study properties and dynamics of biological systems, *J. Am. Med. Inform. Assoc.*, **12**(2):181–199, 2005.
- [61] J. Peterson, *Petri net theory and the modeling of systems*, Englewood Cliffs, NJ, Prectice-Hall, 1981.
- [62] J. Pinney, Petri net representations in systems biology, *Biochemical Society Trans.*, **31**(6):1513–1515, 2003.
- [63] L. Popova-Zeugmann, M. Heiner, and I. Koch, Time Petri nets for modelling and analysis of biochemical networks, *Fundamenta Informaticae*, **67**:149–162, 2005.
- [64] J.M. Proth, Petri nets for modelling and evaluating deterministic and stochastic manufacturing systems, In *Proc. 6th International Workshop on Petri Nets and Performance Models (PNPM'97)*, pp. 2–14, 1997.
- [65] C. Ramchandani, *Analysis of asynchronous concurrent systems by Petri nets*, *Ph.D. Thesis*, Dept. of Electrical Engineering, MIT, 1974.
- [66] V.N. Reddy, M.N. Liebman, and M.L. Mavrovouniotis, Qualitative analysis of biochemical reaction systems, *Comput. Biol. Med.*, **26**(1):9–24, 1996.
- [67] V.N. Reddy, M.L. Mavrovouniotis, and M.N. Liebman, Petri net representations in metabolic pathways, In *Proc. Int. Conf. Intell. Syst. Mol. Biol. 1*, pp. 328–336, 1993.
- [68] A. Saleh, S. M. Srinivasula, S. Acharya, R. Fishel, and E.S. Alnemri, Cytochrome c and dATP-mediated oligomerization of Apaf-1 is a prerequisite for procaspase-9 activation, *J Biol Chem.*, **274**(25):17941–17945, 1999.
- [69] S. Sasagawa, Y. Ozaki, K. Fujita, and S. Kuroda, Prediction and validation of the distinct dynamics of transient and sustained ERK activation, *Nat. Cell Biol.*, **7**(4):365–373, 2005.

-
- [70] C. Scaffidi, S. Fulda, A. Srinivasan, C. Friesen, F. Li, K.J. Tomaselli, K.M. Debatin, P.H. Krammer, and M.E. Peter, Two CD95 (APO-1/Fas) signaling pathways, *EMBO J.*, **17**(6):1675–1687, 1998.
- [71] H. Schulze, M. Ballmaier, K. Welte, and M. Germeshausen, Thrombopoietin induces the generation of distinct Stat1, Stat3, Stat5a and Stat5b homo- and heterodimeric complexes with different kinetics in human platelets, *Experimental Hematology*, **28**:294–304, 2000.
- [72] S. Schuster, T. Dandekar, and D.A. Fell, Detection of elementary flux modes in biochemical networks: a promising tool for pathway analysis and metabolic engineering, *Trends Biotechnol.*, **17**(2):53–60, 1999.
- [73] S. Schuster, D.A. Fell, and T. Dandekar, A general definition of metabolic pathways useful for systematic organization and analysis of complex metabolic networks, *Nature Biotechnol.*, **18**(3):326–332, 2000.
- [74] S. Schuster, T. Pfeiffer, F. Moldenhauer, I. Koch, and T. Dandekar, Structural Analysis of Metabolic Networks: Elementary Flux Mode, Analogy to Petri Nets, and Application to Mycoplasma Pneumoniae, In *German Conference on Bioinformatics 2000*, pp. 115–120, 2000.
- [75] J. Sifakis, Use of Petri Nets for Performance Evaluation, In *Proc. 3rd Intl. Symposium on Modeling and Evaluation*, IFIP, North Holland, pp. 75–93, 1977.
- [76] T. Takai-Igarashi and R. Mizoguchi, Cell signaling networks ontology, *In Silico Biol.*, **4**(1):81–87, 2004.
- [77] K. Takano, S. Taoka, M. Yamauchi, and T. Watanabe, Experimental evaluation of two algorithms for computing Petri net invariants, *IEICE Trans. on Fundamentals*, **E84-A**(11):2871–2880, 2001.
- [78] C.B. Thompson, Apoptosis in the pathogenesis and treatment of disease, *Science*, **267**(5203):1456–1462, 1995.

- [79] S. Troncale, F. Tahi, D. Campard, J.P. Vannier, and J. Guespin, Modeling and simulation with hybrid functional Petri nets of the role of Interleukin-6 in human early haematopoiesis, In *Pacific Symp. on Biocomputing*, vol. 11, pp. 427–438, 2006.
- [80] K. Voss, H. Monika, and I. Koch, Steady state analysis of metabolic pathways using Petri nets, *In Silico Biol.*, **3**(3):367–387, 2003.
- [81] C.H. Weber and C. Vincenz, A docking model of key components of the DISC complex: death domain superfamily interactions redefined, *FEBS Lett.*, **492**(3):171–176, 2001.
- [82] G.R. Wheeler, The modelling and analysis of IEEE 802.6’s configuration control protocol with coloured Petri nets., In J. Billington, M. Diaz, and G. Rozenberg, editors, *Application of Petri Nets to Communication Networks*, vol. 1605 of *Lecture Notes in Computer Science*, Springer, pp. 69–92, 1999.
- [83] P. Widlak, J. Lanuszewska, R.B. Cary, and W.T. Garrard, Subunit structures and stoichiometries of human DNA fragmentation factor proteins before and after induction of apoptosis, *J Biol Chem.*, **278**(29):26915–26922, 2003.
- [84] S. Yamaguchi, *A study on application of Petri net theory to concurrent systems*, PhD thesis, Yamaguchi University, October 2002.
- [85] I. Zevedei-Oancea and S. Schuster, Topological analysis of metabolic networks based on Petri net theory, *In Silico Biol.*, **3**(3):323–345, 2003.
- [86] H. Zou, Y. Li, X. Liu, and X. Wang, An Apaf-1-Cytochrome c multimeric complex is a functional apoptosome that activates procaspase-9, *J Biol Chem.*, **274**(17):11549–11556, 1999.
- [87] <http://www.gene-networks.com/>.
- [88] <http://www.ncbi.nlm.nih.gov/Genbank/>.

-
- [89] <http://www.rcsb.org/pdb>.
- [90] <http://www3.oup.co.uk/nar/database/c/>.
- [91] <http://www.genome.jp/kegg/>.
- [92] <http://www.biobase.de/>.
- [93] <http://www.biocarta.com/>.
- [94] <http://genome.ib.sci.yamaguchi-u.ac.jp/~pnp/>.
- [95] <http://www.ncbi.nlm.nih.gov/entrez/>.

Appendix I: Abbreviation of Substances

Apaf-1:	apoptotic protease activating factor 1
ATP:	adenosine triphosphate
Bad:	Bcl- x_L /Bcl-2 associated death promoter
Bax:	Bcl-2 associated X protein
Bcl-2:	B-Cell lymphoma 2
Bid:	Bcl-2 interacting protein
c-FOS:	c-FBJ osteosarcoma oncogene
caspase:	cysteine-aspartic-acid-proteases
CREB:	cAMP response element-binding protein
CrkL:	Crk (CT10-regulated kinase)-like protein
dATP:	desoxyadenosine triphosphate
DED:	death effector domain
DFF:	DNA fragmentation factor
DFF40:	40kDa unit of DFF
DFF45:	45kDa unit of DFF
DISC:	death inducing signaling complex
ERK:	extracellular signal-regulated kinase
FADD:	Fas-associated death domain protein
Grb2:	growth factor receptor binding protein 2
GAP:	GTPase activating protein
GDP:	guanosine diphosphate
GTP:	guanosine triphosphate
HcpH:	HcpH (hemopoietic cell phosphatase)
hSIE:	human sis-inducible element
Jak:	Janus kinase
MAPK:	mitogen activated protein kinase
MAPKK:	mitogen activated protein kinase kinase

MEK:	MAPK/ERK kinase
Mpl:	myeloproliferative leukemia protein
Pi:	phosphate group
Raf-1:	v-raf-1 murine leukemia viral oncogene homolog 1
Ras:	v-Ha-ras Harvey rat sarcoma viral oncogene homolog
RSK:	90-kDa ribosomal S6 kinase
S5RE:	STAT5 responsive element
Shc:	Src-homology collagen protein
Sos:	Son of sevenless
STAT:	signal transducers and activators of transcription
tBid:	truncated Bid
TNF:	tumor necrosis factor
TRE:	TPA response element